

Dissertation zur Erlangung des Doktorgrades
der Naturwissenschaften an der Fakultät für Biologie
der Ludwig-Maximilians-Universität München



Dynamics of histone modifications

Annette N. D. Scharf

aus

Offenburg

Eingereicht am 23. Juli 2009

Mündliche Prüfung am 24. November 2009

1. Gutachter: Prof. Dr. Peter Becker
2. Gutachter: Prof. Dr. Dirk Eick
3. Gutachter: Prof. Dr. Thomas Cremer
4. Gutachter: Prof. Dr. Michael Boshart
5. Gutachter: PD Dr. Stefan Müller
6. Gutachter: Prof. Dr. Charles David
7. SV: Prof. Dr. Axel Imhof

Ehrenwörtliche Versicherung

Ich versichere hiermit ehrenwörtlich, dass die vorgelegte Dissertation von mir selbständig und ohne unerlaubte Hilfe angefertigt ist.

München, den

(Unterschrift)

Dedicated to my father

Acknowledgments	13
Summary	14
Zusammenfassung	15
1. Introduction	17
1.1 Epigenetics	18
1.2 Chromatin	18
1.3 Histone modifications	21
1.3.1 Acetylation	23
1.3.2 Methylation	24
1.3.2.1 H3K36	25
1.3.2.2 H3K9	26
1.3.2.3 H3K27	26
1.3.2.4 H4K20	27
1.3.3 Demethylation	28
1.4 Histone code	28
1.5 Replicating chromatin	30
1.5.1 Disassembly of parental nucleosomes	30
1.5.2 Relocation of parental histones	31
1.5.3 Deposition of newly synthesized histones	32
1.5.4 Chromatin maturation	33
1.6 Objective	35
2. Materials and Methods	37
2.1 Materials	38
2.1.1 Technical devices	38
2.1.2 Chemicals and consumables	39
2.1.3 Kits and enzymes	41
2.1.4 Plasmids	41
2.1.5 Media	42
2.1.5.1 Media for <i>E. coli</i>	42
2.1.5.2 Media for HeLa cells	42

Table of contents

2.1.6	Antibiotics	43
2.1.7	Antibodies	43
2.1.7.1	Primary antibodies	43
2.1.7.2	Secondary antibodies	43
2.1.8	<i>E. coli</i> strains	43
2.1.9	DNA and protein markers	44
2.1.10	Protease inhibitors	44
2.1.11	Mass spectrometry material	44
2.1.12	Bioinformatic tool	45
2.2	Methods	45
2.2.1	Microbiology methods	45
2.2.1.1	Preparation of competent cells	45
2.2.1.2	Plasmid transformation	46
2.2.1.3	Isolation of Plasmid DNA from <i>E. coli</i>	46
2.2.2	Nucleic acid methods	47
2.2.2.1	Storage of DNA	47
2.2.2.2	DNA quantification	47
2.2.2.3	Agarose gel electrophoresis	48
2.2.2.4	Restriction digest	48
2.2.2.5	Polymerase Chain Reaction	48
2.2.2.6	RT PCR	49
2.2.3	Tissue culture methods	49
2.2.3.1	Cultivation of HeLa cells	49
2.2.3.2	Harvesting of HeLa cells	50
2.2.3.3	Storage of HeLa cells	50
2.2.3.4	Synchronization of HeLa cells	50
2.2.3.5	SILAC labeling	51
2.2.3.6	Flow cytometric analysis of the cell cycle	51
2.2.4	Protein methods	52
2.2.4.1	Protein quantification	52
2.2.4.2	SDS-Polyacrylamid-Gelelectrophoresis	52

2.2.4.3	Coomassie staining.	53
2.2.4.4	Western blotting	53
2.2.4.5	Histone extraction	54
2.2.4.6	MALDI-TOF analysis	55
2.2.4.7	Quantification of MALDI signals.	55
2.2.4.8	Tandem MS	56
2.2.4.9	AspN digest	56
2.2.5	Chromatin methods	57
2.2.5.1	Preparation of chromatin assembly extract from <i>Drosophila</i> embryos.	57
2.2.5.2	Preparation of biotinylated DNA	58
2.2.5.3	Chromatin assembly on immobilized DNA	59
2.2.5.4	Expression and purification of <i>Drosophila</i> histones.	61
2.2.5.5	Octamer reconstitution	63
2.2.5.6	Chromatin assembly by salt dialysis	63
2.2.5.7	HMT assay.	64
3.	Results and Discussion	67
3.1	Results	68
3.1.1	H3K36 methylation during transcription	69
3.1.2	H4K20 monomethylation during chromatin assembly	81
3.1.3	Histone modifications during chromatin assembly <i>in vivo</i>	93
3.2	Discussion	103
3.2.1	H3K36 methylation during transcription	103
3.2.2	H4K20 monomethylation during chromatin assembly	105
3.2.3	Histone modifications during chromatin assembly <i>in vivo</i>	109
3.2.4	General outlook.	113
	References	118
	Abbreviations	131
	Curriculum vitae.	135

First of all, I would like to thank Prof. Dr. Axel Imhof for giving me the opportunity to work on an exciting project and for his continual guidance, support and advice throughout the thesis. His inquisitive nature and extraordinary example as a scientific investigator and mentor are contagious and continuously boosted my motivation for science.

I also want to express my gratitude to Prof. Dr. Peter Becker for always having time for me, his advice and constant support and for providing not only a scientifically motivating environment but also a perfect lab atmosphere.

I would also like to thank Dr. Sandra Hake and Dr. Ana Villar-Garea for being on my internal thesis committee and for their helpful discussions and guidance of my research projects.

I am grateful to all past and present members of the institute for creating a scientifically motivating environment, help whenever needed, discussions and criticism and of course for the fun. Special thanks go to the mass spec team Ana, Christa, Ignasi, Lars, Pierre and Tilman, the HPI team Andreas, Irene and Jochen, the HMT and SMARTER team Jörn, Julia and Simone, the chromatomics team Julian, Teresa and Viola.

I wish to acknowledge my collaborators for their excellent experimental contribution and scientific interest, especially Oliver Bell, Dirk Schübeler, Karin Meier, Alexander Brehm, Elisabeth Kremmer, Volker Seitz and Teresa Barth.

Heartfelt thanks go to Boehringer Ingelheim Fonds for their exceptional generous financial support but also for their valuable personal support. Thank you Claudia, Sabine, Monika and Hermann!

My special thanks go to Tobias, thank you for being who you are.

Histone modifications are crucial for gene expression patterns and silencing and thus for the identity of the cell. This identity is transmitted from one cell generation to the next and consequently histone modification patterns have to be stably maintained during replication. On the other hand histone modifications need to be flexible to adjust the chromatin structure.

A histone modification mark in the context of transcription elongation is H3K36 methylation. Dimethylation of H3K36 accumulates adjacent to promoter regions whereas trimethylation is found at the 3' end of active genes. This thesis research shows a stepwise methylation process for H3K36 emphasizing on a state specific regulatory potential for H3K36 methylation.

Moreover this thesis research used a *Drosophila* assembly extract to dissect maturation processes during and after chromatin assembly. It was found that H4 is acetylated at K5 and K12 prior to deposition onto DNA and during chromatin maturation these acetylation marks are erased. At the same time H4 is monomethylated at K20 by Pr-Set7. In addition it was shown that dl(3)MBT is in a complex with dRpd3 and binds to the monomethylation mark of H4K20. The histone deacetylase dRpd3 removes the acetylation marks at H4K5 and H4K12. The deacetylation of H4K5 and H4K12 can be blocked when using SAH that inhibits methylation of H4K20.

Furthermore this thesis research sought to determine the kinetics by which newly synthesized histones adapt to the modification pattern of the parental histones. Therefore a novel technique was established where newly synthesized histones and their modification patterns can be distinguished from the parental ones by means of mass spectrometry. Histone modification patterns in HeLa cells were compared from old and new histones beyond one cell cycle. In conclusion investigated acetylation patterns from new histones adjusted within less than two hours to the parental state. However, the kinetics of investigated methylation patterns to reestablish the modification pattern from old to new histones was diverse

Histon Modifikationen sind für die Genexpression und für das Stilllegen der Gene ausschlaggebend und somit auch für die Identität der Zelle. Diese Identität wird von einer Zellgeneration zur nächsten übertragen und deshalb müssen die Profile der Histon Modifikationen während der Replikation erhalten bleiben. Auf der anderen Seite müssen Histon Modifikationen flexibel sein, um die Chromatin Struktur anzupassen.

Eine Histon Modifikation im Zusammenhang mit der Elongation der Transkription ist die Methylierung von H3K36. Dimethylierung von H3K36 häuft sich in der Nähe des Promoters an während Trimethylierung am 3' Ende der aktiven Gene gefunden wird. Die vorliegende Studie zeigt eine schrittweisen Methylierung von H3K36 und unterstreicht das Potential der H3K36 Methylierung abhängig vom Methylierungsgrad.

Desweiteren wurde in dieser Arbeit ein *Drosophila* Extrakt benutzt, um die Reifung des Chromatins während und nach des Zusammenbaus zu analysieren. Es wurde gefunden, dass vor dem Zusammenbau des Chromatins H4 an K5 und K12 acetyliert ist und während der Reifung des Chromatins werden diese Acetylierungen gelöscht. Gleichzeitig wird H4 mit Hilfe von Pr-Set7 an K20 monomethyliert. Zusätzlich konnte gezeigt werden, dass dl(3)MBT sich im Komplex mit dRpd3 befindet und an die Monomethylierung von H4K20 bindet. Die Histon Deacetylase dRpd3 löscht die Acetylierungen von H4K5 and H4K12. Die Deacetylierung von H4K5 und H4K12 kann durch SAH blockiert werden, das die Methylierung von H4K20 inhibiert.

Ausserdem untersucht diese Studie die Kinetik, die neu synthetisierte Histone benötigen, um die parentalen Profile der Histon Modifikationen zu adaptieren. Dazu wurde eine neue Technik etabliert, so dass neu synthetisierte Histone inklusive ihrer Modifikationen von parentalen Histonen mit Hilfe von Massenspektrometrie unterschieden werden können. Es wurden die Modifikationsmuster von alten und neuen Histonen über einen Zellzyklus hinweg verglichen. Das Fazit ist, dass Acetylierungsmuster von neuen Histonen weniger als zwei Stunden benötigen, um sich an das parentale Muster anzupassen. Jedoch war die Kinetik der neuen Histone bezüglich der Wiederherstellung der parentalen Methylierungsmuster sehr unterschiedlich.

1. INTRODUCTION

1.1 Epigenetics

The term “epigenetics” was coined by Conrad Waddington in 1942 (Waddington 1942) and defined the interaction between genes and their products that bring the phenotype into being (Goldberg et al. 2007). In 1987 Holiday specified “epigenetics” for situations where changes in DNA methylation resulted in changes in gene activity (Holliday 2006). As the most common definition today, “epigenetics” refers to the study of inheritable changes in gene expression patterns caused by events other than changes in the sequence of the DNA (Probst et al. 2009). These epigenetic changes are stable during cell division and are transferred from one generation to the next. Thus a specific gene expression pattern is maintained contributing to the cell’s identity. The identity of the cell changes in the process of cellular differentiation and epigenetic changes are essential to guide from totipotency to a fully differentiated cell (Boyer, Mathur et al. 2006). The fate of any given cell is determined by epigenetic mechanisms. Each cell type in an organism has its own epigenetic signature that depicts genotype, developmental history and environmental influences and in the end leads to the phenotype of the organism (Morgan et al. 2005). Various cell types, including neurons, muscle cell and lymphocytes, derive from a fertilized oocyte all carrying the same DNA sequence but are obviously distinct from each other. Once acquired a certain identity it is important for a cell to remember its status. This memory effect is provided by epigenetic information (Ng et al. 2008). A failure in memory resulting in abrogation of proper gene expression could promote diseases by altering differentiation concepts or silencing tumor suppressor genes (Gargiulo et al. 2009). Key signatures that regulate cellular memory include DNA methylation, histone variants, chromatin binding proteins, positional information, higher order structures, nuclear RNA and posttranslational histone modifications-all acting on the chromatin template (Figure 1).

1.2 Chromatin

Eukaryotic cells harbor a nucleus of just 10 μm in diameter in which approximately 2 m of genomic DNA is stored. Since the DNA needs to fit into the nucleus and at the same time be accessible, organisms have established ways of packaging DNA into chromatin (Felsenfeld et al. 2003). Chromatin is a highly dynamic structure consisting of DNA and its associated proteins. The basic

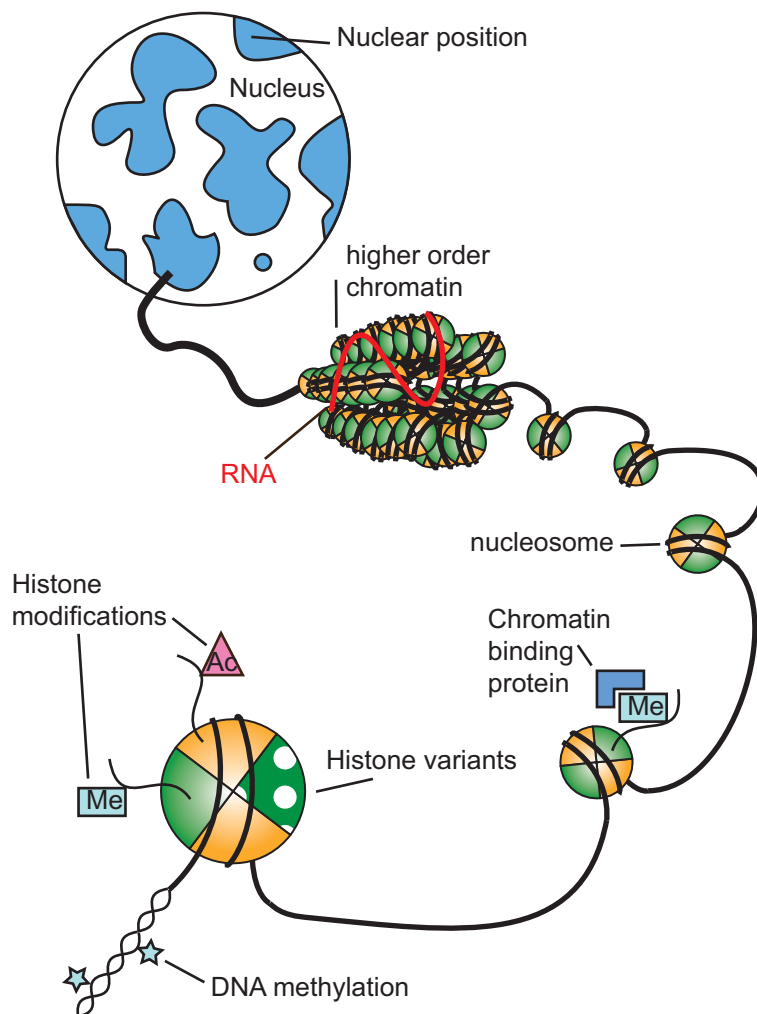


Figure 1: Key signatures in epigenetics. DNA is wrapped around a histone octamer thus forming the nucleosome the basic repetitive unit of chromatin. The DNA can be methylated on cytosine residues and histone can be posttranslational modified by for example methylation or acetylation. These modifications either alone or in combination (histone code) can be read by chromatin binding proteins that process the information further on. Even more complex information is stored in the nucleosome when histone variants are present. Nucleosomal arrays are folded into higher order chromatin structures and potentially linked with non coding RNA. The position of chromatin within the nucleus also encodes information for regulating gene expression.

building block of chromatin is the nucleosome, which consists of two copies of each of the core histone: H2A, H2B, H3 and H4 (Kornberg 1974). Around this histone octamer approximately 147 base pairs of DNA are wrapped in 1.65 superhelical, left handed turns (Luger et al. 1997). Detailed molecular analysis of how the histone protein octamer is structured and the intermolecular interactions between the DNA and the core histones stemmed from crystal structure studies of the nucleosome (Luger et al. 1997). The four core histones are small basic proteins that are composed of an N-terminal tail, a C-terminal tail and a globular domain. The globular domain consists of three α helices connected by two flexible loops and is referred to as the histone fold domain (Luger et al. 1997). The histone fold allows histones to dimerize head to tail in a handshake manner (Arents et al. 1995). The relatively unstructured histone tails are easily accessible as they are protruding

outward from the nucleosome. A variety of posttranslational modification of the tails have been described (Imhof 2003; Fischle, Wang, and Allis 2003b; Kouzarides 2007), however little is known about the conformation of the histone tails and the exact nature of DNA interaction. In crosslinked dinucleosomes the N-terminal tails of H2A and H2B interact with the DNA of the neighboring nucleosome in contrast to the N-terminal tails of H3 and H4 that only exhibit intranucleosomal interactions (Zheng et al. 2003; Wang et al. 2006).

Two nucleosome core particles are separated by the linker DNA, varying in length from 10 to 80 base pairs. Where the linker DNA enters and exits the nucleosome histone, H1 is able to bind forming the so called chromatosome. H1 is larger than the core histones and consists of a globular domain and extended N- and C-terminal tails. Histone H1 participates in nucleosome positioning or spacing and formation of the higher-order chromatin structure (Ramakrishnan 1997; Widom 1998; Thomas 1999; Maier et al. 2008).

The heterogeneous entity enables chromatin to be packed in several levels starting with a formation known as the 11 nm fiber based on its approximate diameter. The fiber comprises repeating units of the nucleosome core and linker DNA separating the individual units (Kornberg 1974). This configuration called “beads on a string” results in a 5 to 10 fold compaction. However, chromatin in living cells consists rather in a more condensed form. To increase the condensation, chromatin is packed into a fiber with the diameter of 30 nm (Marsden et al. 1979). The exact folding of this fiber is still controversial (Bednar et al. 1998; Robinson et al. 2006). Several different models have been proposed to describe the details of how the 30 nm fiber is organized. Two favorable classes of models have been described, the “one-start” and the “two-start” models. In the “one-start” models, the 30 nm fiber resembles a solenoid wherein the nucleosomes are spooled around a central axis with 6-8 nucleosomes per turn and bent linker DNA. On the contrary, the “two-start” models favor straight linker DNA and nucleosomes form a “zigzag” loop that either twists or supercoils (Dorigo et al. 2004; Schalch et al. 2005; Routh et al. 2008). The 30 nm fibers compacts the DNA 50 fold. Little is known about further compaction processes resulting in a condensed mitotic chromosome 1.5 μm in diameter (Belmont 2006). Despite the little knowledge about how it is compacted, the function of the mitotic chromosome is well studied. This structure allows an accurate segregation of the identical copies of the genome and ensures a precise transfer to each daughter cell (Swedlow et al. 2003).

Historically, light-microscopy studies have revealed at least two types of chromatin: heterochromatin that stays condensed after cell division and euchromatin that decondenses during interphase (Grewal et al. 2002; Elgin et al. 2003; Maison et al. 2004). Euchromatin can either be actively transcribed or repressed whereas heterochromatin is commonly defined as transcriptionally repressed appearing in large units at the centromeres and telomeres (Grewal et al. 2007). Heterochromatin can be subdivided into constitutive and facultative heterochromatin. Constitutive heterochromatin remains condensed during the entire lifespan of a cell whereas facultative heterochromatin has the potential to convert between heterochromatin and euchromatin (Craig 2005). The transcriptional status of a gene can also be determined by its spatial position. In the nucleus individual chromosomes occupy distinct regions known as the chromosome territories. On the surface of the territories often actively transcribed genes are found. Territories are separated by interchromatin compartments containing the machinery for nuclear functions (Cremer et al. 2001; 2006).

1.3 Histone modifications

Chromatin is a highly dynamic structure and must keep the balance between being folded as much as needed and being accessible whenever necessary to cope with genome templated processes such as replication, transcription and DNA repair. The functional state of chromatin is partially regulated through posttranslational modifications (PTMs) of histones (Jenuwein et al. 2001) (Figure 2). Thereby these modifications are involved in regulating the gene expression. Numerous types of histone modifications exist and they divide into two groups. To the first group belong acetylation of lysines, phosphorylation of serines and threonines and methylation of arginines and lysines as they convey small chemical groups. Second, there are larger peptides such as ubiquitination and SUMOylation of lysines and ADP-ribosylation of glutamic acid (Imhof 2003; Fischle, Wang and Allis 2003b).

There are several mechanisms how histone posttranslational modifications can influence chromatin. First, histones and their modifications can alter the chromatin structure and thus regulate DNA accessibility (Imhof et al. 1997). For example acetylated histones correlate with a more open chromatin structure. Secondly, PTMs on histones facilitate the binding of a protein to chromatin by creating a specific binding site. A classic example is that methylated H3K9 serves as binding

platform for HP1 (Heterochromatin protein 1) (Lachner et al. 2001; Grewal et al. 2007). Thirdly, modified histones may impede the binding of a factor to chromatin such as phosphorylated H3S10 inhibits the binding of HP1 to methylated H3K9 (Fischle et al. 2003a, 2005; Johansen et al. 2006).

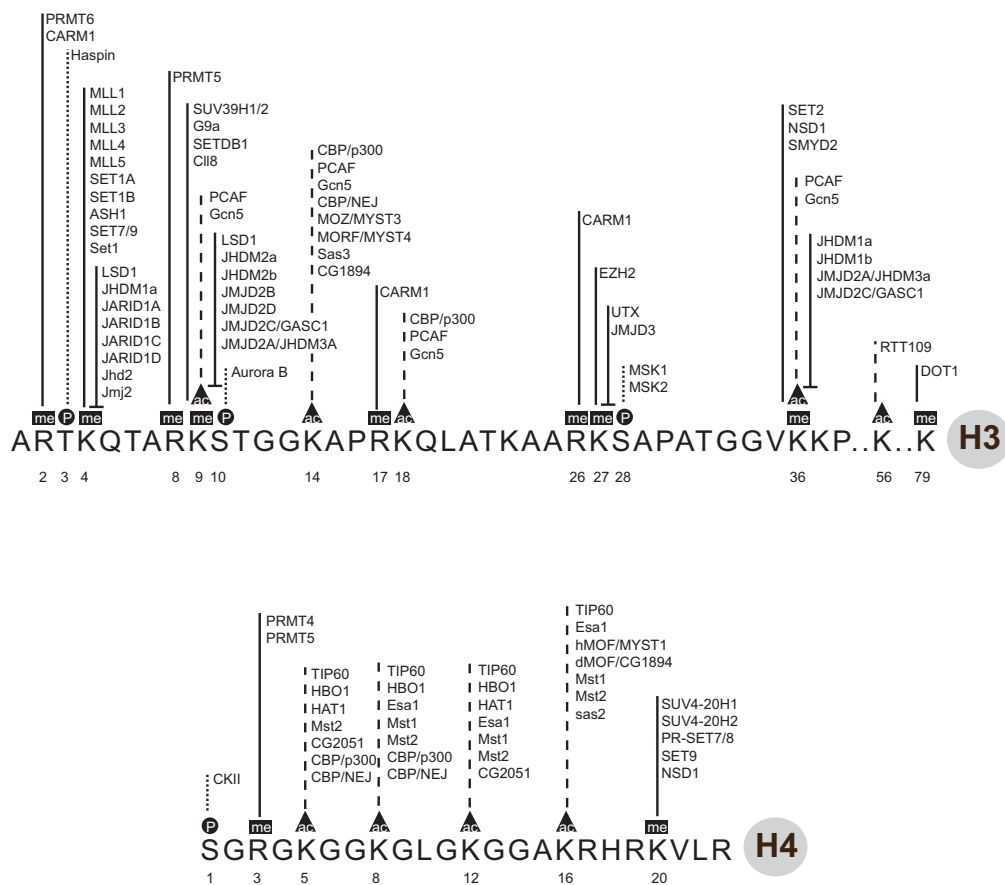


Figure 2: Histone modification map of H3 and H4. Most common sites of acetylation (ac), methylation (me) and phosphorylation (P) on histone H3 and H4 and their corresponding enzymes are depicted. Figure adapted from Abcam.

1.3.1 Acetylation

Acetylation of lysines within the histone tails has an important role in transcription. Genetic studies in *S. cerevisiae* revealed that upon depletion of the histone tails or substitution of H4K5, 8 and 12 to arginines gene activation was affected (Durrin et al. 1991). This correlates acetylation with transcriptionally active chromatin (Hebbes et al. 1994). Setting the acetylation mark is catalyzed by histone acetyltransferases (HAT) and the first of which was isolated in 1996 in *Tetrahymena* (Brownell et al. 1996). The isolated enzyme was homologous to the yeast Gcn5 (General control non-derepressible) a known transcriptional adaptor in *S. cerevisiae* that was found to interact with transcriptional activators. Depending on the substrate specificity and cellular localization histone acetyltransferases can be categorized in either type A or type B. Type A acetyltransferases are localized in the nucleus and modify histones incorporated into chromatin. On the contrary type B acetyltransferases are located in the cytoplasm and acetylate only free histones (Parthun 2007). The sole representative so far identified of type B acetyltransferases is Hat1 and is found to mediate acetylation on H4K5 and K12 (Kleff et al. 1995; Parthun et al. 1996). Acetylation is a reversible mark and histone deacetylases (HDAC) are enzymes that remove acetyl groups from an acetylated amino acid. The first histone deacetylase was also identified in 1996 from cow protein extracts and discovered to be a homologue of yeast Rpd3 (reduced potassium dependency-3) (Taunton et al. 1996). The current model is that activators that are bound to DNA attract HATs to transfer acetyl groups while repressors bind HDACs to remove acetyl groups resulting in alterations of the chromatin template and thus in gene regulation.

Histone acetyltransferases are highly diverse and reside in a variety of multiprotein complexes. At least three main HAT families exist. First the GNAT (Gcn5 related N-acetyltransferase) family includes Gcn5, Hat1 and PCAF (Dyda et al. 2000). The second family is called MYST, an acronym for its founding members Morf, Ybf2, Sas2 and Tip60 (Utley et al. 2003). Both families are highly conserved from yeast to men. Another yet less conserved family is called p300/CBP named for the two proteins p300 and CBP (Giordano et al. 1999; Bannister et al. 1996). Some HATs also possess specific domains known as bromodomains that enable the enzymes to bind to acetylated histones (Zeng et al. 2002).

The numerous HDAC enzymes that remove acetyl groups from histones are categorized into

four groups: Type I, Type II, Type III or Sir2 related enzymes and Type IV. Only the third group needs NAD as a cofactor to catalyze the removal of the acetyl group. HDACs are usually found in several multisubunit complexes. The deacetylase Rpd3 is found in the Sin3 complex as well as the Mi-2/NuRD complex (Yang et al. 2008). Rpd3 comprises a N-terminal deacetylase domain and a C-terminal tail. The activity of HDACs can be reversibly inhibited by small compounds such as sodium butyrate (NaBu) or Trichostatin A (TSA). TSA, a hydroxamic acid is a fermentation product of *Streptomyces* and selectively inhibits HDACs from Type I and II by binding to the catalytic domain of the enzyme (Yoshida et al. 1990). NaBu, a short chain fatty acid is the byproduct of an aerobic bacterial fermentation and occurs naturally in the body. The inhibition potential is less efficient compared to TSA. Noteworthy, HDAC inhibitors have therapeutic potential for treating cancer and other diseases by changing epigenetic pathways (Gallinari et al. 2007).

1.3.2 Methylation

Methylation on histones can either occur on lysines (K) or arginines (R). At the moment there are at least 24 sites of lysines and arginines discovered on histones with the potential to be methylated. On the ϵ -amino groups of lysines one (me1), two (me2) or three (me3) methyl groups can be added whereas the guanidino nitrogen atoms of arginines can only be mono- or dimethylated (Zhang et al. 2001). The combinatorial effect of sites and methylation grade allows a complex alteration of the nucleosome properties and therefore a high potential to regulate important processes within the nucleus. Methylation is associated both with transcriptional repression as well as activation (Jenuwein et al. 2001).

Methyltransferases are grouped in three distinct protein families the PRMT1 (Protein arginine methyltransferase 1) family (catalyzing arginine methylation), the SET-domain family and the non-SET domain proteins DOT1/DOT1L (Ng et al. 2002). The SET domain was first identified in three *Drosophila* proteins: Suppressor of position effect variegation 3-9, SU(VAR)3-9; Enhancer of zeste, E(Z) and Trithorax, Trx (Jones et al. 1993; Tschiersch et al. 1994; Stassen et al. 1995). The first lysine methyltransferase SUV39H was identified in 2000 and specifically methylates lysine 9 on the N-terminal tail of H3 (Rea et al. 2000). By now several methyltransferases and their sites of modification have been identified (Kouzarides 2007). In all cases the methyl donor is S-Adenosyl

methionine (SAM) and is converted during the methylation reaction to S-Adenosyl homocysteine (SAH). There are six well characterized methylation sites on histones: H3 (K4, K9, K27, K36, K79) and H4K20. Methylation at H3K4, K36 and K79 is mostly coupled with active transcription (Ruthenburg et al. 2007; Lee et al. 2007; Steger et al. 2008) whereas the H3K9, K27 and H4K20 trimethylation is linked to transcriptional repression (Ebert et al. 2006). To carry out downstream effects several proteins are known to bind specific to methylation sites. Binding proteins comprise one of the four domains: the chromodomain, the tudor domain, the PHD (Plant homeodomain) finger domain or the WD40-repeat domain (Martin et al. 2005; Wysocka et al. 2006). Lysine histone methylation is one of the most stable epigenetic mark and different biological processes can be attributed depending on the position of the methylation mark.

1.3.2.1 H3K36

In yeast all H3K36 methylation states are mediated by the histone methyltransferase Set2. This enzyme preferentially binds to RNA polymerase II being phosphorylated at Ser-2 within the C-terminal domain (CTD) (Li et al. 2003; Meinhart et al. 2005). As a result of this interaction, Set2 is directed to active genes. Especially at the 3' end of active genes methylation of H3K36 is enriched and it is associated with proper elongation of RNA polymerase II through the coding region (Schaft et al. 2003; Krogan et al. 2003; Bannister et al. 2005). The RNA polymerase needs acetylated nucleosomes, resulting in an accessible chromatin structure, to progress through the coding regions. During transcription inappropriate initiation of transcription needs to be prevented. Therefore H3K36 serves as a binding motif for the recruitment of histone-deacetylase activity Rpd3 (Carrozza et al. 2005). Structural studies have shown the molecular details of how the Eaf3 (Esa1 associated factor 3) subunit of Rpd3 binds histone H3 methylated at lysine K36 (Xu et al. 2008). Eaf3 is also a subunit of the histone acetylase NuA4 (nucleosome acetyltransferase of histone H4) and therefore plays an important role in controlling histone acetylation patterns that in the end distinguishes between coding regions and promoters (Reid et al. 2004). Joshi et al could show that Eaf3 mediates deacetylation of coding regions by interaction of the chromodomain of Eaf3 and methylated H3K36 (Joshi et al. 2005). In mammals other proteins besides Set2 have been shown to possess methyltransferase activity for H3K36 such as the NSD1 protein. Until now little is known about the exact regulation of this site, the interplay between the levels of methylation and the proteins needed to orchestrate.

1.3.2.2 H3K9

The first discovered lysine HMT was the human SUV39H containing a SET domain and known to methylate H3K9 (Rea et al. 2000). Methylation of H3K9 is mostly associated with transcriptionally inactive chromatin (Schotta et al. 2002; Peters et al. 2003) but is also found in transcribed regions of active genes (Vakoc et al. 2005). Different methylation states (me1, me2 or me3) are found within different regions of the genome suggesting various functions of H3K9 methylation (Ebert et al. 2004). H3K9 di- and trimethylation is involved in pericentromeric heterochromatin formation (Ebert et al. 2004, 2006). For this formation additional proteins are needed, first SUV39H methylating histone H3 at K9 creating a binding site for the second protein involved, HP1 (heterochromatin protein 1) that is able to bind via its chromodomain to di- and trimethylated H3K9 (Bannister et al. 2001; Lachner et al. 2001). After the initiation site has been introduced, heterochromatin can spread by the binding of SUV39H to HP1 that in return leads to more methylation of H3K9 resulting in a self enforcing loop (Maison et al. 2004).

1.3.2.3 H3K27

H3K27 methylation is found in euchromatin at gene loci as well as at pericentromeric heterochromatin and at the inactive X in mammals (Heard 2005). The enzyme that has been shown to mediate H3K27 methylation is EZH2 (Enhancer of Zeste homolog 2) or its homologues (Czermin et al. 2002; Cao et al. 2002). It can add up to three methyl groups on this residue and H3K27 trimethylation is currently considered to be the prevailing state involved in biological functions *in vivo* (Kotake et al. 2007; Boyer, Plath, et al. 2006; Fouse et al. 2008). EZH2 in humans or E(Z) in flies is a SET domain containing protein and found in the Polycomb repressive complex 2 (PRC2) (Czermin et al. 2002). One of the functions of PRC2 is the silencing of differentiation genes by altering chromatin folding (Grimaud et al. 2006). A well known target are the *HOX* genes controlling segmentation during development in *Drosophila*. PRC2 and its catalytic subunit EZH2 is conserved throughout species (Holdeman et al. 1998) suggesting to be a well established strategy for gene silencing that uses H3K27 methylation as a repressing mark. Besides PRC2 also PRC1 (Polycomb repressive complex 1; 2) is able to bind to the H3K27 methylation mark. However, PRC2 is required for PRC1 binding to methylated H3K27 (Fischle, Wang, Jacobs, et al. 2003; Min et al. 2003). Genome wide studies

have discovered more than 1000 silenced genes that are co-occupied by PRC1, PRC2 and H3 K27 trimethylation (Bracken et al. 2006).

1.3.2.4 H4K20

H4K20 can be mono- di- or trimethylated *in vivo*. Pr-Set7/SET8 specifically monomethylates histone H4 at lysine 20 in *Drosophila* or human cells respectively (Nishioka et al. 2002; Fang et al. 2002). The same lysine is di- and trimethylated by other histone methyltransferases: Suv4-20h1 and Suv4-20h2 (Schotta et al. 2004, 2008). The enzymes for all three methylation sites share a common SET domain, known to be a conserved motif in most lysine directed HMTs. But Pr-Set7 lacks Pre- and Post SET domains that were thought to be essential for the activity of HMTs showing that these domains are not absolutely required for HMT activity (Fang et al. 2002). Pr-Set7 is so far only identified in higher eukaryotes but not in yeast. A Pr-Set7 null mutation in *Drosophila melanogaster* linked the methyltransferase to gene silencing and suggested that H4K20 monomethylation by Pr-Set7 is essential for mitosis (Karachentsev et al. 2005). Increased expression of Pr-Set7 during S phase is followed shortly by an increase in H4K20 monomethylation during S phase (Tardat et al. 2007; Jørgensen et al. 2007). During S phase Pr-Set7 is expressed at a high level (Tardat et al. 2007) and interacts directly with PCNA (Proliferating cell nuclear antigen) via a PIP box. Defective interaction results in a faulty S phase progression (Jørgensen et al. 2007; Huen et al. 2008) arguing for a cell cycle dependent function of Pr-Set7 and H4K20 monomethylation. H4K20 mono- and trimethylation is low in abundance throughout the cell cycle and the majority of H4K20 is dimethylated. Newly synthesized H4 becomes rapidly dimethylated (Pesavento et al. 2008). The different methylation states fulfill different functions in the cell: Dimethylation is able to recruit different DNA repair factors (Botuyan et al. 2006). Trimethylation of H4K20 is enriched in pericentromeric heterochromatin (Schotta et al. 2008). In contrast, monomethylation is associated with active genes linking this methylation state to transcription (Barski et al. 2007). But the mark was also found to be associated with inactive X chromosome in undifferentiated ES cells suggesting a role in gene silencing (Kohlmaier et al. 2004). Methylation of H4K20 was suggested to inhibit acetylation at H4K16 (Nishioka et al. 2002). These two marks were first shown to be mutually exclusive. However, in contrast to this proposal recent studies revealed that the two marks are regulated independently (Pesavento et al. 2008). Pesavento et al. could show in HeLa cells

by mass spectrometry analysis that the two marks are not mutually exclusive neither under normal regulation *in vivo* nor when hyperacetylation is induced artificially.

1.3.3 Demethylation

Histone modifications are dynamic in order to cope with the needs of the cell. Methylation marks of either lysine or arginine residues are removed by different enzymes. In human and mice methylarginine can be converted to citrulline by peptidylarginine deiminase (PADI). The first identified lysine specific demethylase LSD1 (Lysine-specific demethylase 1) removes methyl groups using FAD (flavin adenine dinucleotide) as a cofactor with specificity towards mono- and dimethylation at H3K4. Metzger et al. could show that LSD1 demethylates mono- and dimethylation of H3K9, hence promoting gene activation (Metzger et al. 2005). A chromatin associated transcriptional repressor (Co-REST) is required as a cofactor for the demethylation (Shi et al. 2004). Interestingly, demethylation activity is reduced in the presence of HDAC inhibitors thus linking demethylase and deacetylase activity (Lee et al. 2006). Another group of demethylases was found containing a common catalytic Jumonji-C (JmjC) domain distinct from LSD1. The JmjC domain requires iron (Fe(II)) and α -ketoglutarate as cofactors to perform an oxidative demethylation reaction (Klose, Kallin, et al. 2006). Demethylase enzymes from the JmjC class are able to remove mono-, di- and trimethylation marks from H3K36, H3K9, H3K27 and H3K4 (Shi et al. 2004; Klose, Yamane, et al. 2006; Xiang et al. 2007) leaving important marks such as H3K79 and H4K20 for which no demethylase activity has been identified yet.

1.4 Histone code

There is a variety of histone modifications existing and still emerging. Many of them are linked to a specific process with DNA as the template. It has been proposed that the combination of different histone modifications results in a “histone code”, which specifies patterns of gene expression. This may create a second level besides the genetic code and adds an additional complexity to the information potential (Jenuwein et al. 2001; Turner 2002).

The code could be a simple binary code where a certain histone modification is either linked to gene activation or repression and also influencing other modification for further processes. As described above certain modifications possess the tendency for either a transcriptionally “on” or “off” state. Inconsistent with the binary code theory some modifications are involved in opposing chromatin states. For example phosphorylation of H3S10 is found at high level in mitotic cells and associated with chromosome condensation. But it also correlates with active genes and euchromatic regions suggesting different roles for the same modification (Johansen et al. 2006). A more general consideration of the histone code proposes that posttranslational histone modifications attract different “writers” and “readers” mostly being chromatin binding proteins. Depending on the writer and reader a distinguishable signal transduction pathway is initiated resulting in a specific process. Schreiber and Bernstein proposed that multiple histone modifications mediate signal switches and act analogous to signal transduction pathways of receptor tyrosine kinases (Schreiber et al. 2002). The signal transduction pathway in the nucleus could start by recruiting a HAT that acetylates the H3 tail. This newly formed binding site is then able to recruit other enzymatic activities and thus propagating the initial signal. They suggest that positive feedback is provided by proteins containing chromo- and bromodomains such as HP1 interacting with Su(var)3-9 and H3K9 methylation. The counteracting influence of H3S10 and H3K9 methylation can be described as an example of negative feedback (Schreiber et al. 2002). In 2004 Henikoff and colleagues also questioned the existence of the histone code since no templated machinery has been identified so far to propagate histone modifications during replication (Henikoff et al. 2004). They postulated that the histone code is not inherited during replication but rather during transcription. Accordingly, replication merely provides an approximate distribution of old and new histones on the daughter strands. The specificity of chromatin states is caused by nucleosomal replacement during transcription with replication independent histone variants. The H3 replacement variant H3.3, for example, is deposited throughout the cell cycle. Outside S phase H3.3 is deposited mostly with euchromatin leading to the proposal that H3.3 marking active chromatin (Henikoff et al. 2004). The histone code hypothesis and epigenetic inheritance still remain to be further investigated.

1.5 Replicating chromatin

Chromatin packages DNA in the nucleus and controls the expression of genes. This crucial structure must be accurately copied to the two daughter strands during replication to maintain information beyond just DNA sequence (Nakatani et al. 2006; Ng et al. 2008). This epigenetic inheritance can be divided into three major parts. At first the nucleosomes on the parental strand are disassembled which allows the replication machinery to access the DNA. Then the disrupted histones are transferred behind the replication fork with the help of chaperones and finally the histones- old and new- assemble onto the DNA daughter strands to rebuild chromatin in an orchestrated manner (Figure 4).

1.5.1 Disassembly of parental nucleosomes

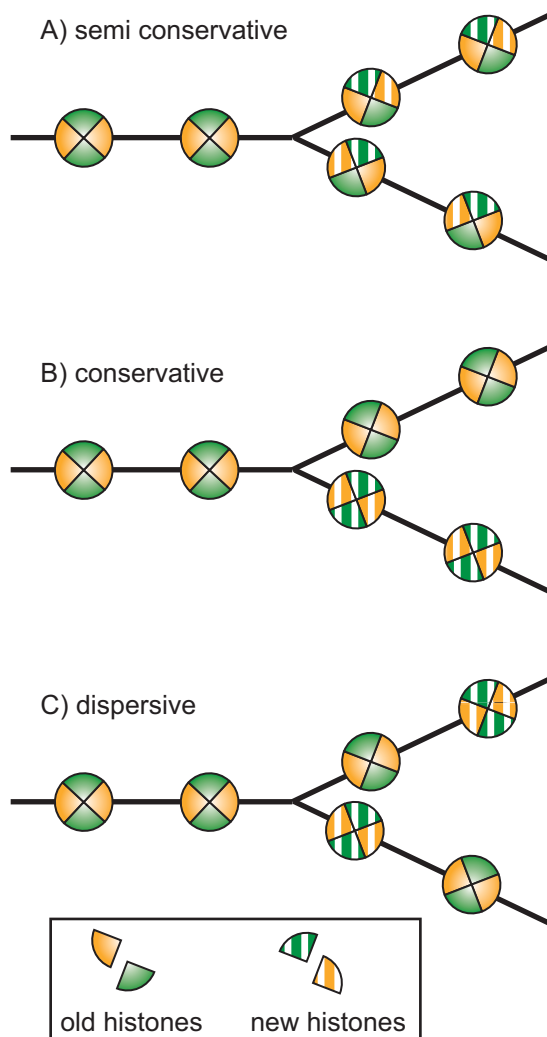
When the replication fork approaches, parental nucleosomes are disrupted ahead of the fork and the nucleosomal octamer is split into two H2A-H2B dimers and a (H3-H4)₂ tetramer (Tagami et al. 2004; Corpet et al. 2009; Probst et al. 2009). Still unclear is the cause of the disruption and whether the replication fork alone drives the disruption or whether additional factors such as chromatin remodeling complexes or chaperones are involved. Chaperones could immediately accept histones from disrupted nucleosomes and could assist the “old” histones to the daughter strands. The H2A-H2B chaperone complex FACT (Facilitates chromatin transcription) was identified in association with MCM (Minichromosome maintenance) proteins (Tan et al. 2006), which constitute a helicase with DNA unwinding activity in front of the replication fork thus linking FACT to replication (Gambus et al. 2006). Another histone chaperone CAF1 (Chromatin assembly factor 1) which is specific for H3-H4 (Verreault et al. 1996) is known to interact with a variety of proteins including PCNA and ASF1 (Anti silencing factor 1) that allows the recruitment of CAF1 to the replication fork (Moggs et al. 2000; Mello et al. 2002, 2001). ASF1 is also associated with the MCM helicase (Groth et al. 2007). When CAF1 activity is reduced severe replication defects, S phase arrest and delayed chromatin assembly occur (Song et al. 2007). Structurally, CAF1 consists of three subunits: p180, p105 and p55 in *Drosophila* and p150, p60 and p48 in humans. The second smallest subunit is known to interact with ASF1 another H3-H4 histone chaperone thereby acting together in histone

deposition (Groth et al. 2005, 2007, 2009).

The interaction of histone chaperones with MCM proteins suggest that chaperones play a key role in disrupting parental nucleosomes and potentially transfer them onto the nascent DNA after the fork.

1.5.2 Relocation of parental histones

To limit the length of exposure of naked DNA, parental nucleosomes are assembled into chromatin as soon as the DNA emerges out of the replisome. There are three common models of distributing



parental nucleosomes on the two daughter strands (Figure 3) (Jackson et al. 1975, 1985; Probst et al. 2009; Groth 2009). First of all the parental histones could, in almost the same manner as DNA and its methylation marks, be deposited in a semi-conservative way (Tagami et al. 2004). Dimers of parental histones distribute evenly onto each daughter strand and dimers of newly synthesized histones complement the nucleosome. This results in a “hemimodified” nucleosome where the

Figure 3: Inheritance of histones at the fork. Three different possibilities for the distribution of parental histones are depicted. A) If the histones are inherited in a semi-conservative manner, then the nucleosomes after the fork are reconstituted equally from old and new histones. B) The conservative way of histone distribution implies that one daughter strand is exclusively associated with old histones and the other strand with only new histones. C) Dispersive histone distribution results in a random sequence of old and new nucleosomes.

old histones and their modification pattern serve as a template to guide the new histones to the appropriate modification pattern. Another possibility is that the distribution of the new versus the old histones follows an asymmetric order where the pre-existing histones all assemble on one daughter DNA molecule whereas the newly synthesized associate with the other daughter strand. To achieve identically daughter strands in terms of histone modifications interstrand communication is necessary. This way of segregating parental and new histones could initiate changes in cell fate and allow reshaping the cells' identity. In the last hypothetical model both old and new histones are assembled randomly onto the daughter strands (Russev et al. 1982). Histone modification pattern are copied from neighboring nucleosomes so that no epigenetic information is lost. This method of restoring histone modification patterns from one nucleosome to its neighboring sounds ideal for repetitive sequences where long arrays of nucleosomes carry the same marks. However, this cannot be applied to chromatin stretches with highly dynamic modification patterns or when single histone modifications are important.

Theoretically it is also possible that all three models described above occur in nature depending on the needs of the cell. There are instances where an exact copy of the chromatin state is necessary and chromatin reorganization leads to catastrophic events within the organism such as cancer (Grønbaek et al. 2007). However, one could also envision that a blank template is needed in order to change the cell fate (Welstead et al. 2008). A combination of the different ways allows the cell to cope with the environment in an either static or dynamic way (Groth et al. 2007, 2009; Probst et al. 2009).

1.5.3 Deposition of newly synthesized histones

DNA doubles during replication as so has the amount of histones. Canonical core histones are synthesized during S phase and the exit of the S phase results in a rapid decrease in histone mRNA levels (Marzluff et al. 2002). Newly synthesized histones are escorted by chaperones such as CAF1 and ASF1 and carry a conserved combination of acetylation marks (Ridgway et al. 2000; Groth et al. 2007). Histone H4 is preacetylated at lysine 5 and 12 and the mark is removed quickly after chromatin assembly and chromatin can mature (Sobel et al. 1995; Loyola et al. 2006). In yeast

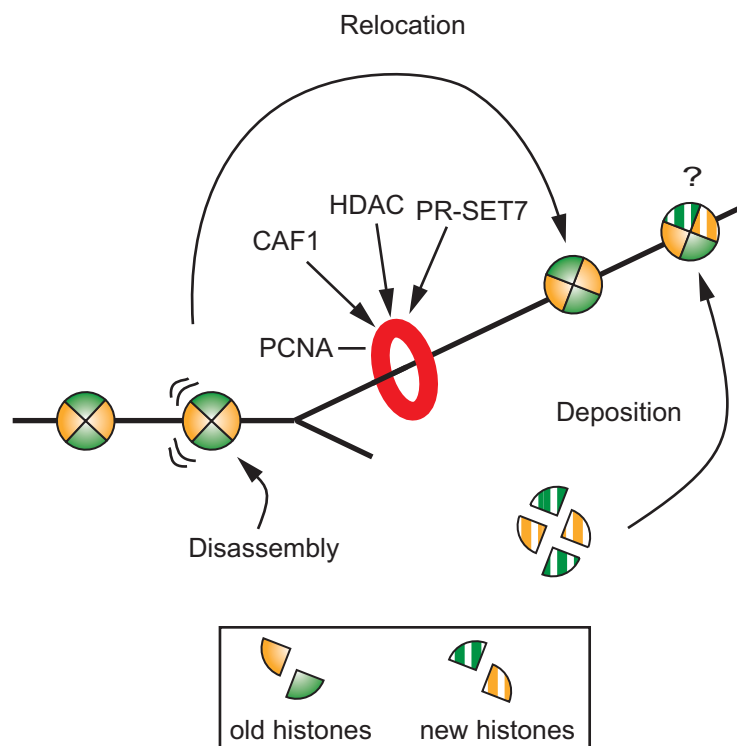


Figure 4: Chromatin at the replication fork. Ahead of the moving fork nucleosomes are disassembled so that the DNA sequence can be accessed. Then the parental histones are relocated behind the replication fork and the fully nucleosome density is completed by the deposition of newly synthesized histones. PCNA serves as a common platform for chromatin binding proteins

H3K56 also serves as a predeposition mark (Masumoto et al. 2005; Das et al. 2009). However, the acetylation patterns of H3 differ from species to species suggesting that the charge state of H3 is more important for further assembly than acetylation on a specific site. Chromatin assembly can be divided in several consecutive steps. H3 and H4 are assembled followed by the addition of two H2A-H2B dimers and in the end the linker histone H1 is added on the chromatin fiber (Benson et al. 2006). Once chromatin is reestablished after the replication fork chromatin and especially its modification pattern may mature with the help of chromatin binding proteins.

1.5.4 Chromatin maturation

On the replication fork PCNA can serve as a docking station for various chromatin binding proteins (Figure 4). For example PCNA is able to recruit histone deacetylase activity (Milutinovic et al. 2002), chromatin remodeling activity (Poot et al. 2004), DNA methyltransferase 1 (Dnmt1) (Chuang et al. 1997) and also the lysine methyltransferase Pr-set7 (Huen et al. 2008). A model for

targeting the replication fork to chromatin assembly and maturation would be that PCNA recruits CAF1 and thereby newly synthesized histones carrying several acetylation marks. At the same time PCNA delivers histone deacetylases to remove the predeposition marks and histone modifying enzymes such as Pr-Set7 to set the new marks (Moldovan et al. 2007). The individual steps of how chromatin maturation is configured are still to be discovered.

1.6 Objective

Chromatin encounters different cellular processes and needs to be able to react adequately without losing its epigenetic information. This flexibility and at the same time stability is obtained by mechanisms including histone modifications. The aim of this work was to gain more insight how histone modification patterns are regulated in detail especially how the patterns are established and maintained during replication, chromatin assembly and transcription.

Part I: Localized H3K36 methylation states define histone H4K16 acetylation during transcriptional elongation in *Drosophila*

During transcription elongation H3K36 methylation is the only mark to be enriched in the 3' end of active genes. However, little was known about the state specific regulation of K36 methylation. The aim of the first part of this thesis was to verify by means of mass spectrometry a stepwise methylation process for methylation on H3K36 that was found in Western blot analysis by our collaborator Oliver Bell.

Part II: Monomethylation of H4K20 facilitates chromatin maturation

Shortly after histones being deposited onto DNA chromatin is assembled. Yet *in vivo* events of chromatin maturation happen quite fast and thus are difficult to investigate. Therefore an *in vitro* approach, using a *Drosophila* extract that is able to assemble DNA into chromatin, is conducted in this thesis research to dissect the dynamics of histone modifications and their binding proteins in detail before and after chromatin assembly.

Part III Establishment of histone modifications after chromatin assembly

Newly synthesized histones possess differential modification patterns when compared to parental histones. However, the detailed kinetics by which the modification patterns are reestablished on the new histones is still unknown. In this thesis research a novel technique (pulsed stable isotope labeling with amino acids) was established and applied to investigate the kinetics by which newly synthesized histones adjust to the modification pattern of the parental histones.

2. MATERIALS AND METHODS

2.1 Materials

2.1.1 Technical devices

Description	Supplier
-20°C Freezer	Liebherr
26°C Incubator	Bachofer
37°C Incubator/ bacteria	Memmert
37°C Incubator/ cells	Thermo scientific
4°C Fridge	Liebherr
-80° Freezer	GFL
Agarose gel chamber	repair shop of Adolf-Butenandt-Institute
Autoclave (Varioklav)	H+P
Balances	Sartorius
Cell counter	Casy Cell Counter, Innovatis
Centrifuges	Eppendorf Centrifuge 5417C Eppendorf miniSpin Heraeus; Kendro (Biofuge pico), Heraeus; Kendro (Cryofuge6000i), Sorvall; Kendro (RC6PLUS) Thermo; Multifuge 3L Sigma; 3-18 Heraeus; Cryofuge 6000i Beckman; Ultracentrifuge (LE-80K)
FACS	FACSCanto, Beckton Dickinson
FPLC	Amersham Biosciences
French press	ThermoSpectronic
Geiger counter	Bachofer
Gel documentation system	Peqlab
Homogenisator	Schütthomgen
Hood	HeraSafe, Thermo Scientific
Imaging system	LI-COR
Incubation shaker	Infors Multitron
Microscope (TC)	Leica DMIL
Microwave	LG
MilliQ-water	Millipore
pH-meter	inoLab pH 720
Pipetboy	Brand
Pipettes	Gilson

Power supply	BioRad (Pac 300), Pharmacia
Proteingel chamber (Novex Mini Cell)	Invitrogen
Rotating wheel	neoLab
Shaker	Roth
Sonifier	Branson
Spectrophotometer	Nanodrop ND1000, Peqlab
Thermocycler	MWG Biotech
Thermomixer (compact)	Eppendorf
Vortex Genie 2™	Bachofer
Water bath (thermomix 1420)	B. Braun
Western blot apparatus	BioRad

2.1.2 Chemicals and consumables

Unless otherwise stated, all common chemicals are purchased in analytical grade from Merck.

Description	Supplier
1.5 ml and 2 ml micro centrifuge tubes	Eppendorf
15 ml and 50ml tubes	Sarstedt
250 ml Centrifuge tubes	Corning
Agarose SeaKem® ME	Biozym
Ampicillin	Roth
Bacto Agar	BD
Bacto Tryptone	BD
Barrier food wrap	Saran
Bradford Reagent	BioRad
BSA 98%	Sigma
BSA purified	NEB
Cellculture flasks	Greiner
Concentration tubes	Microsep 30K Omega
Coomassie G250	Serva
Cryovials	Roth
dCTP, dGTP, bio dATP, bio dUTP	Invitrogen
Dialysis membrane	Spectra/Por, Roth
DMSO	Sigma
dNTP mix	NEB

Materials and Methods

DTT	Roth
Dynabeads M280-Straptavidin	Dynal
EDTA	Sigma
EGTA	Sigma
Ethidium bromide	Sigma
FACS tubes	BD
FCS dialyzed	Sigma
Filter paper Whatman 3MM	Whatman
Filter tips	Roth
Filter unit	Nalgene, 0.2 µm filter holes
Glass pipettes 5 ml and 10 ml	Hirschmann®
Glassware	Schott
Glycogen	Roche
HEPES	Roth
Hiload 16/60 Superdex 200 gel filtration column	GE Healthcare
IPTG	Roche
Kilobasebinder	Dynal
Laboratory film	Parafilm®
NP40	Sigma
Orange G	Sigma
Pasteur pipettes	Brand
PCR-reaction tubes 0.2 ml	Biozym
Penicillin/ Streptomycin	Sigma
Petridishes and tissue culture plates	Greiner, Sarstedt
Pipette tips	Gilson, Brand
PMSF	Sigma
Propidium iodide	Sigma
Protein gel cassettes (disposable)	Invitrogen
Quick spin columns (Sephadex 50)	Roche
Random primer	Promega
Rotiphorese Acrylamid-Bisacrylamidmix	Roth
S-Adenosyl (methyl ³ H)-L-methionine	Amersham Biosciences
SAH	Sigma
SDS	Serva
Sodium butyrate	Sigma
SP-Sepharose column (5ml)	GE Healthcare

β-Mercaptoethanol	Sigma
Syringes and accessories	Roth
TEMED	Roth
Thymidine	Sigma
Tris	Invitrogen
Triton X-100	Sigma
Trypsin/EDTA (TC)	PAA
TSA	Sigma
Tween 20	Sigma
Yeast extract	Difco

2.1.3 Kits and enzymes

Description	Supplier
Klenow	Roche
Maxi- and Midiprep kit	Qiagen
M-MuLV RT + buffer	Fermentas
MNase	Sigma
Proteinase K	Genaxxon
Restriction endocucleases	NEB
RNase A	Roche
RNeasy kit	Qiagen
SILAC kit	Invitrogen
Taq polymerase	NEB

2.1.4 Plasmids

pET3cH2A, pET3cH2B, pET3cH3 and pET3cH4 according to (Morales et al. 2004).

pAI61 according to (Eskeland et al. 2007).

2.1.5 Media

2.1.5.1 Media for *E. coli*

Luria-Bertani (LB) medium

1.0% (w/v) Bacto-Tryptone

1.0% (w/v) NaCl

0.5% (w/v) Bacto-Yeast extract

→ Adjust the pH to 7.0 with 10 M NaOH

The medium was autoclaved for 20 min at 120°C and after cooling down to 60°C the appropriate antibiotics was added. For preparing plates the LB medium was mixed with 1.5% agar.

SOB medium

2% (w/v) Bacto-Tryptone

10 mM NaCl

0.5% (w/v) Bacto-Yeast extract

2.5 mM KCl

10 mM MgCl₂*

→ Adjust the pH to 7.0 with 10 M NaOH

* add before use

The medium was sterilized in an autoclave for 20 min at 120°C.

2.1.5.2 Media for HeLa cells

a) Growth medium

DMEM Glutamax medium (PAA) was supplemented with 50 U/mL Penicillin, 50 µg/mL Streptomycin and 10% heat inactivated FCS. Heat inactivation was performed for 20 min in a waterbath at 56 °C.

b) SILAC medium

Preparation of SILAC medium was performed according to Invitrogen's instructions. 1 l dialyzed DMEM was supplemented with 100 mg L-lysine and 100 mg either unlabeled L-arginine (R⁰ SILAC) or isotopically labeled L-¹²C₆ ¹⁵N₄-arginine/ L-¹³C₆ ¹⁵N₄-arginine (R^{4/10} medium). Prepared

medium was filtered and 10% of dialyzed, heat inactivated FCS, 50 U/mL Penicillin and 50 µg/mL Streptomycin was added. The medium was aliquoted and stored at 4 °C.

2.1.6 Antibiotics

Name	Concentration of the stock solution	Working concentration
Ampicillin	100 mg/ml (1000x) in H ₂ O	100 µg/ml
Chloramphenicol	34 mg/ml (1360x) in Ethanol	25 µg/ml
Kanamycin	10 mg/ml (1000x) in H ₂ O	10 µg/ml
Tetracyclin	5 mg/ml (500x) in Ethanol	10 µg/ml

2.1.7 Antibodies

2.1.7.1 Primary antibodies

Name	Supplier	Dilution
αdl(3)MBT	E. Kremmer	1:1000
αH4K20me ₁	Abcam	1:1000
αRpd3	R. Steward	1:1000

2.1.7.2 Secondary antibodies

Name	Supplier	Dilution
Goat-arabbit	Licor (680nm)	1:5000
Goat-mouse	Licor (680nm)	1:5000

2.1.8 E. coli strains

Strain	Genotype	Supplier
DH5α	F ⁻ Φ80 <i>dlacZ</i> ΔM15 Δ(<i>lacZYA-argF</i>) _{U169} <i>recA1 endA1 hsdR17</i> (<i>r_k⁻</i> , <i>m_k⁺</i>) <i>phoA supE44 λ⁻ thi-1 gyrA96 relA1</i> (Hanahan 1983)	Genentech
BL21 (DE3) pLysS	B F ⁻ <i>dcm ompT hsdS</i> (<i>r_B⁻</i> , <i>m_B⁻</i>) <i>gal λ</i> (DE3) (studier and moffatt 1986)	Stratagene
XL1 Blue	<i>recA1 endA1 gyrA96 thi-1 hsdR17 supE44 relA1 lac</i> [F ['] <i>proAB lacI^qZ</i> ΔM15 Tn 10 (Tet ^r)]	Stratagene

2.1.9 DNA and protein markers

Name	Supplier
1 kb DNA marker	NEB
123 bp ladder	Invitrogen
DNA 100 bp ladder	NEB
peqGOLD Protein Marker IV, II	Peqlab
smart ladder	Eurogentec

2.1.10 Protease inhibitors

Name	Supplier
Aprotinin	Gennaxon
Leupeptin	Gennaxon
Pepstatin (in EtOH)	Gennaxon
PMSF	Sigma
β -glycerolphosphate	Sigma

2.1.11 Mass spectrometry material

Description	Supplier
0.2 ml tubes, strips of 8 (mass spec)	Nunc
0.5 ml tubes	Eppendorf LoBind
Acetonitrile	Sigma
Ammoniumbicarbonate	Sigma
AspN	Roche
Formic acid	Sigma
H ₂ O HPLC grade	Merck
Hydrophobic plate	Applied Biosystems
MALDI-TOF	Voyager-DE TM, Applied Biosystems
Propionic acid	Merck
QSTAR	Applied Biosystems
Speed vac	Eppendorf
TFA	Merck
ZipTips	Millipore μ C18
α -cyano-4-hydroxycinnamic acid	Sigma

2.1.12 Bioinformatic tool

Device	Software
FACS	FACSDIVA, FlowJo
MALDI-TOF	Voyager, Data explorer, Manuelito
Orbitrap	Bioworks, Xcalibur, Peaks, Mascot, Maxquant
QSTAR	Analyst

2.2 Methods

2.2.1 Microbiology methods

2.2.1.1 Preparation of competent cells

E. coli bacteria from glycerol stocks were streaked out on LB plates and incubated o/n at 37°C. From this plate one colony was used to grow a 3 ml LB preculture o/n at 37°C. The next day 1 ml of the preculture was transferred into 500 ml LB medium and grown to an OD at 600 nm of 0.6. The culture was cooled on ice for 10 min and then centrifuged (15 min, 4000 rpm, 4°C, Heraeus Cryofuge 6000i). After centrifugation the supernatant was discarded and the cell pellet was carefully resuspended in 200 ml ice cold TBPI. Cells were incubated on ice for 5 min and afterwards the centrifugation step was repeated. The pelleted cells were then gently resuspended in 20 ml ice cold TBPII. Aliquots of 200 µl were snap frozen in liquid nitrogen, and stored at -80°C. An efficiency of 10⁷ cfu/µg was achieved using this preparation.

TBPI

30 mM KAcetate
 100 mM KCl
 10 mM CaCl₂
 50 mM MnCl₂
 15% (v/v) glycerol
 → filter 0.2 µm, keep at 4°C

TBPII

10 mM PIPES pH 6.5
 75 mM CaCl₂
 10 mM KCl
 15% (v/v) glycerol
 → filter 0.2 µm, keep at 4°C

2.2.1.2 Plasmid transformation

Plasmid DNA was added to 200 µl chemically competent cells that had been thawed on ice. The cell suspension was left on ice for 45 min, and then heat-shocked for 45 sec at 42°C and immediately chilled on ice for 5 min. 500 µl of SOB medium was added and the cells were incubated for 45 min at 37°C in a shaking incubator at 700 rpm (Thermomixer). Transformed cells were plated on LB agar plates supplemented with the appropriate antibiotics and incubated for 12 to 16 h at 37°C.

2.2.1.3 Isolation of Plasmid DNA from *E. coli*

a) Miniprep

Small amounts of plasmid DNA were extracted from *E. coli* by alkaline lysis (Birnboim et al. 1979). LB medium (3 ml) supplemented with the appropriate antibiotics was inoculated with colonies picked from an agar plate of freshly transformed bacteria. The cultures were grown o/n at 37°C shaking at 200 rpm (Infors Multitron). Half of each o/n culture was transferred in a 1.5 ml reaction tube and centrifuged (10 min, 9000 rpm, RT, Eppendorf 5417C). The pelleted bacteria were resuspended in 250 µl P1 to destabilize the bacterial membrane. Afterwards the bacterial suspension is lysed by adding 250 µl P2. The tubes are immediately inverted 5 times to mix the components and left at RT for 5 min. The lysis was stopped by adding 350 µl P3 followed by inverting again for 5 times and then incubating on ice for 10 min. Precipitated proteins and the chromosomal DNA was sedimented by centrifugation (10 min, 13000 rpm, RT, Eppendorf 5417C). The supernatant corresponding to the plasmid DNA was transferred in a new 1.5 ml tube. 600 µl of isopropanol was added and the sample incubated on ice for 30 min and then centrifuged (20 min, 13000 rpm, 4°C, Eppendorf 5417C). The pelleted plasmid DNA was washed with 70% ethanol and recentrifuged (5 min, 13000 rpm, 4°C, Eppendorf 5417C) in case the DNA pellet becomes dislodged during the washing step. The supernatant was discarded and the pellet air dried. The dried pellet was taken up in 25 µl TE.

<u>P1</u>	<u>P2</u>	<u>P3</u>
50 mM Tris pH 8.0	200 mM NaOH	3 M KAcetate pH 5.1
10 mM EDTA	1% (w/v) SDS	
100 µg/ml RNase A		

b) Midiprep

To obtain larger amounts of plasmid DNA, 200 ml of LB medium including the appropriate antibiotics was inoculated with a single colony of an agar plate holding freshly transformed bacteria. The culture was incubated o/n at 37°C at 180 rpm (Infors Multitron). in a shaker. The bacteria was transferred into 250 ml Corning tubes and pelleted by centrifugation (10 min, 4000 rpm, RT, Heraeus Cryofuge 6000i). The further isolation of the plasmid DNA was done with Qiagen Plasmid Midiprep Kit according to the manufacturer`s instructions.

2.2.2 Nucleic acid methods

2.2.2.1 Storage of DNA

DNA was stored in TE buffer at -20°C

TE buffer

10 mM Tris pH 8.0

1 mM EDTA

2.2.2.2 DNA quantification

DNA concentration was quantified by measuring the absorbance at the wavelength of 260 nm in a UV spectrophotometer. One absorbance unit at 260 nm corresponds to a concentration of 50 µg DNA/ml. The purity of the DNA can be judged by the ratio $A(260\text{ nm})/A(280\text{ nm})$ and should lie between 1.8 and 2.0. Lower values indicate protein contamination (Sambrook et al. 2000).

2.2.2.3 Agarose gel electrophoresis

Agarose gel electrophoresis was performed to separate linear DNA fragments by size (Sambrook et al. 2000). The smaller the fragments for analysis the higher the percentage of agarose solution was used ranging from 0.8 to 2% (w/v) in 1x TBE buffer. The agarose solutions were brought to boil in a microwave and were allowed to cool down to approximately 50°C. Then ethidium bromide was added to a final concentration of 1 µg/ml prior to pouring the solution into the gel chambers. After an adequate solidification of the gel, running buffer (1x TBE) was added. Before loading the samples onto the gel they were mixed with 5x loading dye. The electrophoresis was performed with 10 V/cm gel length and smart ladder, 1 kb ladder or 123 bp ladder served as a size standard. The DNA was visualized by UV light (254-366 nm) since the complex of DNA and ethidium bromide is triggered to fluoresce. Gels were documented with the help of a gel documentary system.

1x TBE

90 mM Tris

90 mM Boric acid

2 mM EDTA

5x loading dye

50% (v/v) Glycerol

5 mM EDTA

0.3% (w/v) Orange G

2.2.2.4 Restriction digest

Buffer conditions and temperatures for incubation were used as suggested by the manufacturer. Usually 1 U of the enzyme was applied for 1 µg DNA and incubated for 2–3 h. The reaction products were analyzed by agarose gel electrophoresis.

2.2.2.5 Polymerase Chain Reaction (PCR)

PCR was used to amplify DNA fragments and conducted according to Sambrook et al. For a standard reaction 10 ng of template DNA, 200 pmol of each primer, 200 µM dNTPs, 1 Unit of the appropriate DNA polymerase and the adequate 10x buffer for the polymerase were used (Sambrook et al. 2000). The final volume of 25 µl was added up with ddH₂O. The amplification of the DNA fragments was controlled by agarose gel electrophoresis.

Reaction	Temperature [°C]	Time	
Initial Denaturation	94	2 min	1x
Denaturation	94	1 min	
Annealing	50	30 sec	} 25x
Elongation	72	1 min/kb	
Final Elongation	72	10 min	1x

2.2.2.6 RT PCR

RNA was extracted from snap-frozen HeLa cell pellets using RNeasy kit according to the manufacturer's manual and dissolved in RNase-free water. Total RNA concentration was quantified using a spectrophotometer. Reverse transcription was primed with 250 µg of random primers with 1 µg of total RNA per sample at 70°C for 5 min. The samples were then incubated with 20 U MuLV in 20 µl of buffer containing 1000 µM dNTP and manufacturer's RT buffer for 10 min at 25 °C, then heated up to 37 C for 1 h, 70 C for 10 min, chilled on ice and frozen at -20°C. PCR reaction was conducted with the following primers H3.2 (5'-GCTACCAGAAGTCCACGGAG and 5'-GATGTCCTTGGGCATAATGG) and 18S (5'-TTGTTGGTTTTCGGAAGTACTGAGG and 5'-CATCGTTTATGGTCGGAAGTACTAG).

2.2.3 Tissue culture methods

2.2.3.1 Cultivation of HeLa cells

HeLa cells (classical adherent cervix carcinoma cells) were kept in DMEM medium in 15 cm dishes in a 37°C incubator with a humidified atmosphere of 5% CO₂. Cells were split in a sterile hood every 2 to 3 days in a ratio 1:3 or 1:4 then moved to a new dish and provided with fresh medium in a total volume of 20 ml in order to keep cell density to 2-8x 10⁵ cells/ml. Cells were counted using the CasyCounter according to the manufacturer's manual. Every two month a new frozen cell stock was thawn.

2.2.3.2 Harvesting of HeLa cells

Growth medium was discarded using a vacuum pump and harvesting solution was added on top of the adherent HeLa cells. After 5 min of incubation at 37°C the trypsinized cells were detached by pipetting the harvesting solution up and down. The cell suspension was transferred in a 15 ml tube, centrifuged (3 min, 1200 rpm, RT, Thermo Multifuge) and washed with sterile PBS.

1x Harvesting solution

0.1% (w/v) trypsin

0.04% (w/v) EDTA

in sterile PBS

1x PBS

136 mM NaCl

2.7 mM KCl

4 mM Na₂HPO₄

1.7 mM KH₂PO₄

→ adjust pH to 7.4

2.2.3.3 Storage of HeLa cells

To 5x 10⁶ cells in 1ml DMEM medium, DMSO was added dropwise to a final concentration of 7.5%. The cell suspension was transferred to 1.5 ml freezing vials and gently cooled down to -80°C using a freezing box encased with an isopropanol jacket. The frozen cells were stored in liquid nitrogen (-196°C). To utilize cells in culture, they were quickly thawed in a 37°C waterbath, washed twice with medium (3 min, 1200 rpm, RT, Thermo Multifuge) and seeded in a 15 cm dish for further culturing.

2.2.3.4 Synchronization of HeLa cells

For G1/S phase synchronization a double thymidine block was used. Therefore 2x 10⁵ HeLa cells/ml were seeded in 6 well plates and cultured for 24 h at 37°C in R⁰ SILAC medium. Thymidine was added to a final concentration of 2 mM and incubation was maintained for 16 h. The block was released by exchanging the thymidine-containing medium with R⁰ culture medium. Cells were grown for 9 h before adding again thymidine of 2 mM final concentration for further 16h to synchronize the HeLa cells at the G1/S border. The arrest was finally released by refeeding cells

with thymidine-free R⁴SILAC medium to allow cell cycle progression. Whenever indicated 10 mM NaBu was added directly into the medium and cells were washed twice with PBS before transferring cells into medium without NaBu. Cells were maintained in a 37°C incubator with a humidified atmosphere of 5% CO₂.

2.2.3.5 SILAC labeling (Stable isotope labeling with amino acids in cell culture)

We used three different SILAC DMEM media; R⁰ SILAC (L-arginine), R⁴ (L-¹²C₆ ¹⁵N₄-arginine) and R¹⁰ (L-¹³C₆ ¹⁵N₄-arginine). HeLa cells were synchronized at the G1/S border in R⁰ SILAC medium and released into cell cycle in R⁴ SILAC medium in order to label all newly synthesized histones (Figure 5). For all pulse chase experiments (pSILAC) we fed synchronized cells with R⁴ SILAC medium for 6 h and chased with R¹⁰ SILAC medium. All materials for SILAC labeling were purchased from Invitrogen and prepared according to the manufacturer's instructions.

2.2.3.6 Flow cytometric analysis of the cell cycle

For FACS analysis, cells (1×10^6) were harvested, washed twice in PBS followed by fixation in 70% ethanol at -20°C for a minimum of 1h. Fixed cells were washed in PBS and incubated with 100 µg/ml RNase A in PBS for 30 min at 37°C. Afterwards, propidium iodide to a final concentration of 50 µg/ml was added and the cells were incubated at 37°C for 30 minutes. Samples were stored at 4°C in the dark until analysis on BD Biosciences FACSCanto. A minimum of 10,000 cells was counted and the raw data was analyzed and histograms plotted using FlowJo software.

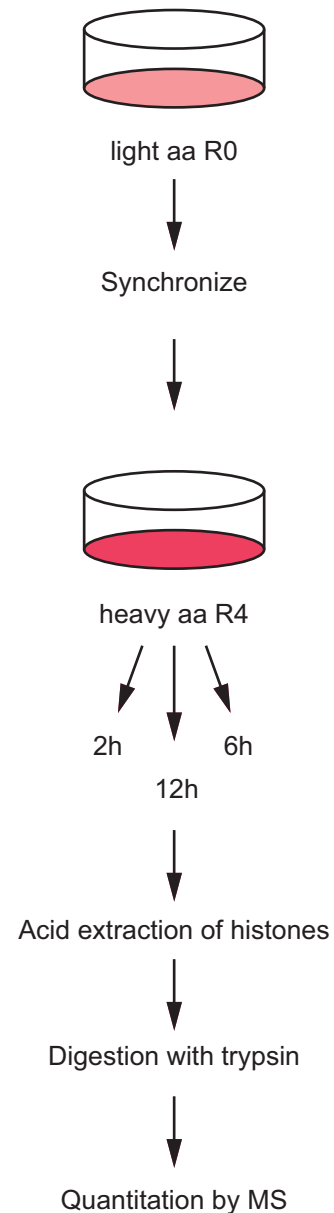


Figure 5: Pulsed SILAC. Schematic view of SILAC labeling of HeLa cells and further preparation procedure.

2.2.4 Protein methods

2.2.4.1 Protein quantification

Protein concentrations were determined using the BioRad Protein Assay according to the manufacture`s instruction. BSA (Bovine serum albumin) was used as a protein standard (Bradford 1976).

2.2.4.2 SDS-Polyacrylamid-Gelelectrophoresis (SDS-PAGE)

Denaturing SDS-Polyacrylamid-Gels were used to separate protein mixtures. This method is based on a discontinuous electrophoresis. One gel consists of a resolving gel ranging from 8–15% and a 5% stacking gel that was poured one after another in disposable gel cassettes. Per gel 6 ml separation gel and 2 ml stacking gel was used. After complete polymerization of the gel it was placed into a chamber filled with SDS running buffer. The protein samples were mixed with Laemmli buffer and denatured for 5 min at 95°C before applying on the gel. Protein markers were used to determine the molecular weight of the samples. Proteins were separated at 200 V for 1 h. Afterwards the gel was further processed either by Coomassie staining or Western blotting.

Separation gel (18%)

0.9 ml H₂O

3.6 ml acrylamid mix (30/0.8)

1.5 ml 1.5 M Tris PH8.8

30 µl 20% (w/v) SDS

30 µl 20% (w/v)APS

3 µl TEMED

Stacking gel (5%)

1.4 ml H₂O

340 µl acrylamid mix (30/0.8)

250 µl 1 M Tris pH 6.8

10 µl 20% (w/v)SDS

10 µl 20% (w/v) APS

2 µl TEMED

SDS Running buffer

25 mM Tris
190 mM glycine
0.1% (w/v) SDS

4 x Laemmli buffer

200 mM Tris pH 6.8
8% (w/v) SDS
40% (v/v) glycerol
0.2% (w/v) bromphenol blue
4.2% (v/v) β -Mercaptoethanol

2.2.4.3 Coomassie staining

The separation gel was shaken for 30 min in fixing/ staining solution on a shaker at RT. To destain the gel was placed into destain solution with a tissue placed aside to bind the excess dye. After achieving the desired level of colouration the gel is documented and dried on a 3 MM Whatmann for 2 h at 80°C in a gel drier.

For mass spectrometry analysis gels were documented and proteins were cut out with a clean scalpel and stored in 0.2 ml tubes with 100 μ l of ddH₂O at 4°C until further analysis.

fixing/ staining solution

50% (v/v) methanol
10% (v/v) acetic acid
0.25% (w/v) Coomassie Brilliant Blue (G-250)

destaining solution

10% (v/v) acetic acid

2.2.4.4 Western blotting

SDS PAGE of protein samples was performed as described above. The gel was removed from the electrophoresis apparatus and soaked for 2 min in 1 x Western blot buffer as well as two 3MM Whatmann papers and two sponges. A nitrocellulose membrane (8 cm x 6.5 cm) was appropriately labeled and pre-wet in Western blot buffer. The blotting sandwich was assembled in the following order: grey bottom support (facing the negative electrode), 1 sponge, 1 piece of 3MM paper, equilibrated gel, membrane, 1 piece of 3MM paper, 1 sponge, clear top support (facing the positive electrode). The assembly was transferred to the blotting apparatus, which was filled with 1 x

Western blot buffer and an ice block for cooling. The proteins were transferred to the membrane by electrophoresis at 400 mA for 1.5 h at 4°C. After transfer the gel was Coomassie stained to determine the blotting efficiency. The membrane was blocked in 5% (w/v) milk in 1x PBS Tween for 1 h at RT on a shaker. Subsequently it was incubated with the primary antibody in 5% (w/v) milk in PBS Tween for 1 h at RT or o/n at 4°C on a shaker. After three washing steps (10 min each) in PBS Tween the membrane was incubated with the fluorescently labeled secondary antibody again for 1 h at RT while shaking. The blot was washed again as above and detected protein was documented and quantifies with an Odyssey system from Li-Cor (Towbin et al. 1979).

1x PBS

136 mM NaCl

2.7 mM KCl

4 mM Na₂HPO₄

1.7 mM KH₂PO₄

→ adjust pH to 7.4 with HCl

1x PBS Tween

1x PBS

0.1% (v/v) Tween 20

Western blot buffer

25 mM Tris

192 mM glycine

0.02% (w/v) SDS

15% (v/v) methanol

2.2.4.5 Histone extraction

HeLa cell pellets were redissolved in 0.4 N HCl in a total volume of 0.5 ml per 1 x 10⁶ cells and rotated for a minimum of 1 h at 4°C. After centrifugation at 13000 rpm (Eppendorf 5417C) for 30 min the supernatant was dialyzed at 4°C against 100 mM ice-cold acetic acid for 3 times 1 h using 6000-8000 MWCO. The sample was concentrated using a speed vac and redissolved in SDS-loading buffer and applied on a SDS-PAGE gel for further analysis.

2.2.4.6 MALDI-TOF analysis

Histones were separated by SDS-PAGE 18%. G250 Coomassie blue stained bands were excised and destained with 50 mM ammonium bicarbonate in 50% (v/v) ACN (Acetonitrile) for 30 min at 37°C. After washing the gel pieces with HPLC grade water, histones were chemically modified by treating with 2 µl propionic anhydride (100%) and 48 µl of ammonium bicarbonate (1M) at 37°C. After 1 h the modified histones were washed with HPLC grade water and digestions were carried out at 37°C overnight with 200 ng sequencing grade trypsin according to the manufacturer's manual. Digestion products were collected and the gel pieces were acid extracted in addition with 25 mM ammonium bicarbonate and afterwards with 5% (v/v) formic acid. The pooled digestions were concentrated using a speed vac and redissolved in 0.1% (v/v) TFA (Trifluor acetic acid). Afterwards the samples were desalted with ZipTip µC18 according to the manufacturer's instructions and directly eluted onto the target plate with a saturated solution of α -cinnamic acid in 0.3 (v/v) TFA and 50% (v/v) ACN. The target plate was loaded into a Voyager DE STR spectrometer and analyzed. Peptide mass fingerprint was analyzed in positive reflector mode (Bonaldi et al. 2004; Villar-Garea et al. 2008).

Settings for peptide mass fingerprint (pmf)

Accelerating voltage	20000 V
Grid voltage	66%
Mass range	500 -2000 Da
Laser intensity	800-1200

2.2.4.7 Quantification of MALDI signals.

To determine all modifications occurring on histones the Manuelito software was used. Spectra were processed and analyzed with the Data Explorer software. For quantification the integrated area of the peaks was used with a signal to noise ratio of 2. The sum of the area from all peaks (monoisotopic) derived from a single peptide was defined as 100 percent. Charts were drawn in Excel.

2.2.4.8 Tandem MS

Cut gel pieces were destained with 50 mM ammonium bicarbonate in 50% (v/v) ACN for 30 min at 37°C. After washing the gel pieces with HPLC grade water, histones were chemically modified by treating with 2 µl propionic anhydride (100%) and 48 µl of ammonium bicarbonate (1M) at 37°C. After 1 h the modified histones were washed with HPLC grade water and digestions were carried out at 37°C overnight with 200 ng sequencing grade trypsin according to the manufacturer's manual. Digested peptides were collected and the gel pieces were acid extracted in addition with 25 mM ammonium bicarbonate and afterwards with 5% (v/v) formic acid. Digestions were pooled and concentrated using a speed vac and next redissolved in 0.1% (v/v) TFA. Afterwards the samples were desalted with Ziptip µC18 according to the manufacturer's instructions and loaded into needle for nanospray. For protein identification samples were directly used for nanospray-ESI-MS/MS, collision-induced spectra were recorded on a QSTAR XL mass spectrometer with manually adjusted collision energies. The resulting spectra were interpreted manually via Manuelito and Analyst.

2.2.4.9 AspN digest

Cut out gel pieces were washed with HPLC grade water and destained with 50 mM ammonium bicarbonate in 50% (v/v) ACN for 30 min at 37°C. After 1 h the modified histones were washed with HPLC grade water and digestions were carried out at 37°C overnight with 40 ng sequencing grade AspN according to the manufacturer's manual. Digestion products were collected and the gel pieces were acid extracted in addition with 25 mM ammonium bicarbonate and afterwards with 5% (v/v) formic acid. The pooled digestions were concentrated using a speed vac and redissolved in 0.1% (v/v) TFA. Afterwards the samples were desalted with ZipTip µC18 according to the manufacturer's instructions and directly eluted onto the target plate with a saturated solution of α -cinnamic acid in 0.3 (v/v) TFA and 50% (v/v) ACN. The target plate was loaded into a Voyager DE STR spectrometer and analyzed. Peptide mass fingerprint was analyzed in positive reflector mode as described before.

2.2.5 Chromatin methods

2.2.5.1 Preparation of chromatin assembly extract from *Drosophila* embryos

From twelve cages *Drosophila* embryos 0 to 90 min after egg laying were collected in a fine sieve. The collection was rinsed with tap water and transferred in embryo wash buffer on ice to stop further development. After four successive collections resulting in approximately 50 ml packed embryos, the pooled harvest was dechorionated. The ice cold wash buffer was exchanged with wash buffer at RT. The volume was adjusted to 200 ml and 60 ml of 13% (v/v) hypochlorite was added. The embryos were stirred vigorously for 3 min, immediately transferred into the collection sieve, and rinsed with tap water for 5 min. The embryos were settled in 200 ml of wash buffer for about 5 min and then the supernatant including the chorions was discarded. Repeated settlings were conducted: one in 0.7% (w/v) NaCl and one in extract buffer at 4°C. Temperature of 4°C was kept for all further processing. The embryo suspension was transferred in a 60-ml glass homogenizer on ice for about 15 min and the volume of settled embryos was determined. The supernatant except 2 ml was discarded and the embryos were subjected to homogenization by one stroke at 3000 rpm and ten strokes at 1500 rpm with a drilling pestle. To the homogenated embryos additional 3.5 mM MgCl₂ was added to increase the total MgCl₂ concentration to 5 mM. The homogenate was subjected to centrifugation for 10 min at 10000 rpm in a SS34 rotor (Sorvall RC6PLUS) to separated nuclei away. The supernatant was further processed by centrifugation for 2 h at 45,000 rpm (Beckman ultracentrifuge LE-80K) in an SW 56 rotor and collected with a syringe, avoiding the top lipid layer. Aliquots of 800 µl were transferred in 1.5 ml tubes and flash frozen in liquid nitrogen and stored at -80°C. Protein concentrations were determined as described above (Becker et al. 1992).

Embryo wash

0.7% (w/v) NaCl

0.05% (v/v) Triton X-100

Extract buffer

10 mM HEPES pH 7.6

10 mM KCl

1.5 mM MgCl₂

0.5 mM EGTA

10% (v/v) glycerol

10 mM β -glycerophosphate*

1 mM DTT*

0.2 mM PMSF*

→ * add fresh before use

2.2.5.2 Preparation of biotinylated DNA

First 500 μ g of the plasmid PAI61 was digested with mix 1: 14 μ l of Sac I (20,000 U/ml) in a total volume of 750 μ l containing 75 μ l BSA (1 μ g/ μ l), 75 μ l 10x NEB buffer and x μ l ddH₂O. Digestion was carried out for 3 h at 37°C. Every hour the tube was vortexed. 1 μ l of the digestion mix was analyzed on an agarose gel to confirm proper linearization. Then a second digestion was carried out by adding 10 μ l Xba I (20,000 U/ml) to the digestion mix 1 as well as additional 5 μ l of BSA (1 μ g/ μ l), 5 μ l 10x NEB buffer 2, 7.5 μ l NaCl (5 M) and 22.5 μ l ddH₂O. The mixture was incubated for 3 h at 37°C. The DNA was precipitated by adding 85 μ l of sodiumacetate pH 5.3 (3 M) and 700 μ l isopropanol. The sample was mixed and incubated on ice for 30 min. The 1.5 ml tube was centrifuged for 30 min at 13000 rpm at 4°C (Eppendorf 5417C). The supernatant was discarded and the pellet washed with 70% ethanol, dried and redissolved in 30 μ l 10x NEB buffer 2 and x μ l ddH₂O. For the biotinylation reaction 80 mM dCTP, 80 mM dGTP, 3 mM dUTP biotinylated, 3 mM dATP biotinylated and 10 U Klenow was added. The final volume of the reaction was 300 μ l. The sample was incubated for 2 h at 37°C before the Klenow enzyme was heat inactivated for 20 min at 70°C. To remove all nucleotides that have not been incorporated 3 sepharose G50 columns were used. The columns were centrifuged twice (1 min, 1000 rpm, 4°C, Sigma 3-18) and the flow through discarded. To each column 100 μ l of the sample was applied and centrifuged for 2 min at 2000 rpm (Sigma 3-18) at 4°C. The flow through was collected and the DNA concentration determined.

2.2.5.3 Chromatin assembly on immobilized DNA

Per reaction 2 µg DNA (PAI61) was immobilized to 0.6 µg paramagnetic streptavidin coated beads. Beads were washed with 2 M Dynawash and to the packed beads the DNA was added as well as 1x volume of TE and 2x volume of kilobasebinder. Samples were incubated for 1 h at RT on a metal-free rotating wheel and then washed three times with 1 M Dynawash and three times with TE. After the extensive washing, beads were blocked with BSA (1.5 µg/ µl) in EX100 for 30 min at RT on a rotating wheel. Then beads were washed with EX-NP40. At time point zero immobilized DNA on beads was mixed with 160 µl assembly extract (DREX) together with an ATP regenerating system (McNap) and the total volume increased to 240 µl with EX100. The reaction was conducted by rotating for 1-6 h at 26°C. The assembly reaction was stopped and either subjected to micrococcal nuclease digestion or mass spectrometry (Sandaltzopoulos et al. 1994).

1 M Dynawash

10 mM Tris HCl pH 8

1 mM EDTA

1 M NaCl

2 M Dynawash

10 mM Tris HCl pH 8

1 mM EDTA

2 M NaCl

EX100

10 mM HEPES pH 7.6

100 mM NaCl

1.5 mM MgCl₂

0.5 mM EGTA

10% (v/v) glycerol

1 mM DTT*

0.2 mM PMSF*

→ * add fresh before use

EX-NP40

10 mM HEPES pH 7.6

1.5 mM MgCl₂

0.5 mM EGTA

10% (v/v) glycerol

0.05% (v/v) NP-40

McNap

3mM ATP

30 mM creatine phosphate

10 µg creatine kinase / ml

3 mM MgCl₂

1 mM DTT

a) **Micrococcal nuclease digestion**

Immobilized chromatin was washed once with EX100 and twice with EX300. Beads were resuspended in 240 µl EX100/MgCl₂ (5 mM). The digestion was started by adding 360 µl MNase mix. After 30, 60 sec and 3 min the reaction was stopped by taking out 200 µl from the mixture and immediately transferring into a new tube containing 50 µl stop solution. After adding 20 µg of RNase A the samples were incubated for 30 min at 37°C. Then 50 µg of Proteinase K and SDS (final concentration 0.015%) were added and the samples were incubated for at 37°C. After 3 h the DNA solution was subjected to precipitation by adding 20 µg glycogen, adjusting the salt concentration with ammonium acetate (2 M final concentration) and adding 0.6 volumes of ice-cold ethanol. After mixing, the solution was incubated for 30 min at -20°C and afterward centrifuged (30 min, 13000 rpm, 4°C, Eppendorf 5417C). The pelleted DNA was washed with 70% ethanol and then air dried. The DNA was redissolved in 1x loading dye and analyzed by gel electrophoresis.

MNase Sigma: 500 U lyophilized vial was resuspended in 850 µl EX50 buffer and aliquoted in 50 µl aliquots: Concentration is 50 U /µl (Boehringer units).

MNase mix

5 mM CaCl₂

2.5 U MNase

in EX100

5x loading dye

50% (v/v) Glycerol

5 mM EDTA

0.3% (w/v) Orange G

b) **Mass spectrometry and Western blot**

The chromatin was subjected to several washes: 1x EX100, 2x EX500/300, 1x EX100 and then

resuspended in 1x Laemmli, boiled for 5 min at 95°C. Proteins are separated on an 18% SDS gel either cut out for mass spectrometry or further analyzed by Western blotting.

EX300

10 mM HEPES pH 7.6

300 mM NaCl

1.5 mM MgCl₂

0.5 mM EGTA

10% (v/v) glycerol

1 mM DTT*

0.2 mM PMSF*

→ * add fresh before use

EX500

10 mM HEPES pH 7.6

500 mM NaCl

1.5 mM MgCl₂

0.5 mM EGTA

10% (v/v) glycerol

1 mM DTT*

0.2 mM PMSF*

→ * add fresh before use

2.2.5.4 Expression and purification of *Drosophila* histones

Every individual core histone was transformed in BL21(DE3)pLys using 1 µg of pET-histone expression plasmid. The transformation mix was directly added to 200 ml LB and incubated for 1 h at 37°C before adding the appropriate concentration of ampicillin and chloramphenicol. After incubating o/n 20 ml of the preculture was transferred to 10x 500 ml LB containing the appropriate antibiotics. The bacterial growth was monitored until OD₅₉₅ reached a value of 0.6. An aliquot of 500 µl was taken for testing the expression and the histone expression as induced by adding IPTG to a final concentration of 1 mM for 2 h. A second aliquot of 500 µl was taken and OD₅₉₅ was determined. The remaining culture was centrifuged (4000 rpm, 20 min, RT, Heraeus Cryofuge 6000i) and the pellet frozen down at -20°C. To test the expression the equal number of cells from samples before and after the induction was loaded on an 18% SDS gel.

In order to prepare inclusion bodies the bacterial pellet was resuspended with 15 ml wash buffer and homogenized by pipetting up and down with a 25 ml plastic pipette. The homogenate was subjected to the French press (3-6 runs at 1000 psi) and afterwards to sonification (5 min, pulse 5 sec on/ 5 sec off, 70% amplitude). The sample was centrifuged in a SS 34 rotor (Sorvall RC6 PLUS) for 20 min at 18000 rpm at 4°C. The pellet was washed with 40 ml triton-wash buffer and again

Materials and Methods

centrifuged as before. Then two more consecutive washes were conducted with 40 ml wash buffer without triton X-100 and the pellet containing the inclusion bodies frozen at -20°C for at least 30 min.

Then the inclusion bodies needed to be unfolded. Therefore 1 ml DMSO and 25 ml unfolding buffer were added to the pellet and homogenized with a 5 ml plastic pipette. For 1 h the mixture is rotated on a wheel at RT to allow unfolding of inclusion bodies and then spun in a SS34 rotor (Sorvall RC6 PLUS) for 20 min, 18000 rpm at 4°C. The supernatant is dialyzed against 3x 1 l of Sau 200 at 4°C (6-8000 MW cut off). The dialyzed fraction was centrifuged (SS34, 10 min, 18000 rpm, 4°C) to remove undissolved material and histones were purified via a SP Sepharose column, washed with 25 ml Sau200 and eluted with a gradient of Sau600. Fractions are analyzed on a 18% SDS gel and pooled according to the purity of the fractions. Histone pools were dialyzed against 3x 1 l of ddH₂O, the concentration was determined ($OD_{276} / \epsilon_{276} * MW$) and 4 mg aliquots were flash frozen and stored in -80°C (Luger et al. 1999).

Wash buffer

50 mM Tris pH 7,5
100 mM NaCl
1 mM EDTA pH 8,0
5mM β-mercapto EtOH*
0.2 mM PMSF*
→ * add fresh before use

Triton wash buffer

as wash buffer
1% (v/v) Triton X-100

Unfolding buffer

7 M guanidium
20 mM Tris pH 7.5
10 mM DTT
→ prepare freshly

SAU 200

7 M Urea
20 mM sodiumacetate pH 5.2
200 mM NaCl
1 mM EDTA pH 8
5 mM β-mercapto EtOH
→ prepare freshly

	MW	ϵ_{276} (cm/M)
H2A	11.960	4050
H2B	13.774	6070
H3	15.273	4040
H4	11.236	5400

2.2.5.5 Octamer reconstitution

Lyophilized recombinant histones were dissolved in unfolding buffer with a final concentration of 2 mg/ml. H3 and H4 were mixed in an equimolar ratio, whereas H2A and H2B were added with an 20% excess. The histone mix was dialyzed 3 times against 1 l of refolding buffer at 4°C. Precipitations were removed by a centrifugation step (SS34, 5000 rpm, 10 min, 4°C). The supernatant was concentrated to approximately 2 ml in concentration tubes (SS34 rotor, 7900 rpm, 30 K cut off, 4°C, approximately 20 min). The concentrated sample was purified over a gel filtration column (Hiload Superdex 200). The column was equilibrated to refolding buffer, the flow rate set to 1 ml/min and 1 ml fractions were collected. The fractions were analyzed on an 18% SDS gel and suitable fractions containing stoichiometric histone octamers were frozen in 50% (v/v) glycerol at -20 °C after determining the octamer concentration ($A_{276} = 0.45$ for 1 mg/ml) (Luger et al. 1999; Morales et al. 2004).

Refolding buffer

2 M NaCl

10 mM Tris pH 7.5

1 mM EDTA

5 mM β -mercapto EtOH*

→ * prepare freshly

2.2.5.6 Chromatin assembly by salt dialysis

A usual assembly reaction contained 500 μ g DNA (PAI61) to which 600 μ g of recombinant octamers were added as well as 60 μ g BSA, 2 M NaCl, 10 mM Tris pH 8 filled up with ddH₂O to a total volume

of 500 μ l. The mixture was transferred in a dialyzing membrane with a cut off of MW 6000-8000. The filled membrane was placed in 200 ml DB2000 (high salt) to where continuously 1.8 l DB50 (low salt) was pumped for approximately 12 h at a speed of 2.5 ml/min.

To check the correct assembly of chromatin an MNase digest was performed. To 20 μ l salt assembled nucleosomes 17 μ l MNase mix was added and mixed well. The digestion was stopped after 20, 60 and 120 sec by transferring 12 μ l to a tube ready prepared with 5 μ l stop solution. To each tube 20 μ g RNase A was added and incubated for 30 min at 37°C. Then 50 μ g Proteinase K was added for 1 h at 37°C. For precipitation 20 μ g glycogen was added, salt concentration adjusted with ammonium acetate (2 M final concentration) and 0.6 volumes of ice-cold ethanol was added. After mixing, the solution was incubated for 30 min at -20°C and afterward centrifuged (30 min, 13000 rpm, 4°C, Eppendorf 5417C). The pelleted DNA was washed with 70% ethanol and then air dried. The DNA was redissolved in 1x Orange G and analyzed by gel electrophoresis.

DB50

50 mM NaCl

10 mM Tris pH 8

1 mM EDTA

1mM β -mercapto EtOH

0.01% (v/v) NP40

DB2000

2M NaCl

10 mM Tris pH 8

1 mM EDTA

1mM β -mercapto EtOH

0.01% (v/v) NP40

Stop solution

4 % SDS

100 mM EDTA

2.2.5.7 HMT assay

10 μ l chromatin from 880 ng DNA that was salt assembled to chromatin, was used as a substrate. 0.5 μ g/ μ l BSA, 50 mM DTT, HMTase buffer and 50 ng of enzyme (PrSet7) was added and filled up with water to a total volume of 20 μ l per reaction. Additionally 1 μ Ci S-Adenosyl (methyl 3 H)-L-methionine is added and the samples are incubated for 1h at 30°C. The total reaction was spotted on a p81 filter, dried and washed 3 times 5 min in 1x HMTase buffer. The filter papers were dried

and the amount of incorporated ^3H -methyl groups was measured by a scintillation counter in cpm. When using SAH the indicated concentration was added to the HMT assay.

1x HMTase buffer

12.5 mM Tris pH 7.8

2.5 mM MgCl_2

50 mM NaCl

3. RESULTS AND DISCUSSION

3.1 Results

Major progress has been made towards identifying key player imposing epigenetic marks and the processes involved in epigenetic inheritance meaning stably transmitting epigenetic information and in epigenetic reversibility allowing the cell to adjust to its needs. Key signatures are posttranslational histone modifications that are thought to create specific chromatin structures. These structures possess various functions in DNA packaging, gene expression or gene silencing and they have to cope with the challenge to be reversible and just as well stable inheritable. This dual function is regulated by histone modifications. Histone marks act alone or in a combinatorial manner and are set and removed coordinately. Notably, site specific marks correlate well with particular biological functions including transcriptional elongation or chromatin maturation and they need to be copied during DNA replication from parental histones to newly synthesized histones. In this thesis specific histone modifications and the assigned biological function were investigated. First, a stepwise pathway for H3K36 methylation involved in transcriptional elongation was described. Second, kinetics of H4K20 monomethylation and its interaction partners were explored and linked to chromatin maturation. And at last, the kinetics of inheritance of histone modification patterns during replication was dissected.

3.1.1 H3K36 methylation during transcription

H3K36 trimethylation has been shown to be enriched towards the 3' end of active genes. To better understand the connection of chromatin and transcriptional elongation, it is essential to understand how H3K36 trimethylation is regulated. Therefore H3K36 methylation was characterized in *Drosophila*. In this study, H3K36 methylation was analyzed in terms of distribution, regulation and read out. It is the only known modification so far associated with elongation of transcription (Bannister et al. 2005; Barski et al. 2007). When dissecting the regulatory pathway of methylation at this site, it became clear that methylation marks are added in a stepwise manner, where two different enzymes are involved.

Oliver Bell, Christiane Wirbelauer, Marc Hild, **Annette N.D. Scharf**, Michaela Schwaiger, David M. MacAlpine, Frederic Zilberman, Stephen P. Bell, Axel Imhof, Dan Garza, Antoine H. F. M. Peters and Dirk Schübeler. Localized H3K36 methylation states define histone H4K16 acetylation during transcriptional elongation in *Drosophila*. *EMBO*, 2007 Dec 12; 26 (24): 4974-84.

Declaration of contribution to "Localized H3K36 methylation states define histone H4K16 acetylation during transcriptional elongation in Drosophila": The study was initiated by Dirk Schübeler and Oliver Bell. I contributed and prepared Figure 3E, wrote the corresponding figure legends and material and method section. The manuscript was written by Dirk Schübeler. The final version of the manuscript was revised with the help of Axel Imhof and me.

Localized H3K36 methylation states define histone H4K16 acetylation during transcriptional elongation in *Drosophila*

Oliver Bell¹, Christiane Wirbelauer¹,
Marc Hild², Annette ND Scharf³, Michaela
Schwaiger¹, David M MacAlpine^{4,6},
Frédéric Zilbermann¹, Fred van Leeuwen⁵,
Stephen P Bell⁴, Axel Imhof³, Dan Garza²,
Antoine HFM Peters¹ and Dirk Schübeler^{1,*}

¹Friedrich Miescher Institute for Biomedical Research, Maulbeerstrasse, Basel, Switzerland, ²Novartis Institutes for Biomedical Research, Cambridge, MA, USA, ³Adolf-Butenandt Institute, University of Munich, Munich, Germany, ⁴Department of Biology, Howard Hughes Medical Institute, Massachusetts Institute of Technology, Cambridge, MA, USA and ⁵Netherlands Cancer Institute, Amsterdam, The Netherlands

Post-translational modifications of histones are involved in transcript initiation and elongation. Methylation of lysine 36 of histone H3 (H3K36me) resides promoter distal at transcribed regions in *Saccharomyces cerevisiae* and is thought to prevent spurious initiation through recruitment of histone-deacetylase activity. Here, we report surprising complexity in distribution, regulation and readout of H3K36me in *Drosophila* involving two histone methyltransferases (HMTases). Dimethylation of H3K36 peaks adjacent to promoters and requires dMes-4, whereas trimethylation accumulates toward the 3' end of genes and relies on dHyph. Reduction of H3K36me3 is lethal in *Drosophila* larvae and leads to elevated levels of acetylation, specifically at lysine 16 of histone H4 (H4K16ac). In contrast, reduction of both di- and trimethylation decreases lysine 16 acetylation. Thus di- and trimethylation of H3K36 have opposite effects on H4K16 acetylation, which we propose enable dynamic changes in chromatin compaction during transcript elongation.

The EMBO Journal (2007) 26, 4974–4984. doi:10.1038/sj.emboj.7601926; Published online 15 November 2007

Subject Categories: chromatin & transcription

Keywords: chromatin; histone methyltransferases; histone modifications; transcription; transcription elongation

Introduction

Nucleosomal packaging provides a barrier for protein binding to DNA and for the processivity of DNA and RNA polymerases. Changes in chromatin structure involve ATP-depend

ent remodeling of nucleosomes and numerous post-translational modifications of histones (Felsenfeld and Groudine, 2003). Depending on the modification and the targeted residue, these alterations can affect sequence accessibility for DNA-binding proteins or create recognition modules for effector proteins with defined functions (Jenuwein and Allis, 2001; Peters and Schubeler, 2005). Indeed, chromatin modifications appear involved in all steps of transcription, such as initiation, elongation and termination (Sims *et al*, 2004). A large body of work links histone H3 modifications, such as lysine 4 methylation and lysine 9 and 14 acetylation to RNA polymerase recruitment at the promoter. Recent genome-wide studies revealed that these active modifications are present at transcribed genes, yet occur preferentially at the promoter and adjacent downstream regions. This suggests a shared chromatin profile consisting of several histone tail modifications involved in early events of transcription (Robert *et al*, 2004; Schubeler *et al*, 2004; Pokholok *et al*, 2005; Barski *et al*, 2007).

Although extensive knowledge exists on promoter-proximal events, less is known about the cross talk between the elongating polymerase and chromatin. Several chromatin-associated proteins are implicated in aiding transcriptional elongation. Some affect histone acetylation (Wittschieben *et al*, 1999; Winkler *et al*, 2002), whereas others show nucleosomal remodeling or histone chaperone activity (Belotserkovskaya *et al*, 2003; Kaplan *et al*, 2003; Mason and Struhl, 2003; Morillon *et al*, 2003). These findings suggest that nucleosomes are acetylated and mobilized during transcriptional elongation. Moreover, high levels of transcription cause nucleosomal displacement, leading to reduced nucleosomal density, which in metazoa appears to be compensated in part by depositing nucleosomes that contain the variant histone H3.3 (Lee *et al*, 2004; Mito *et al*, 2005; Schwartz and Ahmad, 2005; Wirbelauer *et al*, 2005). Thus, although chromatin opening is required for gene activation at promoters, transcription itself causes chromatin disruption, which appears to be compensated by reestablishing a compact chromatin state.

Methylation of lysine 36 of histone H3 (H3K36me) is the only covalent histone modification reported to be enriched in the 3' end of active genes (Bannister *et al*, 2005; Kizer *et al*, 2005; Pokholok *et al*, 2005; Rao *et al*, 2005; Barski *et al*, 2007; Mikkelsen *et al*, 2007). Therefore, understanding the regulation of this modification is likely to shed light on the interplay between chromatin and transcriptional elongation. In *S. cerevisiae*, all lysine 36 methylation is mediated by Set2 histone methyltransferase (HMTase), which is directed to active genes through interaction with elongation-competent RNA polymerase II (Krogan *et al*, 2003; Li *et al*, 2003; Xiao *et al*, 2003; Kizer *et al*, 2005). In turn, Set2-methylated nucleosomes signal for cooperative binding of two subunits of the Rpd3S complex (Li *et al*, 2007a), resulting in

*Corresponding author. Friedrich Miescher Institute for Biomedical Research, Maulbeerstrasse 66, Basel 4058, Switzerland.

Tel.: +41 61 69 78269; Fax: +41 61 69 73976;

E-mail: dirk@fmi.ch

⁶Present address: Duke University Medical Center, Department of Pharmacology and Cancer Biology, Durham, NC 27710, USA

Received: 2 September 2007; accepted: 24 October 2007; published online: 15 November 2007

recruitment of histone-deacetylase activity to the body of active genes (Carrozza *et al*, 2005; Joshi and Struhl, 2005; Keogh *et al*, 2005). Thus, H3K36 methylation has been proposed to be involved in the maintenance of repressive chromatin structure. Indeed, loss of Rpd3 recruitment by deletion of *SET2* results in an increase of spurious intragenic initiation events (Carrozza *et al*, 2005; Li *et al*, 2007b). This supports a function for H3K36me in compensating for transcription-coupled disruption and hyperacetylation of chromatin, which otherwise could unmask cryptic promoters. However, because deacetylation interferes with transcriptional initiation, mechanisms need to be in place to ensure that H3K36me-mediated HDAC recruitment does not occur in vicinity of active promoters.

Little is known about potentially different chromosomal distributions or functions of the mono-, di- or trimethylated states of H3K36. Interestingly, two recently identified histone demethylases in the human genome have been shown to demethylate either preferentially H3K36me2 (Tsukada *et al*, 2005) or H3K36me3 (Klose *et al*, 2006; Whetstone *et al*, 2006) opening the possibility of enzymatically regulated differential turnover of H3K36 methylation states.

To investigate function and regulation of this residue in a higher eukaryote, we have characterized H3K36 methylation in *Drosophila melanogaster*. We show that dimethylation and trimethylation of H3K36 have distinct chromosomal localization, and we suggest that these methylation states rely on separate HMTases. Importantly, we find that H3K36 methylation states show antagonistic cross talk to H4 acetylation at lysine 16 (H4K16ac), which has been shown to directly influence packaging of higher-order chromatin (Dorigo *et al*, 2003; Shogren-Knaak *et al*, 2006).

These findings suggest opposing functions for H3K36 methylation states in *Drosophila* to regulate chromatin acetylation and presumably compaction during transcriptional elongation in higher eukaryotes.

Results

Global distribution of H3K36 di- and trimethylation in *Drosophila* cells

To address if H3K36me associates with repressive or permissive chromatin in metazoa, we determined the nuclear localization of H3K36me2 and H3K36me3 in *Drosophila* Kc cells. Similar to other euchromatic marks such as H3K4 methylation (Wirbelauer *et al*, 2005), both H3K36 methylation states are largely excluded from the transcriptionally inert heterochromatin but are highly enriched in the transcriptionally active euchromatic regions of the nucleus (Figure 1A).

This nuclear localization reflects the presence of both H3K36 methylation states at active genes, as we find both enriched at the ectopically expressed histone variant H3.3 (Figure 1B). H3.3 is deposited at active genes, which are subject to transcription-coupled nucleosomal displacement events (Mito *et al*, 2005; Schwartz and Ahmad, 2005; Wirbelauer *et al*, 2005). This confirms previous observations by mass spectrometry of endogenous H3.3 in *Drosophila* Kc cells (McKittrick *et al*, 2004) and suggests that both H3K36 methylation states are enriched at sites of active transcription.

To investigate the chromosomal distribution of lysine 36 methylation, we performed chromatin-immunoprecipitation

(ChIP) using antisera specific for H3K36me2 or H3K36me3. DNA from enriched chromatin was compared to input chromatin by comparative hybridization to a DNA microarray representing chromosome 2L of the *Drosophila* genome in a 2 kb tiling resolution (MacAlpine *et al*, 2004; Schubeler *et al*, 2004). In addition, we determined the chromosomal distribution of H3K4me3, which we and others have previously shown to occur promoter proximal at active genes (Bernstein *et al*, 2005; Pokholok *et al*, 2005; Wirbelauer *et al*, 2005). The resulting distribution on chromosome 2L confirms these previous studies, as we find preferential enrichment of H3K4me3 at the 5' end of active genes (Figure 1C and D). H3K36me3, in contrast, shows a different localization, as it is highly enriched toward the 3' end of active genes as previously reported for *S. cerevisiae* (Pokholok *et al*, 2005). The distribution of H3K36me2 with preferential distribution toward the 5' end is remarkably different, although this distribution is less pronounced than that of H3K4me3 (Figure 1C and D). Together, this chromosome-wide analysis revealed different distributions of di- and trimethylated lysine 36, with trimethylation localizing toward the 3' end and dimethylation being adjacent to the promoter.

Before proceeding with further analysis, we confirmed the specificity of the antibodies. We did not detect cross-reactivity against different methylation states of H3K36 when tested against peptides, suggesting that both antibodies are selective for either the di- or trimethylated state of this residue (Supplementary Figure 1A). We note that not all tested commercial antibodies showed equally high levels of discrimination in this assay (Supplementary Figure 1A), which might explain why a differential distribution of di- and trimethylation of H3K36 has not been reported previously. To test for potential cross-reactivity to regions of histone H3 outside of the peptides used, we tested both antibodies against ectopically expressed H3.3 in which H3K36 had been mutated to alanine. This point mutation leads to a loss of detection for each antibody (Supplementary Figure 1B), indicating that both are specific for defined H3K36 methylation states in the context of full-length histone H3.

Next, we determined the distribution of H3K36 methylation states at a subset of genes using real-time PCR (RT-PCR) and previously published amplicons with a spatial resolution of approximately 750 bp (as compared to over 2000 bp of the microarray) (Wirbelauer *et al*, 2005). This enabled us to relate the observed enrichments to our existing datasets of other histone tail modifications, RNA polymerase II (RNA-Pol II) and the replacement histone H3.3 (Wirbelauer *et al*, 2005). This analysis confirmed that H3K36me3 is biased toward the 3' end of active genes (Figure 2A and B). It also verified a different distribution for H3K36me2, as this mark was most abundant at a region between the 5' peak of H3K4me3 and the 3' peak of H3K36me3 (Figure 2B). The observed distribution is not cell line-specific, as similar results were obtained at the same set of genes in a second *Drosophila* cell line, SL2 (data not shown).

We conclude that three chromatin signatures can be distinguished along active genes based on H3 tail modifications. A promoter-proximal region of high H3K4 methylation, an intermediate region characterized by a peak in H3K36me2 and a further 3' region characterized by high H3K36me3. Thus, different K36 methylation states mark discrete regions of transcribed genes.

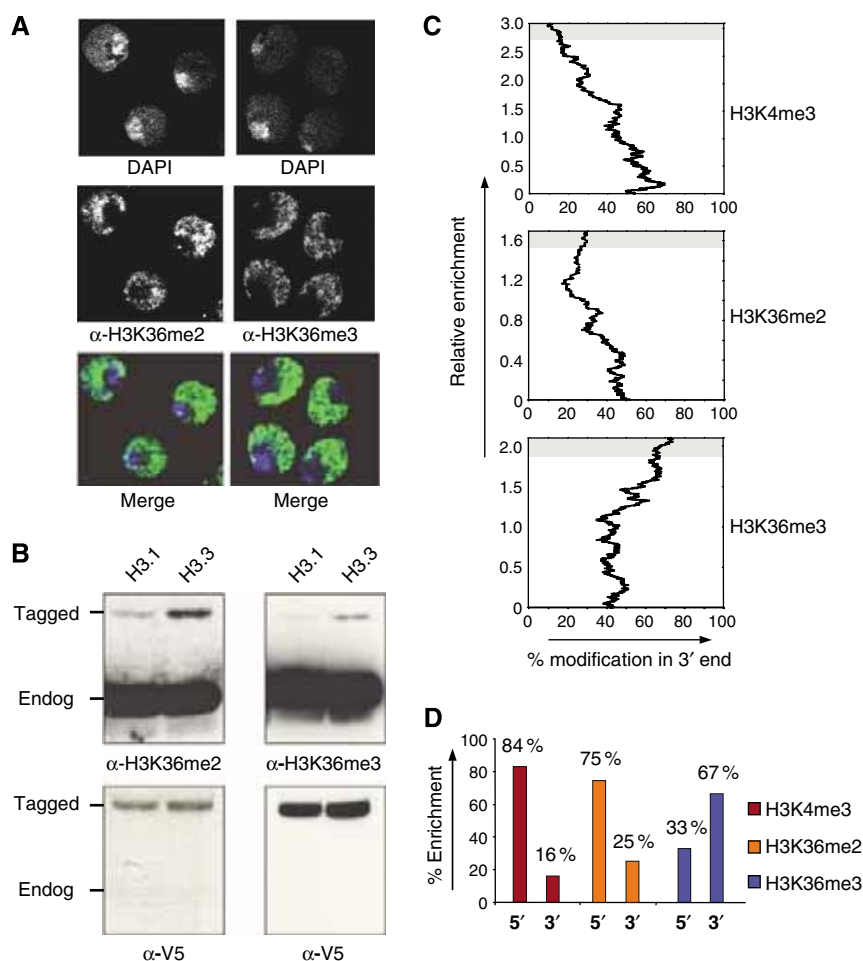


Figure 1 Nuclear and chromosomal localization of H3K36me2 and H3K36me3. **(A)** *Drosophila* Kc cells were stained with DAPI in combination with antibodies specific to H3K36me2 and H3K36me3. Merged pictures are pseudo-colored with antibody staining in green and DAPI staining in blue. The heterochromatic chromocenter is visible in these cells as a region with high signal for DAPI, whereas the euchromatin shows weaker DAPI staining. Both methylation states of H3K36 strongly stain euchromatin and are excluded from the transcriptionally inert chromocenter. **(B)** H3K36me2 and H3K36me3 are enriched at the variant histone H3.3. Histones were isolated from Kc cells expressing either epitope-tagged H3.1 or H3.3 (Wirbelauer *et al*, 2005) and analyzed by western blot. This analysis finds H3K36me2 and H3K36me3 enriched at H3.3 compared to canonical H3.1. Detection of the V5-epitope tag serves as a loading control. **(C)** Chromosome-wide analysis of the distribution of H3K4me3 and H3K36me2/me3 relative to the 5' or 3' end of coding regions. Following ChIP, DNA from input and bound fraction were co-hybridized to a microarray representing the complete *Drosophila* chromosome 2L (see Materials and methods). To determine the relative enrichment for either the 5' or 3' end of genes, we focused on tiles that were within genes and either contained the 5' or 3' end. We ignored those that were intergenic or mid-genic. The 5' and 3' end tiles (2105 for H3K4me3, 2041 for H3K36me2, 2123 for H3K36me3) were ranked according to their ChIP enrichment, and then we asked if tiles that are highly enriched are biased toward the 5' or 3' end. Note that enrichment of 3' end tiles implies absence from 5' tiles. Shown is a moving average (% , $n = 100$) of tiles in the 3' end relative to enrichment. This illustrates a preferential 5' position of tiles enriched for H3K4me3 (85% of enriched regions reside at a 5' end of a gene) and a 3' bias for tiles enriched for H3K36me3 (67% of enriched tiles are at the 3' end). H3K36me2 shows a 5' bias in this analysis similar to H3K4me3, yet less pronounced. **(D)** Summary of chromosomal array with 2 kb resolution. The bar chart shows the abundance in 5' or 3' positions for those sequences with the highest enrichment in each modification (upper 10% of tiles, illustrated with a gray background in C).

Two proteins mediate H3K36 methylation in *Drosophila*

To gain further insights into the underlying enzymatic regulation and function, we sought to identify the proteins responsible for H3K36 methylation based on homology to the SET domain sequence of the single H3K36 HMTase in *S. cerevisiae* (Set2) (Supplementary Figure 2A). We performed an RNAi screen against putative HMTases and used bulk analysis of H3K36me2 and H3K36me3 levels by western blot as a readout for loss of function. This identified two SET domain-containing proteins (CG4976 and CG1716) (Figure 3A) that upon knockdown showed reduced levels of H3K36 methylation (Figure 3B and D). Thus, we find that at

least two putative HMTases are involved in H3K36 methylation in flies. To ensure specificity of the RNAi, we raised specific antibodies against both proteins (see Material and methods), which confirmed efficient protein reduction upon addition of dsRNA (Figure 3C). We named CG1716 as '*Drosophila* Hypb' (dHypb) based on homology to the human HMTase HYPB (Sun *et al*, 2005). CG4976, in contrast, shows homology to the nuclear-receptor-binding SET-domain-containing protein (NSD) family of SET domain proteins (Supplementary Figure 2B) and has previously been annotated as *Drosophila* Mes-4 (dMes-4) based on its similarity to a SET domain-containing protein in the *C. elegans*

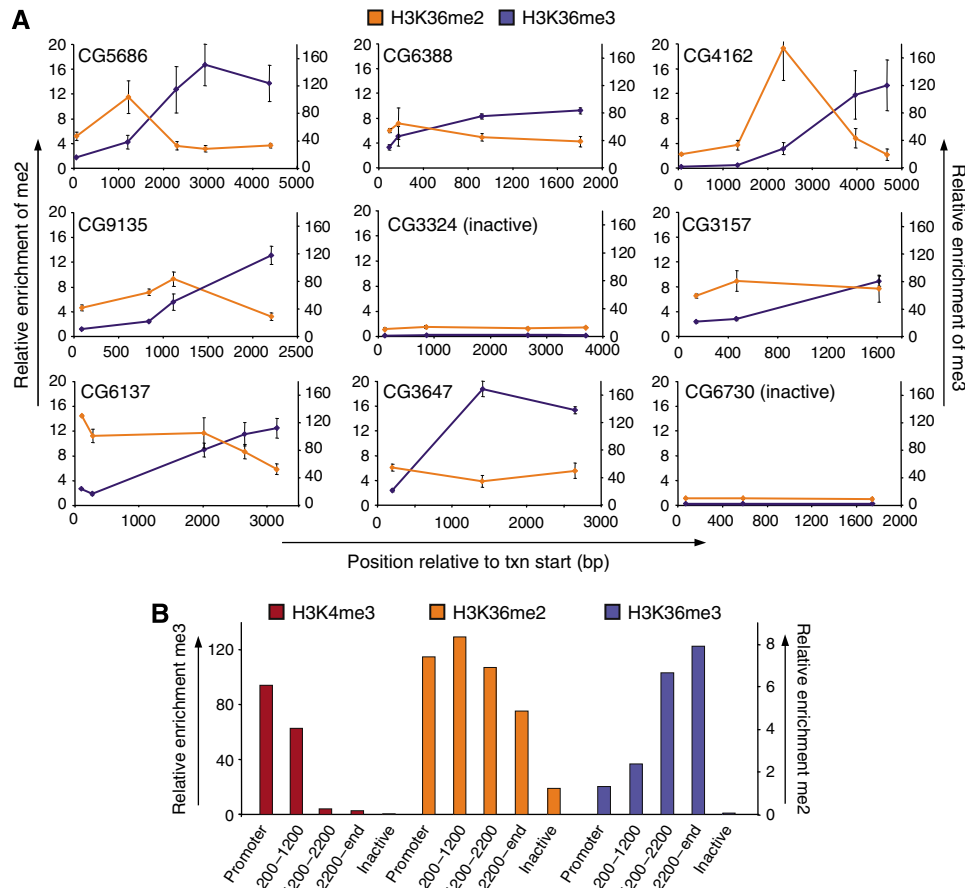


Figure 2 High-resolution analysis of di- and trimethylation of H3K36 at individual genes. **(A)** ChIP analysis in *Drosophila* Kc cells along the body of several genes using antibodies specific for H3K36me2 or H3K36me3 and quantification by RT-PCR. Enrichments were normalized to nucleosomal abundance determined with an antibody against the C-terminus of H3. Shown is average and standard deviation from at least three independent repeats starting with cells at different passages. X-axis reflects the base-pair position relative to the transcriptional start site. Y-axis reflects enrichment (bound/input normalized to an intergenic control). H3K36me2 (orange line, scale on the left), H3K36me3 (blue line, scale on the right). Numbers in graphs are gene IDs according to Flybase. **(B)** Summary of individual genes. Probes at active genes shown in A were grouped according to the distance from the transcriptional start site (promoter $n = 5$, 200–1200 bp $n = 8$, 1200–2200 bp $n = 4$, 2200-end bp $n = 7$). All probes at inactive genes were grouped separately (inactive $n = 7$). For each group, the average enrichment for each modification was calculated. Values for H3K4me3 and H3K36me3 are according to the left scale, values for H3K36me2 are according to the right scale. This representation illustrates a strong 5' bias for H3K4me3, an intermediate 5' bias for H3K36me2 and a strong 3' bias for H3K36me3.

genome. In worms, Mes-4 is required for H3K36 methylation at autosomes in early embryo and is necessary for germline viability (Bender *et al*, 2006).

When we compared the levels of di- versus trimethylation of H3K36 upon reduction of dHypb or dMes-4, we noted a striking difference. RNAi against dMes-4 reduces di- and trimethylation, suggesting that the activity of this enzyme is required for both methylation states (Figure 3D). Knockdown of dHypb, in contrast, results in the downregulation of trimethylation alone, whereas levels of dimethylation slightly increase. This result is in disagreement with the recent study that reported reduction of dimethylation following RNAi knockdown of CG1716 in flies (Stabell *et al*, 2007). However, we point out that the authors relied for detection on an antibody that we found cross-reactive with trimethylated lysine 36 peptide (Supplementary Figure 1A), possibly accounting for this discrepancy.

To validate the differential effects on lysine 36 methylation by an antibody-independent approach, we analyzed histones isolated from either control or RNAi-treated cells by mass spectrometry. We compared the levels of H3K27 and H3K36 methylation within the peptides comprising amino acids

27–40 of histone H3. To determine the changes in methylation of H3K36, we analyzed the mono-, di- and trimethylated isoforms and measured the levels of H3K36 methylation relative to the methylation at H3K27 by nanospray MS/MS (see Materials and methods). This confirmed the downregulation of both di- and trimethylation of H3K36 upon loss of dMes-4, whereas loss of dHypb reduced trimethylation alone (Figure 3E). In addition, we observed a modest increase of K36me2 in the dHypb knockdown in line with the results obtained by western blot; however, the low abundance of K36me2 relative to K27me2 precludes a robust quantification.

dHypb is essential for fly development

To examine whether changes in H3K36 methylation states would influence organismal development, we generated transgenic fly lines harboring an RNAi construct complementary to either dMes-4 or dHypb message under the control of a GAL4-inducible promoter (see Materials and methods). Transcription of the respective RNAi construct was triggered by crossing in a fly strain that expresses the GAL4 activator ubiquitously under the control of the tubulin promoter. Induction of the dMes-4 RNAi construct led to a detectable

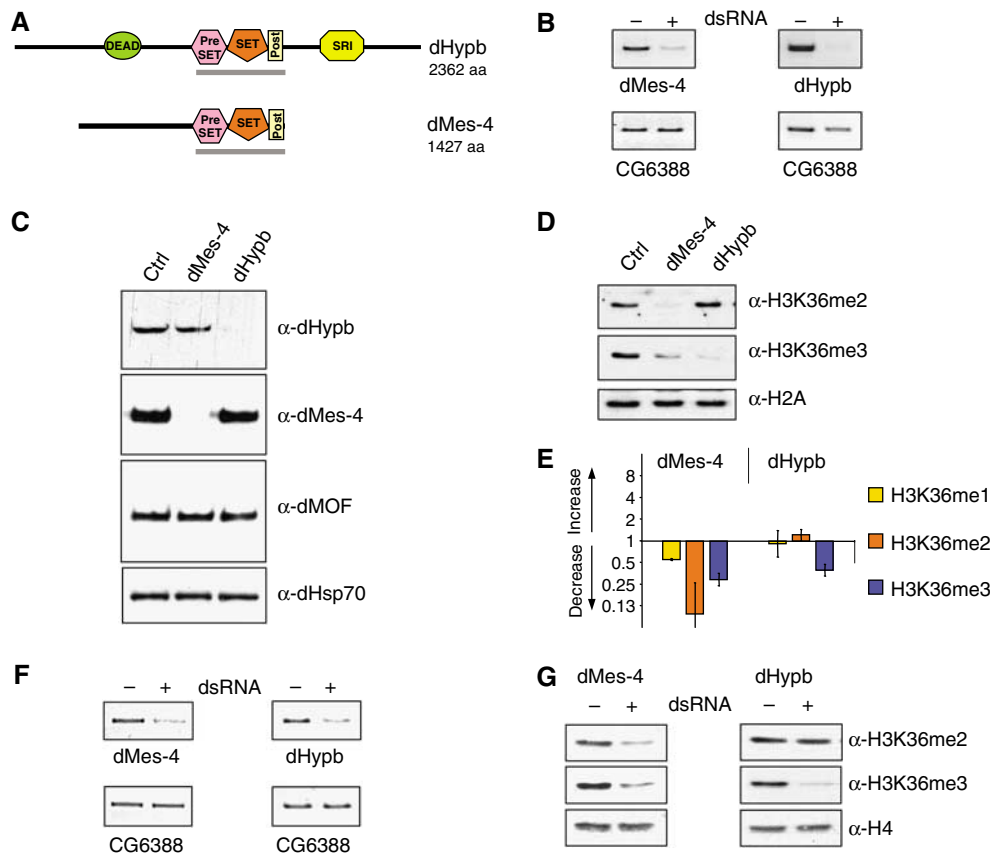


Figure 3 Identification of *Drosophila* SET domain proteins involved in H3K36 methylation. (A) Domain structure of full-length HMTase proteins as predicted by the SMART software (EMBL). DEAD = ATP dependant helicase domain, SRI = Set2 Rpb1 interacting domain. The gray bar indicates protein fragments tested for HMTase activity *in vitro*. (B) Validation of mRNA knockdown in cultured Kc cells. RT-PCR of target message in the absence (-) or presence (+) of dsRNA reveals efficient mRNA knockdown. The gene expression of CG6388 is unaffected in both knockdowns and serves as a loading control. (C) Validation of protein reduction. Western blot using antibodies specific for dMes-4 and dHypb in the absence (-) or presence (+) of dsRNA reveals efficient reduction of the targeted proteins in Kc cells. dHsp70 and dMOF are unaffected by RNAi knockdown and serve as loading control. (D) Reductions of dMes-4 and dHypb have specific effects on global levels of H3K36 methylation. Loss of dHypb results in the reduction of H3K36me3 and coinciding increase of H3K36me2. Knockdown of dMes-4 leads to a reduction in both H3K36me2 and H3K36me3. H2A serves as loading control. Global levels of H3 and H4 were unaffected (Supplementary Figure 5A). (E) Mass spectrometry analysis of H3K36-methylated peptides. MS-MS analysis of mono-, di- or trimethylated H3K36 moieties following knockdown of putative HMTases in *Drosophila* Kc cells. The bar chart displays fold changes in the abundance of H3K36 methylation states relative to untreated control cells. (F) Knockdown of putative *Drosophila* H3K36 HMTases *in vivo*. RT-PCR from larvae uninduced (-) or induced (+) for targeted knockdown of either dMes-4 or dHypb mRNA *in vivo*. Reduced transcript abundance is detected in the presence of GAL4 driver under the control of a ubiquitously expressed (tubulin) promoter. CG6388 mRNA levels serve as loading control. (G) Western blot analysis of H3K36 methylation states in fly larvae mirror the observations in cultured cells. Reduction of dMes-4 message results in the reduction of H3K36 di- and trimethylation, whereas dHypb RNAi specifically downregulates H3K36me3. Levels of total H4 serve as loading control.

reduction of target mRNA (Figure 3F), yet only in a subset of fly lines. Those with reduced expression of dMes-4 mRNA showed a decrease of both K36me2 and K36me3 at larval stages, confirming the results from cell culture (Figure 3G). In the case of dHypb, induction of the RNAi transgene efficiently reduced dHypb mRNA (Figure 3F) and led to decreased levels of H3K36me3, confirming the results in cultured cells (Figure 3G and D). Moreover, postzygotic depletion of dHypb levels was lethal at the larvae-pupae transition with 100% penetrance observed in multiple independent integration sites of the RNAi construct (see Materials and methods) in agreement with a recent report (Stabell *et al*, 2007). We conclude that reducing HMTase levels in flies mirror the chromatin effects seen in cultured cells and that a strong reduction of dHypb is lethal, suggesting that dHypb-mediated H3K36me3 is essential for development.

dHypb shows HMTase activity at histone H3 *in vitro*

To test the enzymatic activity of both enzymes *in vitro*, we expressed fragments containing pre-SET, SET and post-SET domains as GST-tagged fusion proteins using Baculovirus infection of insect cells (Supplementary Figure 3B). Recombinant proteins were purified and incubated with radioactively labeled SAM as methyl donor and histones purified from calf thymus as a substrate. HMTase activity was reproducibly detected for dHypb by measuring radioactive incorporation into histones. Subsequent gel separation of labeled products revealed that dHypb methylates preferentially histone H3 (Figure 4A). Unlike dHypb, dMes-4 displayed only weak activity under various conditions tested (data not shown). Although this might reflect the lack of necessary cofactors, it precluded us from further defining dMes-4 activity *in vitro*.

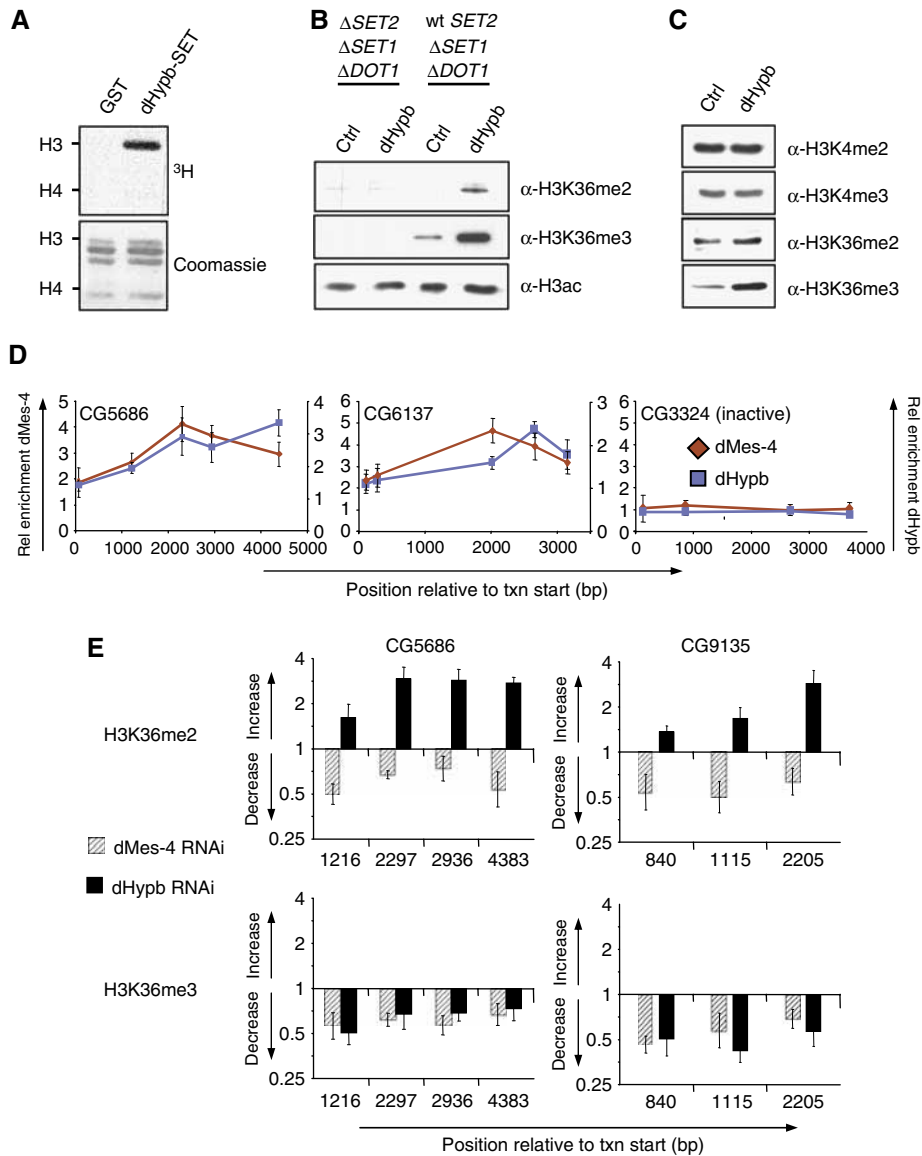


Figure 4 dHypb methylates lysine 36 *in vitro* and colocalizes with dMes-4 at active genes. (A) dHypb shows histone-methyltransferase activity *in vitro*. Recombinant protein fragments containing pre- and post-SET domain (dHypb: aa 1351–1553, shown as gray bar in Figure 3A) were incubated with radioactive SAM and histones from calf thymus as substrates. Shown in the upper panel is the reaction product that was separated by SDS–PAGE and incorporated radioactivity measured by exposure to film. The lower panel displays Coomassie-stained SDS–PAGE gel and serves as loading control. Recombinant dHypb-SET shows HMTase activity to histone H3 in this assay. (B) dHypb methylates H3K36 *in vitro*. Western blot analysis displays H3K36 di- and trimethylation levels of HMTase assay with recombinant full-length dHypb using mutant yeast nuclear extracts deficient for H3K4me, K36me and K79me ($\Delta SET2$, $\Delta SET1$, $\Delta DOT1$) or K4me and K79me (*wt SET2*, $\Delta SET1$, $\Delta DOT1$) as a substrate. A dHypb-dependent increase of di- and trimethylation is obtained only with chromatin substrate from *wt SET2* strain, suggesting that dHypb requires premethylated lysine 36 substrate for its activity. (C) Western blot analysis of *Drosophila* Kc-overexpressing dHypb shows a specific increase in trimethylation. A similar experiment with full-length dMes-4 in Kc cells did not reveal robust changes in H3K36 methylation (data not shown). (D) ChIP analysis using antibodies generated against endogenous dMes-4 and dHypb along the body of two active genes (CG6137 and CG5686) and one inactive gene (CG3324). Shown is average and standard deviation from at least three independent repeats. X-axis reflects the base-pair position relative to the transcriptional start site. Y-axis reflects enrichment (bound/input normalized to an intergenic control). (E) dMes-4 and dHypb define distinct methylation states in Kc cells. Levels of H3K36 methylation states in RNAi and control cells were compared with ChIP followed by RT–PCR analysis. Shown is the ratio of H3K36me enrichments (fold change, Y-axis) of RNAi over control cells relative to the position from the transcriptional start site (X-axis) of two actively transcribed genes. RNAi against dHypb leads to a reduction of H3K36me3 in the coding region with a coinciding increase of H3K36me2 predominantly toward the 3' end. Loss of dMes-4 leads to a reduction of both H3K36me2 and H3K36me3.

To gain insights into dHypb specificity, we incubated recombinant full-length protein with nuclear extracts from yeast strains that lack K4me, K36me and K79me of histone H3 or K4me and K79me only (Figure 4B and Material and methods). Subsequent western blotting revealed a dHypb-

dependent increase in di- and trimethylation of lysine 36, yet only when supplied with yeast chromatin positive for mono-, di- and trimethylation of H3K36 (Figure 4B). In contrast, no methylation was detected in mutant extracts deficient for any lysine 36 methylation. Whereas these results demonstrate

that dHyph mediates H3K36 methylation *in vitro*, they also indicate that its activity relies on the presence of premethylated lysine 36 substrate.

To address if a similar specificity can be observed *in vivo*, we ectopically expressed dHyph in *Drosophila* Kc cells. Upon overexpression, we found only H3K36me3 levels to be increased (Figure 4C and Supplementary Figure 3C), which is in agreement with the reduction of trimethylation observed upon knockdown of dHyph.

In conclusion, we found that dHyph methylates H3K36 *in vitro*, yet requires premethylated lysine 36 substrate for its activity. Combined with the specific changes of trimethylation observed *in vivo*, our results suggest that dHyph is responsible for the trimethylated state of lysine 36 in *Drosophila*.

dMes-4 and dHyph localize at sites of H3K36 methylation at active genes

As both dMes-4 and dHyph show distinct effects on H3K36me2 and H3K36me3 upon knockdown *in vivo*, we asked if both act at the same genes. To test for chromosomal binding, we carried out ChIP using antibodies specific for endogenous dMes-4 or dHyph and quantified enrichments by RT-PCR. This revealed that both enzymes colocalize to actively transcribed genes, while being absent from an inactive gene (Figure 4D). The distributions of both HMTases are largely overlapping, with highest relative abundances downstream of the promoter at sites of di- and trimethylation of H3K36 (compare Figure 2A).

H3K36 methylation states occur enzyme-specific at individual genes

To test if recruitment of either enzyme mediates defined methylation states, we reduced the level of either one of the two enzymes by RNAi and determined the local effect on H3K36me by ChIP analysis at individual genes. Reduction of

dHyph at selected genes results in reduced presence of trimethylation and coincident increase of dimethylation (Figure 4E). This finding suggests that the slight upregulation of bulk H3K36me2 levels detected by western blot and mass spectrometry (Figure 3D and E) reflects an increase at intragenic regions, which are trimethylated in untreated cells. In contrast, reduction of the endogenous levels of dMes-4 coincides with a decrease of both H3K36me2 and H3K36me3 not only in bulk (Figure 3D), but also at individual genes (Figure 4E). One possible interpretation of these results is that both enzymes act consecutively at the same set of genes to mediate distinct patterns of di- and trimethylation of H3K36.

Specific cross talk between H4 lysine 16 acetylation and H3K36 methylation states

In *S. cerevisiae*, H3K36 methylation has been reported to recruit an HDAC-containing complex, resulting in deacetylation of the 3' end of actively transcribed genes (Carrozza *et al*, 2005; Joshi and Struhl, 2005; Keogh *et al*, 2005). No direct comparison between localization of di- and trimethylation of H3K36 has been reported in budding yeast; however, loss of the only H3K36 methylase Set2 results in hyperacetylation of both histones H3 and H4 within reading frames (Carrozza *et al*, 2005; Joshi and Struhl, 2005; Keogh *et al*, 2005).

We therefore examined whether H3K36 methylation in flies shows a similar cross talk to histone acetylation and whether the di- and trimethylated states of H3K36 in *Drosophila* have separate functions in this pathway. Reduction of H3K36 trimethylation by dHyph knockdown in female Kc cells resulted in significant upregulation of bulk levels of H4 acetylation at lysine 16 (Figure 5A). Although this hyperacetylation is reminiscent of global hyperacetylation reported in yeast *SET2* mutants (Carrozza *et al*, 2005; Joshi and Struhl, 2005; Keogh *et al*, 2005; Li *et al*, 2007b), it

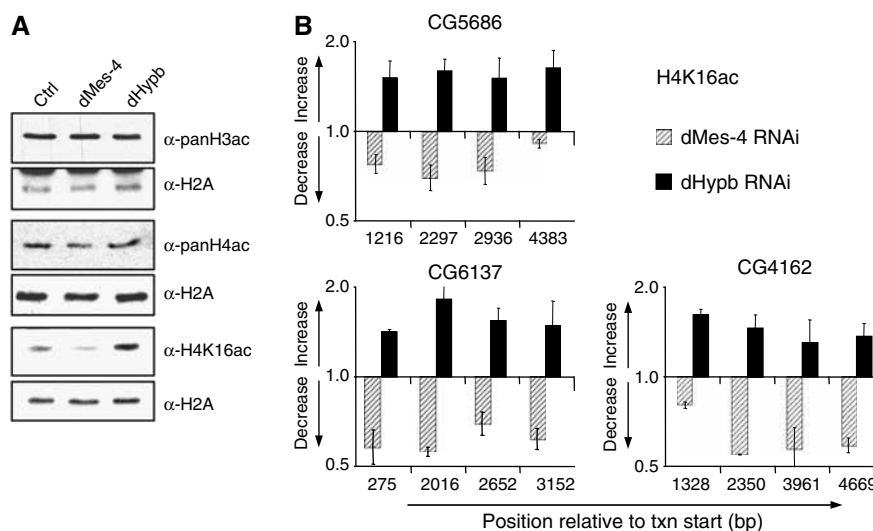


Figure 5 Differential cross talk between H3K36 methylation states and H4K16 acetylation. (A) Knockdown dMes-4 or dHyph has specific effects on the acetylation of H4K16. Levels of H3 and H4 acetylation in bulk histones were measured upon RNAi by western blot analysis. In *Drosophila* Kc cells, knockdown of dMes-4 results in a reduction, whereas knockdown of dHyph leads to an increase of H4K16 acetylation. No changes were detected at other residues on H4 (Supplementary Figure 3A). (B) ChIP analysis of H4K16 acetylation changes upon knockdown of dMes-4 and dHyph. Shown is the ratio of H4K16ac enrichments (fold change, Y-axis) of RNAi over control cells relative to the position from the transcription start site (X-axis) of three actively transcribed genes. These results suggest that the changes in bulk acetylation of histones occur at the same chromosomal positions that change levels of H3K36 methylation states.

appeared to be specific for H4K16, as no change was detected at other lysine residues tested (Figure 5A and Supplementary Figure 3A). In contrast, reduction of H3K36 di- and trimethylation upon knockdown of dMes-4 had the inverse effect, as acetylation at lysine 16 of histone H4 was globally decreased. Together, these data reveal a cross talk between methylation of H3K36 and acetylation of H4 in *D. melanogaster*, however, in a more intricate way than what has been reported for *S. cerevisiae*. Notably, the knockdown of dMes-4 resulted in the reduction of both di- and trimethylation similar to a SET2 mutant, yet it did not result in increased H4 acetylation, which appears to require decline of trimethylation in the presence of dimethylation.

Next, we measured H4K16ac by ChIP to test if changes in global levels reflect acetylation differences at genes that lose H3K36me after HMTase knockdown. In untreated Kc cells, H4K16 acetylation peaked at the promoter and was present to a lesser extent throughout coding regions (Supplementary Figure 5). After knockdown of dHypb, H4K16ac increased at sequences that showed reduced levels of H3K36 trimethylation. In contrast, acetylation decreased at chromosomal positions, which also had reduced di- and trimethylation after dMes-4 RNAi (Figure 5B). These results are in agreement with bulk changes observed by western blot analysis. Importantly, the acetylation changes occur preferentially at H4K16, as other residues tested in ChIP appear unaffected (H3K9/K14ac, H4K8ac, H4K12ac; Supplementary Figure 4 and data not shown).

We conclude that H3K36me2 and H3K36me3 inversely influence H4K16 acetylation at transcribed regions in the *Drosophila* genome.

Discussion

In this study, we provide a comprehensive analysis of the distribution and regulation of the only described chromatin modification associated with transcriptional elongation in *D. melanogaster*. Our results suggest a novel regulatory pathway involving two enzymes, different localization of di- and trimethylation of H3K36 and cross talk of these methylation states to acetylation of lysine 16 of histone H4 (Figure 6A and B), a modification previously shown to prevent formation of compact chromatin.

Spatially defined H3K36 methylation states

Analogous to previously described euchromatic histone modifications, di- and trimethylation of H3K36 are enriched at transcribed genes; yet both show unique distributions downstream of 5'-biased modifications such as H3K4me (Bernstein *et al*, 2005; Pokholok *et al*, 2005; Wirbelauer *et al*, 2005). H3K36me3 peaks in the 3' end, whereas H3K36me2 shows an intermediate distribution (Figure 6A). A previous analysis of H3K36me2 and H3K36me3 in chicken erythrocyte genes did not deduce a differential distribution; however, only two genes were compared (Bannister *et al*, 2005). Thus, whereas the actual conservation of H3K36 methylation patterns in other metazoa needs to be tested, the spatial and functional differences that we report for *Drosophila* might be shared by eukaryotes that encode multiple H3K36 methylases.

We, furthermore, note that despite the topographic differences between H3K36me2, H3K36me3 and H3K4me3, all tested modifications are equally enriched at the replacement

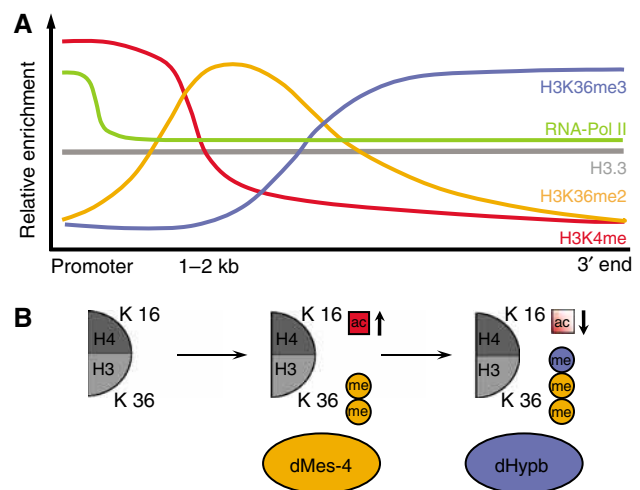


Figure 6 Summary model of H3K36 distribution and function in *Drosophila*. (A) Summary of the distribution of several H3 tail modifications along an exemplified active gene. A peak in promoter-proximal marks such as H3K4me followed by a region high in H3K36me2 and a 3'-specific region marked by high levels of H3K36me3, both depending on separate HMTases (this study). (B) Model of a differential cross talk to H4K16 acetylation at autosomes. dMes-4-dependent H3K36me2 leads to increased H4K16 acetylation, which is compensated by dHypb-catalyzed H3K36me3.

histone H3.3 (Figures 1B and 6A and Wirbelauer *et al*, 2005). This is in agreement with our previous observation that the distribution of this variant histone throughout coding regions does not mirror the complex pattern of underlying tail modifications (Wirbelauer *et al*, 2005).

Two enzymes mediate H3K36 methylation states

The consequences of protein knockdown suggest that dMes-4 is required for dimethylation and that dHypb mediates trimethylation (Figure 3D and E). This model is supported by the *in vitro* activity of dHypb (Figure 4A and B) and localization of both enzymes to the same genes (Figure 4D). Thus, a stepwise mechanism for lysine 36 methylation seems plausible in which dMes-4 mediates dimethylation, which is substrate for dHypb-mediated trimethylation. Methylation-state-specific HMTases have been described for H3K76 involved in cell-cycle regulation of *Trypanosoma brucei* (Janzen *et al*, 2006). Our findings suggest similar enzyme specificity for H3K36 methylation at active genes. As such, it is different from the regulation of H3K4 methylation, where trimethylation depends on the presence of cofactors (Steward *et al*, 2006). We also note that both H3K4 di- and trimethylation peak at the 5' end, whereas H3K36 di- and trimethylation mark distinct intragenic regions, which supports a differential recruitment of the HMTases along the transcribed gene (Figure 6). The absence of lysine 36 methylation at the promoter might reflect acetylation at this residue (H3K36ac), which has recently been reported in *S. cerevisiae*. In yeast, Gcn5-dependent H3K36 acetylation predominantly localizes to active promoters and inversely correlates with methylation, suggesting that its presence precludes methylation from the 5' end of the transcription unit (Morris *et al*, 2006).

Work in budding yeast suggests that targeting of Set2 involves physical interaction with the phosphorylated CTD of RNA polymerase II via a Set2 Rpb1 interacting (SRI)

domain (Kizer *et al*, 2005). Indeed, domain prediction algorithms identify a similar SRI domain in the C-terminal region of dHyb (Figure 3A), and a recent study reports physical interaction with hyperphosphorylated RNA polymerase (Stabell *et al*, 2007). Moreover, loss of Set2 leads to elevated levels of histone acetylation similar to a loss of dHyb. Together, these observations suggest that targeting of H3K36me3 involves interaction with elongating RNA polymerase and that dHyb is the functional *Drosophila* equivalent to yeast Set2.

dMes-4, in contrast, shows homology to human and mouse NSD1, WHSC1 (also referred to as NSD2 or MMSET) and WHSC1-L (NSD3) (Supplementary Figure 2B). This family of NSDs has been implicated in several human malignancies, including protein fusions in cancer (Jaju *et al*, 2001; Wang *et al*, 2007). Moreover, haploinsufficiency of NSD1 causes Sotos syndrome, a neurological disorder (Kurotaki *et al*, 2002). NSD1 has been reported to methylate H3K36 *in vitro* (Rayasam *et al*, 2003) and to interact with transcription factors (Huang *et al*, 1998). It is conceivable that the mammalian NSD class of proteins shares activity and function that we report for dMes-4.

Cross talk of H3K36 methylation states to histone acetylation suggests opposing roles in regulating chromatin compaction on autosomes

Our results indicate that, in metazoa, di- and trimethylation of H3K36 exert different effects on the level of histone acetylation throughout coding regions (Figure 6B). Reduction of trimethylation coincides with specific upregulation of H4 acetylation. This trans-histone effect on acetylation is reminiscent of the phenotype of a *SET2* deletion in budding yeast (Carrozza *et al*, 2005; Joshi and Struhl, 2005; Keogh *et al*, 2005). Here, we show that, in *Drosophila*, upregulation occurs preferentially at lysine 16, a residue that plays a particular role in chromatin compaction, as *in vitro* and *in vivo* evidence established that its acetylation is sufficient to prevent formation of higher-order structure (Corona *et al*, 2002; Dorigo *et al*, 2003; Shogren-Knaak *et al*, 2006). This points toward a function of H3K36me3 in mediating a more compact chromatin structure at the 3' end of *Drosophila* genes either actively by recruiting an HDAC in analogy to yeast or passively by interfering with the acetylation of H4K16.

In light of these results, it is unexpected that reduction of di- and trimethylation of H3K36 through knockdown of dMes-4 does not increase H4 acetylation. Hence, the increase of dimethylation in the dHyb knockdown is required for hyperacetylation of H4, indicating that dimethylation has a function distinct from trimethylation and possibly recruits an H4K16 HAT activity. The HAT MOF has been shown in human cells to be responsible for H4K16ac (Smith *et al*, 2005; Taipale *et al*, 2005) and is assumed to be present in various complexes. Interestingly, human MOF has recently been shown to interact with the H3K4 methylases MLL (Dou *et al*, 2005), suggesting that parallel chromatin pathways can recruit H4K16 acetylation to different regions along the gene.

Together, our results suggest that H3K36 methylation states regulate acetylation levels of H4K16 at transcribed genes. Such opposing behavior provides a rationale for independent regulation by dMes-4 and dHyb and, moreover, could justify regulated demethylation of this residue. Indeed,

histone demethylases specific for H3K36me2 (Tsukada *et al*, 2005) and H3K36me3 (Whetstone *et al*, 2006) have recently been described in the human genome, making a scenario of precise targeting and removal of individual H3K36 methylation states possible. Such network of setting and reverting-defined K36 methylation states with opposing effects on chromatin structure could be utilized to mediate cycles of chromatin opening and compaction that coincide with passage of the polymerase. If this is indeed the case, this could facilitate dynamic chromatin changes to temporarily allow polymerase passage or access for RNA-processing activities involved in splicing, termination or transport.

Materials and methods

ChIP and RT-PCR

ChIPs of histone modifications and PCR quantifications were carried out as described (Wirbelauer *et al*, 2005). Minor modifications and further details are provided in Supplementary data.

Microarray hybridization and analysis

Input and antibody-bound DNA were separately amplified and labeled as described (Schübeler *et al*, 2004), except using indirect labeling via aminoallyl-modified nucleotides. Labeled DNA was co-hybridized to a chromosomal tiling array representing chromosome 2L of the *Drosophila* genome in a 2 kb tiling resolution as described (MacAlpine *et al*, 2004). Two repeats (including dye swap) starting from independent ChIP experiments were carried out. After hybridization and washing, slides were scanned (Axon) and fluorescent reads were analyzed according to the standard normalization and filtering criteria in the GenePix software package (Axon). Repeats showed high reproducibility (H3K4me3 $R=0.98$, H3K36me2 $R=0.91$, H3K36me3 $R=0.92$), so that average value from two experiments could be used in further analysis. Complete datasets are available at GEO database (accession number GSE9414).

Antibodies

A detailed description of purchased and generated antibodies is provided in Supplementary data.

Mass spectrometry

A total of 5–10 pmol of acid-extracted histones were separated by SDS-PAGE. Coomassie blue-stained bands corresponding to histone H3 were excised and subjected to chemical modification to derive free amino groups of lysine residues (Greiner *et al*, 2005). Digestions were carried out overnight with sequencing-grade trypsin (Promega, Madison, WI, USA), according to the manufacturer's protocol. MALDI spectra were acquired (Bonaldi *et al*, 2004) for identification and determination of global changes. To compare methylation levels of H3K27 and H3K36, doubly charged peptides of H3 containing amino acids 27–40 to collision-induced decay were subjected to fragmentation and fragment spectra were analyzed in a Q-STAR XL mass spectrometer. For quantification, the relative intensities of the y8 and the y9 fragment ions that either carried methyl groups (K36me) or not (K27me) were compared.

Preparation of Kc cell nuclei and SDS-PAGE western blot analysis

Detailed protocols are provided in Supplementary data.

Fly strains and transgenes

Details are provided in Supplementary data.

HMTase assays

Detailed protocols are provided in Supplementary data.

Note added in proof

During the review of this manuscript, Larschan *et al* reported that H3K36 trimethylation mediated by dHyb has an additional function for dosage compensation of the male X-chromosome in *Drosophila*.

Supplementary data

Supplementary data are available at *The EMBO Journal* Online (<http://www.embojournal.org>).

Acknowledgements

We thank Elena Aritonovska for assistance, Tianke Wang for sharing unpublished results, FMI core facilities for generation of antisera (Susanne Schenk) and peptide synthesis (Franz Fischer), Michael Rebhahn for support in bioinformatics, Floor Frederiks for

help with yeast strains, members of the Schübeler lab for advice during the course of the projects and comments on the manuscript and Susan Gasser and Matthew Lorincz for critical reading of the manuscript. We acknowledge support by the Novartis Research Foundation (to AP and DS) and the EU 6th framework program (NOE 'The Epigenome' LSHG-CT-2004-503433 to AP, FvL and DS and LSHG-CT-2006-037415 to AI and DS). SPB is supported by the Howard Hughes Medical Institute and the National Institutes of Health (GM52339). MS and AS are predoctoral fellows of the Boehringer Ingelheim foundation.

References

- Bannister AJ, Schneider R, Myers FA, Thorne AW, Crane-Robinson C, Kouzarides T (2005) Spatial distribution of di- and tri-methyl lysine 36 of histone H3 at active genes. *J Biol Chem* **280**: 17732–17736
- Barski A, Cuddapah S, Cui K, Roh TY, Schones DE, Wang Z, Wei G, Chepelev I, Zhao K (2007) High-resolution profiling of histone methylations in the human genome. *Cell* **129**: 823–837
- Belotserkovskaya R, Oh S, Bondarenko VA, Orphanides G, Studitsky VM, Reinberg D (2003) FACT facilitates transcription-dependent nucleosome alteration. *Science* **301**: 1090–1093
- Bender LB, Suh J, Carroll CR, Fong Y, Fingerling IM, Briggs SD, Cao R, Zhang Y, Reinke V, Strome S (2006) MES-4: an autosome-associated histone methyltransferase that participates in silencing the X chromosomes in the *C. elegans* germ line. *Development* **133**: 3907–3917
- Bernstein BE, Kamal M, Lindblad-Toh K, Bekiranov S, Bailey DK, Huebert DJ, McMahon S, Karlsson EK, Kulbokas III EJ, Gingeras TR, Schreiber SL, Lander ES (2005) Genomic maps and comparative analysis of histone modifications in human and mouse. *Cell* **120**: 169–181
- Bonaldi T, Imhof A, Regula JT (2004) A combination of different mass spectroscopic techniques for the analysis of dynamic changes of histone modifications. *Proteomics* **4**: 1382–1396
- Carrozza MJ, Li B, Florens L, Suganuma T, Swanson SK, Lee KK, Shia WJ, Anderson S, Yates J, Washburn MP, Workman JL (2005) Histone H3 methylation by Set2 directs deacetylation of coding regions by Rpd3S to suppress spurious intragenic transcription. *Cell* **123**: 581–592
- Corona DF, Clapier CR, Becker PB, Tamkun JW (2002) Modulation of ISWI function by site-specific histone acetylation. *EMBO Rep* **3**: 242–247
- Dirigo B, Schalch T, Bystricky K, Richmond TJ (2003) Chromatin fiber folding: requirement for the histone H4 N-terminal tail. *J Mol Biol* **327**: 85–96
- Dou Y, Milne TA, Tackett AJ, Smith ER, Fukuda A, Wysocka J, Allis CD, Chait BT, Hess JL, Roeder RG (2005) Physical association and coordinate function of the H3 K4 methyltransferase MLL1 and the H4 K16 acetyltransferase MOF. *Cell* **121**: 873–885
- Felsenfeld G, Groudine M (2003) Controlling the double helix. *Nature* **421**: 448–453
- Greiner D, Bonaldi T, Eskeland R, Roemer E, Imhof A (2005) Identification of a specific inhibitor of the histone methyltransferase SU(VAR)3-9. *Nat Chem Biol* **1**: 143–145
- Huang N, vom Baur E, Garnier JM, Lerouge T, Vonesch JL, Lutz Y, Chambon P, Losson R (1998) Two distinct nuclear receptor interaction domains in NSD1, a novel SET protein that exhibits characteristics of both corepressors and coactivators. *EMBO J* **17**: 3398–3412
- Jaju RJ, Fidler C, Haas OA, Strickson AJ, Watkins F, Clark K, Cross NC, Cheng JF, Aplan PD, Kearney L, Boulwood J, Wainscoat JS (2001) A novel gene, NSD1, is fused to NUP98 in the t(5;11)(q35;p15.5) in *de novo* childhood acute myeloid leukemia. *Blood* **98**: 1264–1267
- Janzen CJ, Hake SB, Lowell JE, Cross GA (2006) Selective di- or trimethylation of histone H3 lysine 76 by two DOT1 homologs is important for cell cycle regulation in *Trypanosoma brucei*. *Mol Cell* **23**: 497–507
- Jenuwein T, Allis CD (2001) Translating the histone code. *Science* **293**: 1074–1080
- Joshi AA, Struhl K (2005) Eaf3 chromodomain interaction with methylated H3-K36 links histone deacetylation to Pol II elongation. *Mol Cell* **20**: 971–978
- Kaplan CD, Laprade L, Winston F (2003) Transcription elongation factors repress transcription initiation from cryptic sites. *Science* **301**: 1096–1099
- Keogh MC, Kurdiani SK, Morris SA, Ahn SH, Podolny V, Collins SR, Schuldiner M, Chin K, Punna T, Thompson NJ, Boone C, Emili A, Weissman JS, Hughes TR, Strahl BD, Grunstein M, Greenblatt JF, Buratowski S, Krogan NJ (2005) Cotranscriptional set2 methylation of histone H3 lysine 36 recruits a repressive Rpd3 complex. *Cell* **123**: 593–605
- Kizer KO, Phatnani HP, Shibata Y, Hall H, Greenleaf AL, Strahl BD (2005) A novel domain in Set2 mediates RNA polymerase II interaction and couples histone H3 K36 methylation with transcript elongation. *Mol Cell Biol* **25**: 3305–3316
- Klose RJ, Yamane K, Bae Y, Zhang D, Erdjument-Bromage H, Tempst P, Wong J, Zhang Y (2006) The transcriptional repressor JHDM3A demethylates trimethyl histone H3 lysine 9 and lysine 36. *Nature* **442**: 312–316
- Krogan NJ, Kim M, Tong A, Golshani A, Cagney G, Canadien V, Richards DP, Beattie BK, Emili A, Boone C, Shilatifard A, Buratowski S, Greenblatt J (2003) Methylation of histone H3 by Set2 in *Saccharomyces cerevisiae* is linked to transcriptional elongation by RNA polymerase II. *Mol Cell Biol* **23**: 4207–4218
- Kurotaki N, Imaizumi K, Harada N, Masuno M, Kondoh T, Nagai T, Ohashi H, Naritomi K, Tsukahara M, Makita Y, Sugimoto T, Sonoda T, Hasegawa T, Chinen Y, Tomita Ha HA, Kinoshita A, Mizuguchi T, Yoshiura Ki K, Ohta T, Kishino T *et al* (2002) Haploinsufficiency of NSD1 causes Sotos syndrome. *Nat Genet* **30**: 365–366
- Larschan E, Alekseyenko AA, Gortchakov AA, Peng S, Li B, Yang P, Workman JL, Park PJ, Kuroda MI (2007) MSL complex is attracted to genes marked by H3K36 trimethylation using a sequence-independent mechanism. *Mol Cell* **28**: 121–133
- Lee CK, Shibata Y, Rao B, Strahl BD, Lieb JD (2004) Evidence for nucleosome depletion at active regulatory regions genome-wide. *Nat Genet* **36**: 900–905
- Li B, Gogol M, Carey M, Lee D, Seidel C, Workman JL (2007a) Combined action of PHD and chromo domains directs the Rpd3S HDAC to transcribed chromatin. *Science* **316**: 1050–1054
- Li B, Gogol M, Carey M, Pattenden SG, Seidel C, Workman JL (2007b) Infrequently transcribed long genes depend on the Set2/Rpd3S pathway for accurate transcription. *Genes Dev* **21**: 1422–1430
- Li B, Howe L, Anderson S, Yates III JR, Workman JL (2003) The Set2 histone methyltransferase functions through the phosphorylated carboxyl-terminal domain of RNA polymerase II. *J Biol Chem* **278**: 8897–8903
- MacAlpine DM, Rodriguez HK, Bell SP (2004) Coordination of replication and transcription along a *Drosophila* chromosome. *Genes Dev* **18**: 3094–3105
- Mason PB, Struhl K (2003) The FACT complex travels with elongating RNA polymerase II and is important for the fidelity of transcriptional initiation *in vivo*. *Mol Cell Biol* **23**: 8323–8333
- McKitterick E, Gafken PR, Ahmad K, Henikoff S (2004) Histone H3.3 is enriched in covalent modifications associated with active chromatin. *Proc Natl Acad Sci USA* **101**: 1525–1530
- Mikkelsen TS, Ku M, Jaffe DB, Issac B, Lieberman E, Giannoukos G, Alvarez P, Brockman W, Kim TK, Koche RP, Lee W, Mendenhall E, O'Donovan A, Presser A, Russ C, Xie X, Meissner A, Wernig M, Jaenisch R, Nusbaum C *et al* (2007) Genome-wide maps of chromatin state in pluripotent and lineage-committed cells. *Nature* **448**: 553–560

- Mito Y, Henikoff JG, Henikoff S (2005) Genome-scale profiling of histone H3.3 replacement patterns. *Nat Genet* **37**: 1090–1097
- Morillon A, Karabetsou N, O'Sullivan J, Kent N, Proudfoot N, Mellor J (2003) Isw1 chromatin remodeling ATPase coordinates transcription elongation and termination by RNA polymerase II. *Cell* **115**: 425–435
- Morris SA, Rao B, Garcia BA, Hake SB, Diaz RL, Shabanowitz J, Hunt DF, Allis CD, Lieb JD, Strahl BD (2006) Identification of histone H3 lysine 36 acetylation as a highly conserved histone modification. *J Biol Chem* **282**: 7632–7640
- Peters AH, Schubeler D (2005) Methylation of histones: playing memory with DNA. *Curr Opin Cell Biol* **17**: 230–238
- Pokholok DK, Harbison CT, Levine S, Cole M, Hannett NM, Lee TI, Bell GW, Walker K, Rolfe PA, Herbolsheimer E, Zeitlinger J, Lewitter F, Gifford DK, Young RA (2005) Genome-wide map of nucleosome acetylation and methylation in yeast. *Cell* **122**: 517–527
- Rao B, Shibata Y, Strahl BD, Lieb JD (2005) Dimethylation of histone H3 at lysine 36 demarcates regulatory and nonregulatory chromatin genome-wide. *Mol Cell Biol* **25**: 9447–9459
- Rayasam GV, Wendling O, Angrand PO, Mark M, Niederreither K, Song L, Lerouge T, Hager GL, Chambon P, Losson R (2003) NSD1 is essential for early post-implantation development and has a catalytically active SET domain. *EMBO J* **22**: 3153–3163
- Robert F, Pokholok DK, Hannett NM, Rinaldi NJ, Chandy M, Rolfe A, Workman JL, Gifford DK, Young RA (2004) Global position and recruitment of HATs and HDACs in the yeast genome. *Mol Cell* **16**: 199–209
- Schübeler D, MacAlpine DM, Scalzo D, Wirbelauer C, Kooperberg C, van Leeuwen F, Gottschling DE, O'Neill LP, Turner BM, Delrow J, Bell SP, Groudine M (2004) The histone modification pattern of active genes revealed through genome-wide chromatin analysis of a higher eukaryote. *Genes Dev* **18**: 1263–1271
- Schwartz BE, Ahmad K (2005) Transcriptional activation triggers deposition and removal of the histone variant H3.3. *Genes Dev* **19**: 804–814
- Shogren-Knaak M, Ishii H, Sun JM, Pazin MJ, Davie JR, Peterson CL (2006) Histone H4-K16 acetylation controls chromatin structure and protein interactions. *Science* **311**: 844–847
- Sims III RJ, Belotserkovskaya R, Reinberg D (2004) Elongation by RNA polymerase II: the short and long of it. *Genes Dev* **18**: 2437–2468
- Smith ER, Cayrou C, Huang R, Lane WS, Cote J, Lucchesi JC (2005) A human protein complex homologous to the *Drosophila* MSL complex is responsible for the majority of histone H4 acetylation at lysine 16. *Mol Cell Biol* **25**: 9175–9188
- Stabell M, Larsson J, Aalen RB, Lambertsson A (2007) *Drosophila* dSet2 functions in H3-K36 methylation and is required for development. *Biochem Biophys Res Commun* **359**: 784–789
- Steward MM, Lee JS, O'Donovan A, Wyatt M, Bernstein BE, Shilatifard A (2006) Molecular regulation of H3K4 trimethylation by ASH2L, a shared subunit of MLL complexes. *Nat Struct Mol Biol* **13**: 852–854
- Sun XJ, Wei J, Wu XY, Hu M, Wang L, Wang HH, Zhang QH, Chen SJ, Huang QH, Chen Z (2005) Identification and characterization of a novel human histone H3 lysine 36-specific methyltransferase. *J Biol Chem* **280**: 35261–35271
- Taipale M, Rea S, Richter K, Vilar A, Lichter P, Imhof A, Akhtar A (2005) hMOF histone acetyltransferase is required for histone H4 lysine 16 acetylation in mammalian cells. *Mol Cell Biol* **25**: 6798–6810
- Tsukada YI, Fang J, Erdjument-Bromage H, Warren ME, Borchers CH, Tempst P, Zhang Y (2005) Histone demethylation by a family of JmjC domain-containing proteins. *Nature* **439**: 811–816
- Wang GG, Cai L, Pasillas MP, Kamps MP (2007) NUP98-NSD1 links H3K36 methylation to Hox-A gene activation and leukaemogenesis. *Nat Cell Biol* **9**: 804–812
- Whetstone JR, Nottke A, Lan F, Huarte M, Smolnikov S, Chen Z, Spooner E, Li E, Zhang G, Colaiacovo M, Shi Y (2006) Reversal of histone lysine trimethylation by the JMJD2 family of histone demethylases. *Cell* **125**: 467–481
- Winkler GS, Kristjuhan A, Erdjument-Bromage H, Tempst P, Svejstrup JQ (2002) Elongator is a histone H3 and H4 acetyltransferase important for normal histone acetylation levels *in vivo*. *Proc Natl Acad Sci USA* **99**: 3517–3522
- Wirbelauer C, Bell O, Schubeler D (2005) Variant histone H3.3 is deposited at sites of nucleosomal displacement throughout transcribed genes while active histone modifications show a promoter-proximal bias. *Genes Dev* **19**: 1761–1766
- Wittschieben BO, Otero G, de Bizemont T, Fellows J, Erdjument-Bromage H, Ohba R, Li Y, Allis CD, Tempst P, Svejstrup JQ (1999) A novel histone acetyltransferase is an integral subunit of elongating RNA polymerase II holoenzyme. *Mol Cell* **4**: 123–128
- Xiao T, Hall H, Kizer KO, Shibata Y, Hall MC, Borchers CH, Strahl BD (2003) Phosphorylation of RNA polymerase II CTD regulates H3 methylation in yeast. *Genes Dev* **17**: 654–663

3.1.2 H4K20 monomethylation during chromatin assembly

Immediately after histone deposition, DNA is assembled into chromatin and chromatin maturation begins in order to fulfill the needs of the cell. Due to the speed, maturation processes are difficult to follow *in vivo* and we made use of an *in vitro* approach. By using an *in vitro* chromatin assembly system (Becker et al. 1992) the dynamics of histone modifications was analyzed before and after chromatin assembly. In agreement with what has been described before H4 histones carry a diacetyl mark at lysine 5 and 12 prior to deposition onto chromatin (Sobel et al. 1995; Benson et al. 2006; Loyola et al. 2006). Immediately after deposition of H4 lysine 20 is monomethylated by Pr-Set7. The monomethylase prefers nucleosomes as a substrate. The monomethylation mark is recognized by dl(3)MBT (Lethal(3)malignant brain tumor-like 3) (Jeesun Kim et al. 2006; Haitao Li et al. 2007) however not alone but in a complex with dRpd3 followed by the deacetylation of H4K5 and K12. This chain of consecutive steps seems to support chromatin maturation.

Annette N.D. Scharf, Karin Meier, Volker Seitz, Alexander Brehm, Axel Imhof. Monomethylation of lysine 20 on histone H4 facilitates chromatin maturation. *MCB*, 2009 Jan; 29 (1): 57-67.

Declaration of contribution to “Monomethylation of lysine 20 on histone H4 facilitates chromatin maturation”: The project was conceived by Axel Imhof and me. Experiments for Figure 4 and 5f were performed by Volker Seitz and experiments for Figure 6b, c, d were performed by Karin Meier. Karin Meier also wrote the corresponding figure legends and material and method sections. Antibody generation against dl(3)MBT was conducted by Elisabeth Kremmer. All assembly and SAH experiments and all corresponding mass spectrometry results and immunoblots as well as MNase digestions were performed by me (Figure 1; 2; 3; 4a, b, c, d, e and 6a, e). I prepared all corresponding figures, legends and material and method sections. I wrote the manuscript with the help of Axel Imhof and Alexander Brehm.

Monomethylation of Lysine 20 on Histone H4 Facilitates Chromatin Maturation[∇]

Annette N. D. Scharf,¹ Karin Meier,² Volker Seitz,¹† Elisabeth Kremmer,³
Alexander Brehm,² and Axel Imhof^{1*}

Munich Centre of Integrated Protein Science and Adolf-Butenandt Institute, Ludwig Maximilians University of Munich, Schillerstr. 44, 80336 Munich, Germany¹; Institut für Molekularbiologie und Tumorforschung (IMT), Philipps-Universität Marburg, Emil-Mannkopff-Str. 2, 35033 Marburg, Germany²; and Helmholtz Zentrum München, Institute of Molecular Immunology, Marchioninistraße 25, 81377 Munich, Germany³

Received 23 June 2008/Returned for modification 6 August 2008/Accepted 22 October 2008

Histone modifications play an important role in shaping chromatin structure. Here, we describe the use of an in vitro chromatin assembly system from *Drosophila* embryo extracts to investigate the dynamic changes of histone modifications subsequent to histone deposition. In accordance with what has been observed in vivo, we find a deacetylation of the initially diacetylated isoform of histone H4, which is dependent on chromatin assembly. Immediately after deposition of the histones onto DNA, H4 is monomethylated at K20, which is required for an efficient deacetylation of the H4 molecule. H4K20 methylation-dependent dl(3)MBT association with chromatin and the identification of a dl(3)MBT-dRPD3 complex suggest that a deacetylase is specifically recruited to the monomethylated substrate through interaction with dl(3)MBT. Our data demonstrate that histone modifications are added and removed during chromatin assembly in a highly regulated manner.

All DNA in a eukaryotic cell is assembled into chromatin to fit it into the restricted nuclear space and to organize the genome (29, 56). As the DNA content of a cell doubles during S-phase of the cell cycle, the cell has to provide sufficient histone molecules to package the newly replicated DNA into chromatin. This is achieved mainly by a coupling of histone and DNA synthesis (37). The progression of the DNA replication machinery disrupts the nucleosome in front of the replication fork, which is then reassembled onto the newly synthesized DNA strands in a random manner (15, 20). The remaining gaps are subsequently filled up with newly translated histone molecules, leading to a mosaic pattern of new and old histone octamers (2, 21). This process is assisted by the action of nuclear chaperones, which bind to the histones before deposition (14, 34). The newly deposited histones are more loosely associated with the DNA than the bulk histones and mature slowly into a more stable chromatin structure. Assembly is achieved via an ordered deposition of H3 and H4, followed by the binding of H2A/H2B dimers and finally the interaction of the linker histone H1 with the chromatin fiber (19–22, 49).

Posttranslational modifications of histone molecules are generally considered to play an important role during the establishment and maintenance of chromatin structures. The combination of histone modifications has been proposed to

constitute a “histone code” (23, 55), which is involved in the maintenance of epigenetic information. However, it is unclear how histone modifications are replicated during cellular division and DNA repair when newly translated histones are deposited onto the DNA.

Modification marks can be stably maintained through multiple mitotic divisions (3, 23, 30, 55). However, for most histone modifications, the molecular mechanisms that regulate this maintenance have so far remained elusive. A key aspect of this maintenance or reestablishment of modification patterns is the precise copying of histone modification patterns from the parental histone to the newly synthesized ones. As the newly synthesized histones carry a specific histone modification pattern that is distinct from the histones found within chromatin (32), this copying not only involves a deposition of particular marks but also the removal of others. Newly synthesized histone H4 is acetylated at position K5 and K12 (5, 32, 50). Recently, a class II histone deacetylase (HDAC) activity (Thd2) has been isolated that specifically deacetylates the replication-dependent H4 modifications in *Tetrahymena thermophila* (48). Thd2 localizes specifically to the micronucleus of the ciliate and is involved in chromatin maturation, which further demonstrates the importance of the deacetylation for chromatin fiber formation. Histone H3 is acetylated mainly at K9 and K14 in HeLa cells and at K14 and 23 in *Drosophila* cells, suggesting a lower degree of conservation of the H3 acetylation sites (7, 32, 50). This acetylation pattern is rapidly removed when histones are deposited. In the case of H4, deacetylation happens within minutes, making the analysis of the diacetylated H4 isoform during chromatin assembly difficult (5, 40).

In order to get a better understanding of the processes that occur during histone deposition, we performed a detailed,

* Corresponding author. Mailing address: Histone Modifications Group, Munich Centre of Integrated Protein Science and Adolf-Butenandt Institute, Ludwig Maximilians University of Munich, Schillerstr. 44, 80336 Munich, Germany. Phone: 49 89 218075420. Fax: 49 89 218075440. E-mail: Imhof@lmu.de.

† Present address: Universitätsklinikum Heidelberg, Klinik für Anaesthesiologie, Im Neuenheimer Feld 110, 69120 Heidelberg, Germany.

[∇] Published ahead of print on 10 November 2008.

time-resolved analysis of histone modifications during chromatin assembly. The use of an *in vitro* assembly system allows a precise analysis of the turnover of histone H4 modification during histone deposition, which is difficult to analyze *in vivo* due to its low half-life. We find that deacetylation is nonprocessive in that either the acetyl group at K12 or the one at K5 is removed from the H4 molecule independently of each other. After deposition, H4 is rapidly monomethylated at K20, which facilitates the subsequent deacetylation through the recruitment of a complex containing dl(3)MBT and the deacetylase dRpd3.

MATERIALS AND METHODS

Antibodies and immunoblotting. Polyclonal anti-dl(3)MBT antibody was raised in rabbits conjugated with three unrelated specific peptides (P1, PSGED KTRSTQKNNKQNTSASC; P2, YFERPLYDRPGRRPSAC; and P3, CLPEQS QTNGYKTDHHDQELS; Peptide Specialty Laboratories). For generation of monoclonal anti-dl(3)MBT antibodies, rats were immunized with either peptide P1 or P3 (antibodies MBT P1 6E6 and MBT P3 8F10, both isotype immunoglobulin G1) (see above). Anti-glutathione *S*-transferase (anti-GST) antibody was produced in rats. Anti-dRpd3 and anti-dHDAC3 antibodies were generous gifts from J. Müller and B. Turner, respectively. Monoclonal mouse anti-FLAG M2 antibody is commercially available (Sigma). For immunoblotting, proteins were transferred onto a polyvinylidene difluoride membrane (Roth), probed with the indicated antibodies, detected with enhanced chemiluminescence-labeled secondary antibodies, and detected using the Immobilon Western kit (Millipore).

Chromatin assembly extract (*Drosophila* assembly extract [DREX]). Zero to 90 min after egg laying, *Drosophila* embryos were rinsed in water and allowed to settle into embryo wash buffer (0.7% NaCl, 0.05% Triton X-100) on ice to arrest further development. After four successive collections, the pooled harvest was dechorionated. The wash buffer was decanted and replaced with wash buffer at room temperature, and the volume was adjusted to 200 ml. After the addition of 60 ml of 13% hypochlorite, the embryos were stirred vigorously for 3 min, poured back into the collection sieve, and rinsed extensively with tap water. Then they were allowed to settle in 200 ml of wash buffer for about 3 min, after which the supernatant (containing the chorions) was aspirated off. Two more settlings were performed, one in 0.7% NaCl and one in extract buffer (10 mM HEPES [pH 7.6], 10 mM KCl, 1.5 mM MgCl₂, 0.5 mM EGTA, 10% glycerol, 10 mM 3-glycerophosphate, 1 mM dithiothreitol [DTT], and 0.2 mM phenylmethylsulfonyl fluoride [PMSF], added freshly) at 4°C. The embryos in extract buffer were settled in a 60-ml glass homogenizer on ice for about 15 min, and the volume of the packed embryos was estimated. The supernatant was aspirated, and the embryos were homogenized by one complete stroke (3,000 rpm) and 10 strokes at 1,500 rpm with a pestle connected to a drill press. Homogenate was supplemented with an additional 3.5 mM MgCl₂ from a 1 M MgCl₂ stock solution and quickly mixed (final MgCl₂ concentration, 5 mM). Nuclei were pelleted by centrifugation for 10 min at 10,000 rpm in an SS34 rotor (Sorvall). The supernatant was clarified by centrifugation for 2 h at 45,000 rpm (190,000 × *g*) in an SW 56 rotor (Beckman) and collected with a syringe, avoiding the floating layer of lipids. Aliquots (300 to 500 μl) were frozen in liquid nitrogen. Protein concentrations were determined with the Bradford assay, using bovine serum albumin (BSA) as the standard (4).

Chromatin assembly on immobilized DNA. One microgram of rRNA was immobilized onto 0.3-mg paramagnetic streptavidin beads (Dynal) in EX100 buffer (10 mM HEPES [pH 7.6], 100 mM NaCl, 1.5 mM MgCl₂, 0.5 mM EGTA, 10% [vol/vol] glycerol, 0.2 mM PMSF, 1 mM DTT) and, after being washed extensively, blocked for 30 min with BSA (1.75 μg/μl) in EX100. The DNA on the beads was concentrated on a magnetic concentrator (Dynal) and resuspended in a total volume of 240 μl containing 80 μl DREX and ATP regenerating system (3 mM ATP, 30 mM creatine phosphate, 10 μg creatine kinase/ml, 3 mM MgCl₂, and 1 mM DTT). Whenever indicated, TSA was added in a total concentration of 50 nM sodium butyrate in a final concentration of 2 mM, and *S*-adenosyl-homocystein (SAH) was added as stated. The reaction mixture was rotated at 26°C for the denoted time period in order to reconstitute chromatin. After extensively washing the chromatin with EX500 (10 mM HEPES [pH 7.6], 500 mM NaCl, 1.5 mM MgCl₂, 0.5 mM EGTA, 10% [vol/vol] glycerol, 0.2 mM PMSF, 1 mM DTT), it was subjected to mass spectrometry, micrococcal digestion, or Western blotting.

Expression and purification of recombinant proteins. dl(3)MBT cDNA was obtained from the Berkeley *Drosophila* Genome Project (clone no. LD05287). This sequence was used for generation of a vector expressing FLAG-tagged

dl(3)MBT [pPac-FLAGdl(3)MBT] (9) by PCR (details available upon request). For generation of a stable S2 line, cells (8 × 10⁶) cultured at 26°C in Schneider's *Drosophila* medium (10% fetal bovine serum; Sigma) were cotransfected with 20 μg pPacFLAG-dl(3)mbt and 1 μg pPuro (a kind gift from E. Izaurralde) using calcium phosphate transfection according to standard procedures. Two days posttransfection, cells were selected for 4 to 6 weeks using 5 μg/ml puromycin (Sigma), clones were picked and expanded, and expression was verified by Western blotting. For baculovirus-mediated expression, FLAG-tagged dl(3)MBT and a FLAG-tagged construct containing the three MBT domains were cloned into pVL1392. Virus production and protein purification have been previously described (10). A construct containing the three MBT domains of dl(3)MBT was cloned into pGex4T1 by PCR (details available upon request). Expression and purification of GST fusion proteins were performed following standard procedures.

Histone purification and nucleosome assembly by salt dialysis. Recombinant histones or histones purified from *Drosophila* embryos (native histones) were expressed, purified, and reconstituted into octamers as described previously (12). Chromatin was reconstituted by salt dialysis overnight at 4°C using NaCl concentrations of 2 M to 0.1 M.

HDAC assay. HDAC assays were performed as described before (10). In some reactions, 500 μM TSA was added.

Immunoprecipitations. Four hundred micrograms of S2 nuclear extract was incubated with 50 μl monoclonal antibodies in a final volume of 350 μl phosphate-buffered saline for 2 h at 4°C with rotation. Five microliters of Protein G beads (GE Healthcare) was added, and incubation was continued for 1 h. Following extensive washing with phosphate-buffered saline, beads were used immediately for HDAC assays (see above). FLAG immunoprecipitations (FLAG-IP) were carried out with S2 nuclear extracts (400 μg total protein) and 5 μl anti-FLAG agarose (Sigma) in a total volume of 400 μl FLAG-IP buffer (25 mM HEPES [pH 7.6], 12.5 mM MgCl₂, 0.1 mM EDTA [pH 8.0], 10% glycerol, 0.1% NP-40, 150 mM NaCl). Incubation was performed for 3 h at 4°C with rotation. After being extensively washed with FLAG-IP, buffer beads were either used immediately in HDAC assays or analyzed by Western blotting. In some experiments prior to immunoprecipitation, nuclear extracts were incubated for 30 min with ethidium bromide (50 μg/ml).

Mass spectrometry. Histones were separated by sodium dodecyl sulfate-polyacrylamide gel electrophoresis (SDS-PAGE). Coomassie blue-stained bands were excised. Digestions were carried out overnight with 200 ng sequencing grade trypsin (Promega); in this case, histones were chemically modified beforehand by being treated with propionic anhydride to convert free amino groups to propionic amides of lysine residues. In order to purify the peptides from the contaminating salts or acrylamide, the peptide solution was passed over a pipette tip containing small amounts of C₁₈ reversed phase material (ZipTip; Millipore). After three 10-μl wash steps with 0.1% trifluoroacetic acid, the bound peptides were eluted with 1 μl of prepared matrix solution (saturated α-cyanohydroxycinnamic-acid [Sigma] dissolved in 50% acetonitrile [vol/vol], 0.3% trifluoroacetic acid [vol/vol]) directly onto the target plate. Samples were air dried to allow cocrystallization of the peptides and the matrix. The target plate was loaded in a Voyager DE STR spectrometer, and spectra were analyzed using the in-house-developed software Manuelito. For tandem mass spectrometry (MS-MS), collision-induced decay spectra were recorded on a Q-Star XL instrument with manually adjusted collision energies. Fragment spectra were interpreted manually.

Methyltransferase activity. Assays were carried out in 25 μl of methyltransferase buffer (50 mM Tris-HCl [pH 8.0], 0.5 mM DTT) containing the indicated substrate and 500 nCi *S*-adenosyl-(methyl-³H)-L-methionine (25 μCi/ml) (Amersham) as the methyl donor. Reactions were stopped by spotting 20 μl on P81 filter paper. Filter papers were then washed three times for 10 min in 50 mM carbonate buffer (pH 9.2) and dried, and ³H incorporation was measured by scintillation counting.

Micrococcal nuclease digestion. Chromatin from 2 μg DNA was resuspended in EX100 containing 5 mM CaCl₂ and 100 Boehringer units of MNase (Sigma). After 30, 90, and 300 s at room temperature, the digestion was stopped by adding 4% SDS and 100 mM EDTA. The suspension was subjected to RNase A and proteinase K treatment, and precipitated DNA was separated onto a 1.3% agarose gel. A 123-bp ladder (Invitrogen) was used as a size marker.

Nuclear extract preparation. Nuclear extracts from S2 cells were prepared as described previously (35).

Peptide pull-down assay. H4 peptides comprising amino acids 16 to 25 with K20 that were either unmodified or mono-, di-, or tri-methylated were coupled to SulfoLink coupling gel (Pierce) via a C-terminal cysteine according to the manufacturer's protocol. Immobilized peptides were preblocked with 1 μg/μl BSA in binding buffer (25 mM Tris [pH 8.0], 150 mM NaCl, 2 mM EDTA, 0.5%

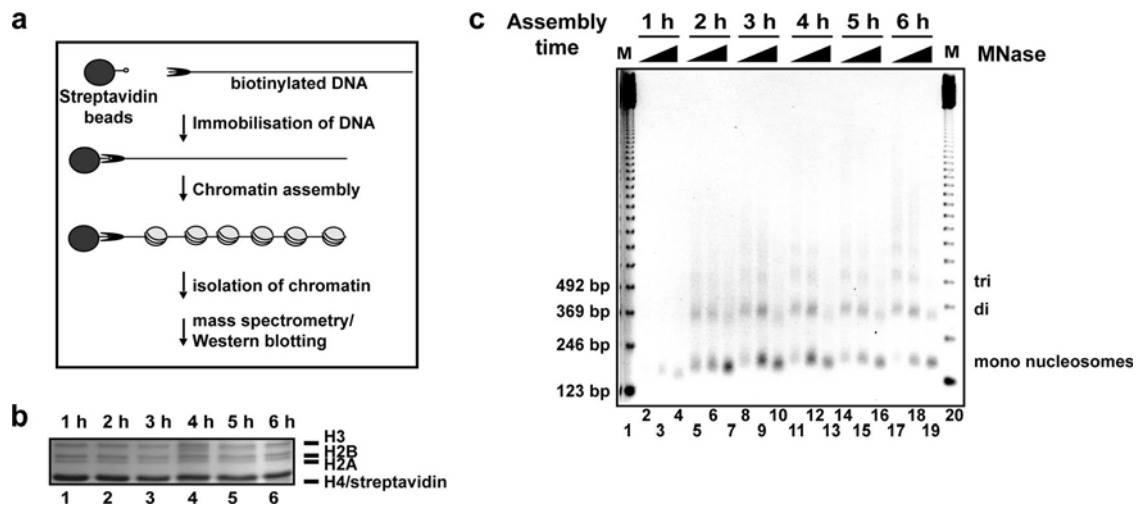


FIG. 1. DREX-mediated chromatin assembly. (a) Scheme of chromatin reconstitution protocol. The DNA used for chromatin assembly is a linearized biotinylated fragment containing 12 repeats of a 5S nucleosome positioning sequence. Two micrograms of DNA bound to paramagnetic beads was reconstituted into chromatin for 1 to 6 h at 26°C using 80 μ l DREX. (b) Corresponding histones stained with Coomassie blue. When boiling streptavidin-coated beads, a strongly stained streptavidin band appeared at the same molecular weight as H4. It is therefore labeled H4/streptavidin. (c) Micrococcal nuclease digestion pattern of the reconstituted chromatin. M, lanes containing the 123-bp ladder as a molecular weight marker; MNase, micrococcal nuclease.

NP-40) for 1 h at 4°C. Recombinant GST-3MBT or FLAG-tagged 3MBT were incubated with preblocked immobilized peptides for 2 h at 4°C in binding buffer with agitation. After extensive washing with binding buffer, peptide-bound protein was analyzed by Western blotting.

RESULTS

In order to determine the kinetics of histone modifications during chromatin assembly, we used a well-characterized S-150 chromatin assembly extract (4) prepared from early *Drosophila* embryos. This extract can be used to assemble large fragments of DNA into an ordered nucleosomal array that closely resembles the chromatin structure observed in vivo (6). For our experiments, we used an array of nucleosome positioning sequences derived from the sea urchin 5S rRNA gene (16). The linearized DNA was biotinylated and subsequently immobilized using magnetic streptavidin beads (4, 12) (Fig. 1a). Although the histone deposition is very fast and occurs within the first hour (4) (Fig. 1b), properly spaced chromatin can be detected only after 4 to 5 h of assembly, as judged by micrococcal nuclease digestion (Fig. 1c). Histones carry specific modifications before deposition onto chromatin in vivo (5, 14, 32), which are rapidly removed after they have been loaded onto DNA. Therefore, we tested whether we could observe similar modification kinetics in the in vitro assembly system.

In accordance with the modifications that were observed on storage histones in *Drosophila* and *Xenopus* embryos early in development (7, 11, 46), histone H4 is found acetylated at the N terminus in a mainly diacetylated form in the extract that we used for assembly (Fig. 2a). We mapped the position of the two acetyl groups to positions K5 and K12 using MS/MS (Fig. 2c). In order to investigate the dynamic changes of histone modifications, chromatin was isolated at various times during assembly and the modification patterns were analyzed by mass spectrometry and Western blotting. As seen in vivo and in the *Xenopus* assembly system (46), the diacetyl form of H4 is

deacetylated during chromatin assembly. Interestingly, the deacetylation is relatively slow, with a half-time of 150 min for the diacetylated form as measured by mass spectrometry and Western blotting (Fig. 2b and data not shown). The deacetylation is not a rapid processive event, as we see an intermediate accumulation of the monoacetylated form (Fig. 2b).

In addition to that, we do not observe a preferred order of deacetylation, as acetyl groups are removed from K5 and K12 with similar kinetics independently of each other (data not shown). The deacetylation is inhibited by the addition of HDAC inhibitors, such as sodium butyrate or TSA, suggesting that class I or class II HDAC activity is targeted to the newly assembled chromatin (Fig. 2d; compare to Fig. 2b for a 0-h time point). During longer assembly times, we do observe some residual deacetylation in the presence of TSA and butyrate, albeit with a much lower efficiency (Fig. 2d). No significant deacetylation occurs when the extract is incubated for the same time in the absence of DNA, showing that the process of assembly is essential for the removal of the acetyl groups (Fig. 2b).

We next wondered whether additional modifications would influence the deacetylation of H4K5 and H4K12. The only methylation that we observed on any histone within the 6 h of chromatin assembly is a monomethylation of H4 at lysine 20. This methylation is strictly dependent on the assembly of H4 into chromatin, as it is not detected in H4 isolated from the assembly extract prior to the addition of DNA (Fig. 3b, lane 1). Monomethylation of H4K20 in H4 increases during assembly as judged by mass spectrometry and Western blotting (Fig. 3). We do not observe a further methylation of H4 during chromatin assembly, leading to di- or trimethylated forms.

The key monomethylase specific for H4 is PR-SET7 (43). As the enzyme is clearly present in DREX, as judged by Western blotting (data not shown), we hypothesized that this enzyme is responsible for the modification in the extract. In order to

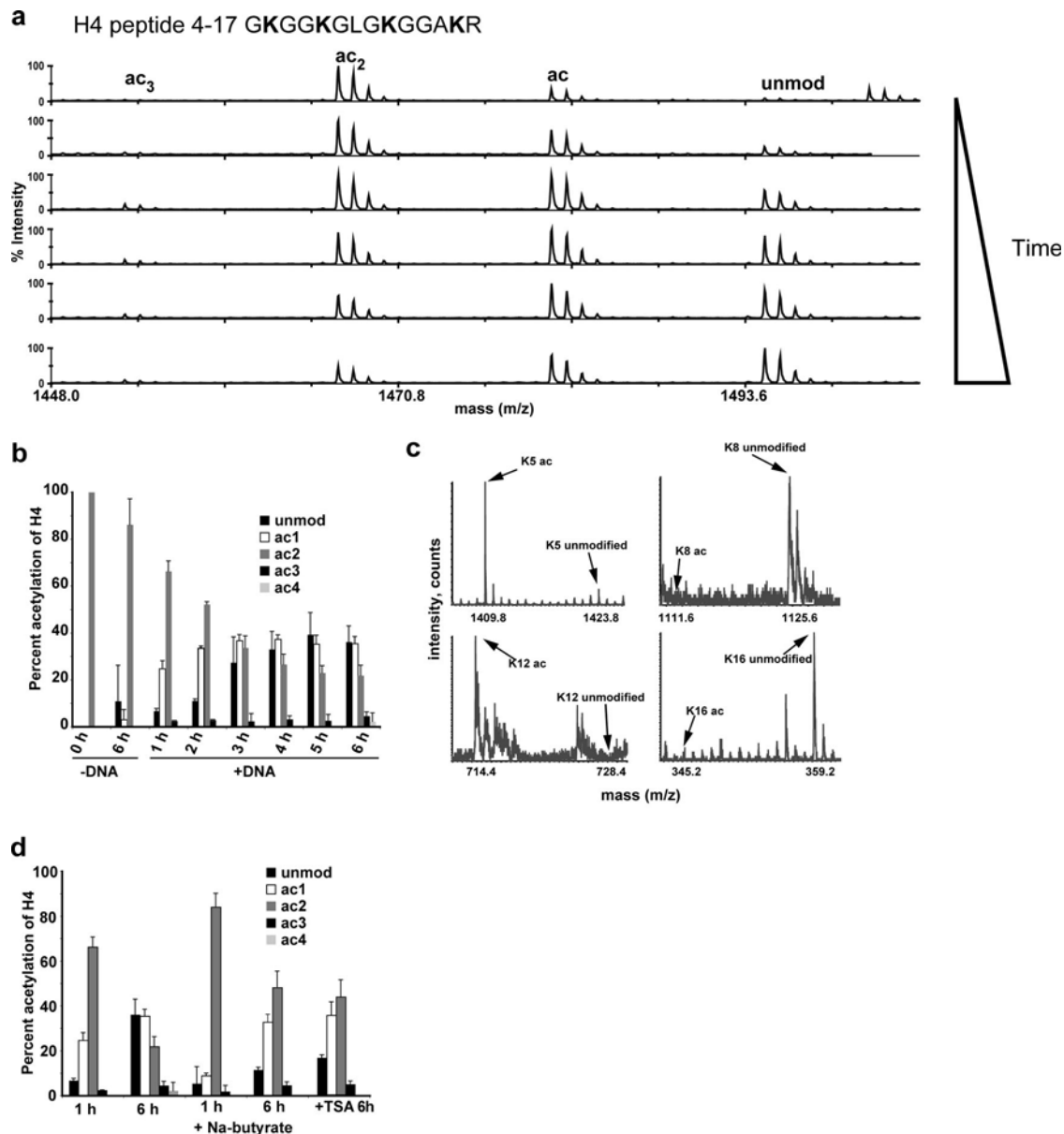


FIG. 2. Dynamics of modifications on H4 peptide 4-17 during DREX assembly. (a) Top, sequence of H4 peptide 4-17; bottom, time course analysis of H4 peptide 4-17 by matrix-assisted laser desorption ionization–time of flight (MALDI-TOF) analysis. Chromatin was reconstituted as described above. The reconstitution was stopped after 1, 2, 3, 4, 5, and 6 h, chromatin attached to paramagnetic beads was washed, and histones were separated by 18% SDS-PAGE. H4 was cut out and subjected to mass spectrometric analysis. (b) Quantification of MALDI-TOF data that are shown in panel a. As a control, DREX was incubated at 26°C without DNA for 0 h or 6 h and labeled as –DNA 0 h/6 h. unmod, unmodified; ac, acetylation. (c) MS-MS spectra generated from the diacetylated peak from 1 h DREX assembly. (d) Quantification of MALDI-TOF analysis. HDAC inhibitors were added to the chromatin assembly reaction, and H4 was analyzed as described above. TSA, trichostatin A; Na-butyrate, sodium butyrate.

better study the *Drosophila* PR-SET7 enzyme, we expressed the full-length protein in bacteria and studied its enzymatic properties (Fig. 4). The recombinant PR-SET7 enzyme is a very efficient nucleosomal methyltransferase but only poorly methylates recombinant H4 when it is not within a nucleosomal context (Fig. 4a and b). As it methylates preacetylated H4 in our system, we tested whether PR-SET7 may methylate chromatin that is acetylated on K5 and 12 preferentially. In order to do this, we fully acetylated H4 on positions 5 and 12

using a recombinantly expressed yHAT1 enzyme (38), assembled it into chromatin, and investigated its ability to serve as a substrate for PR-SET7. Consistent with the substrate requirements of the human enzyme, we do not find an effect on the methylation efficiency after acetylation at positions 5 and 12 in vitro (Fig. 4c and d).

The dependency of PR-SET7 on the presence of nucleosomal DNA and the fact that the enzyme does not distinguish between differentially acetylated substrates let us conclude that

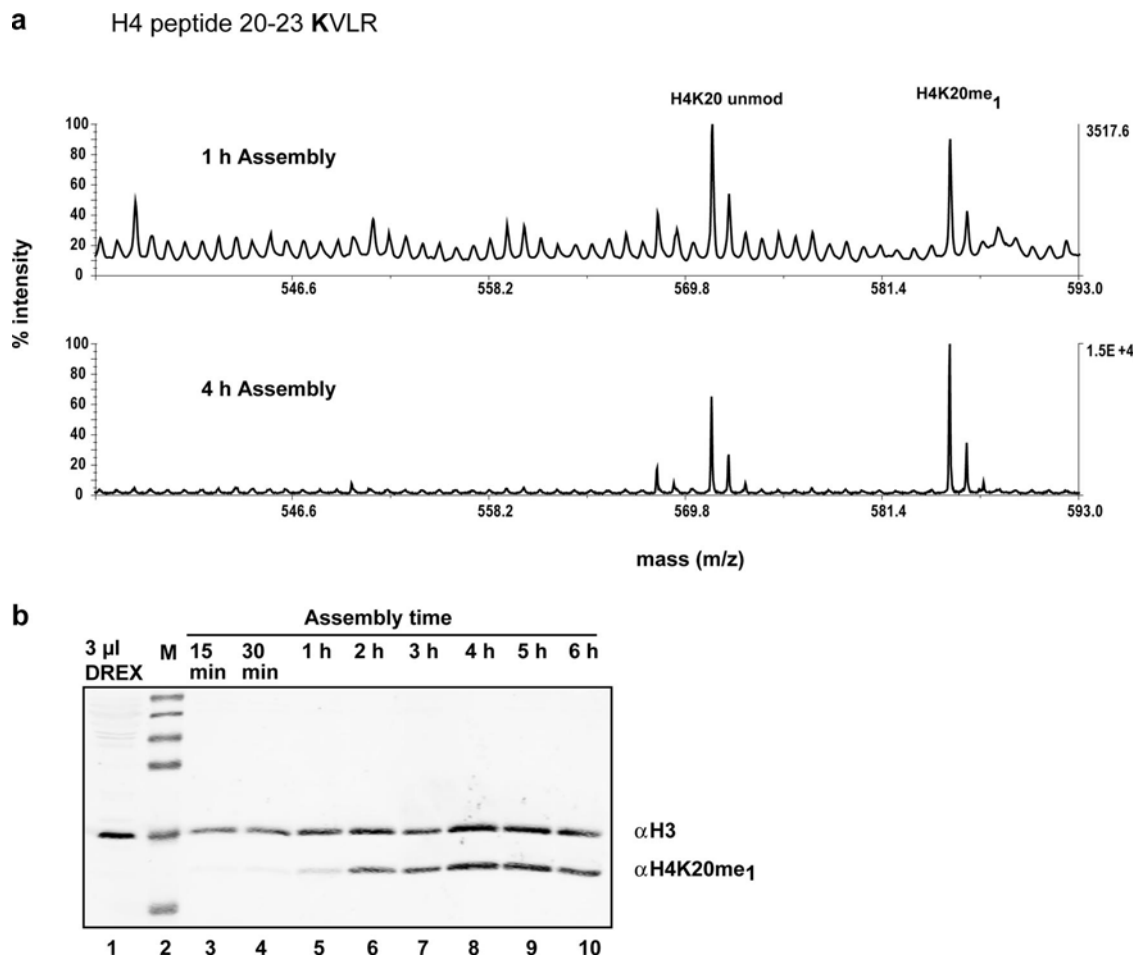


FIG. 3. H4 becomes monomethylated at K20 after assembly. (a) Chromatin was assembled as shown before using DREX. Corresponding histones were separated by 18% SDS-PAGE and then digested with AspN prior to mass spectrometric analysis. Also shown is a comparison of posttranslational modifications of the H4 peptide 20-23 1 h (top) and 4 h (bottom) after the assembly reaction. (b) Western blot analysis of kinetics of H4K20me₁. H3 is serving as a loading control. M, molecular weight marker; α H3, anti-H3; α H4K20me₁, anti-H4K20me₁.

PR-SET7 senses the proper nucleosome assembly rather than the acetylation state of the histone.

In order to study the effect of monomethylation on the process of histone modification maturation, we used SAH to inhibit methyltransferase activity during chromatin assembly. SAH is the reaction product of all methyltransferases that use SAM as cofactors and acts as a competitive inhibitor. In order to test which concentration to use in the assembly reaction, we first analyzed whether PR-SET7 could indeed be inhibited by SAH. In vitro methyltransferase assays showed that a concentration of 500 μ g/ml very efficiently inhibits PR-SET7 (Fig. 5a). When we used SAH in an assembly, we could indeed reduce the level of monomethylation in a concentration-dependent manner (Fig. 5b and d, top). However, we did not observe a major difference in chromatin spacing or in the level of chromatin assembly as judged by nuclease digestion (Fig. 5c).

When we determined the degree of H4 deacetylation of untreated chromatin with the SAH-treated chromatin, we found a substantially increased level of H4 acetylation when monomethylation is inhibited by SAH, arguing for a decrease in acetylation efficiency in the presence of SAH (Fig. 5d, bottom). This was not due to an inhibition of HDAC's presence in

the assembly extract, as the overall levels of HDAC activity in the extract did not decrease (Fig. 5e). Therefore, we wondered whether a specific deacetylase may be targeted to the monomethylated chromatin in order to ensure efficient deacetylation. We first tested the hypothesis that the most abundant deacetylase in the extract, dRpd3, may preferentially deacetylate a premethylated peptide. However, we did not observe a significant increase in the HDAC activity of recombinant dRpd3 when a K20-methylated H4 peptide was used as substrate (Fig. 5f). Another possible explanation for our observation could be that the deacetylase responsible for the removal of the acetyl groups from K5 and K12 after chromatin assembly is brought to methylated H4 by an additional targeting factor. However, HDAC complexes identified to date lack domains capable of binding methylated H4K20. One of the domains that binds monomethylated H4K20 in vitro is the MBT domain (28, 31, 54). *Drosophila* sp. have three genes that code for MBT-containing proteins SCM, dSMBT, and dl(3)MBT. Mutations in SCM and dSfmbt result in homeotic transformations, whereas mutations in dl(3)MBT show effects on the cell cycle, such as a block in mitosis (58). The cell cycle phenotype displayed by dl(3)MBT mutants is consistent with a role in chromatin as-

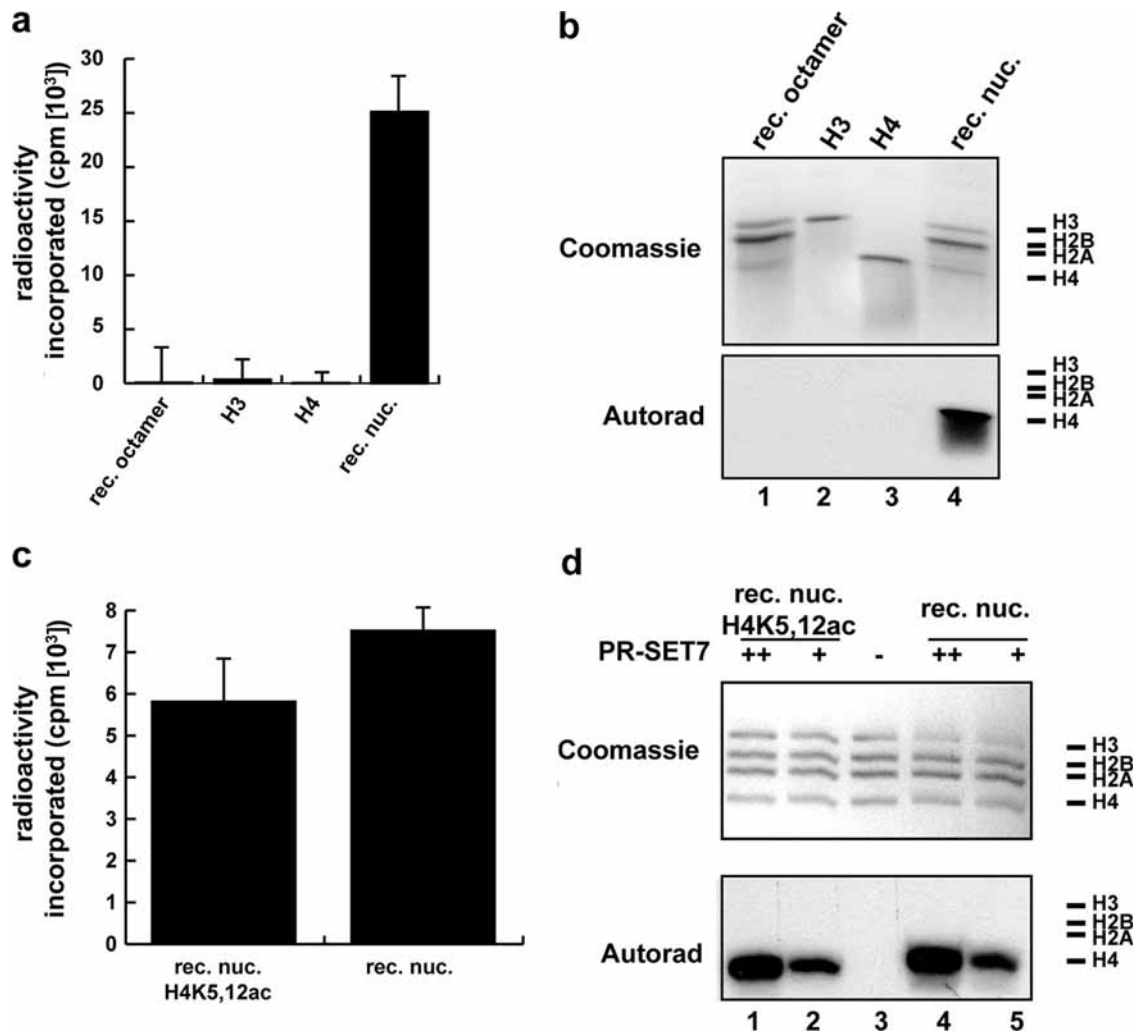


FIG. 4. PR-SET7 needs nucleosomes as a substrate. (a) Recombinant dPR-SET7 was cloned into a pMyb vector, expressed in bacteria, purified over chitin affinity chromatography according to the manufacturer's instructions (New England Biolabs), and assayed for HMTase activity on different substrates. The histogram shows the radioactivity incorporated. rec. nuc., recombinant nucleosomes; rec. octamer, recombinant octamer. (b) Autoradiography of the experiment described for panel a. (c) Methylation of recombinant nucleosomes and nucleosomes acetylated at K5 and K12 by dPR-SET7. (d) Autoradiography of the experiments described for panel c.

sembly. Moreover, similar phenotypes have been observed in neuroblasts that are deficient for PR-SET7 (43).

We wondered whether dl(3)MBT might be recruited to chromatin during assembly. To check this, we used an antibody that specifically recognizes the dl(3)MBT protein and observed an efficient recruitment of this protein to in vitro-assembled chromatin similar to the monomethylation of H4K20 (Fig. 6a). We then verified that the MBT domains of dl(3)MBT can indeed bind to methylated histone H4 tails in vitro. We incubated a GST fusion containing the three dl(3)MBT MBT domains with immobilized histone H4 peptides. As has been shown previously for the human orthologue, the dl(3)MBT MBT domains bound to histone H4 tails in this assay and displayed a strong preference for mono- and dimethylated H4K20 (54) (Fig. 6b). The MBT domains of dl(3)MBT bound more strongly to tails with a methylated K20 residue than to the unmodified tail (Fig. 6b, compare lanes 2 to 5). In contrast to human hl(3)MBTL1 (31), dl(3)MBT bound with increased

affinity to all three methylated H4K20 peptides with an enhanced affinity for H4K20me₁ and H4K20me₂. To exclude the possibility that a posttranslational modification may influence dl(3)MBT's ability to distinguish between the differentially methylated peptides, we also expressed FLAG-tagged MBT domains using a baculoviral expression system. Binding studies using the protein expressed in a eukaryotic system did not differ significantly from the bacterially expressed protein (Fig. 6b, compare top and bottom). These results suggest that dl(3)MBT has the potential to specifically associate with H4K20-methylated H4 tails during chromatin assembly. We then investigated if dl(3)MBT associates with HDAC activity. We generated an S2 line stably expressing FLAG-tagged dl(3)MBT. Anti-FLAG immunoprecipitates were generated from this line and control S2 cells and subjected to HDAC assays in vitro (Fig. 6c, top). Whereas immunoprecipitation from control extracts yielded only background HDAC activity, immunoprecipitates from FLAG-tagged dl(3)MBT-containing

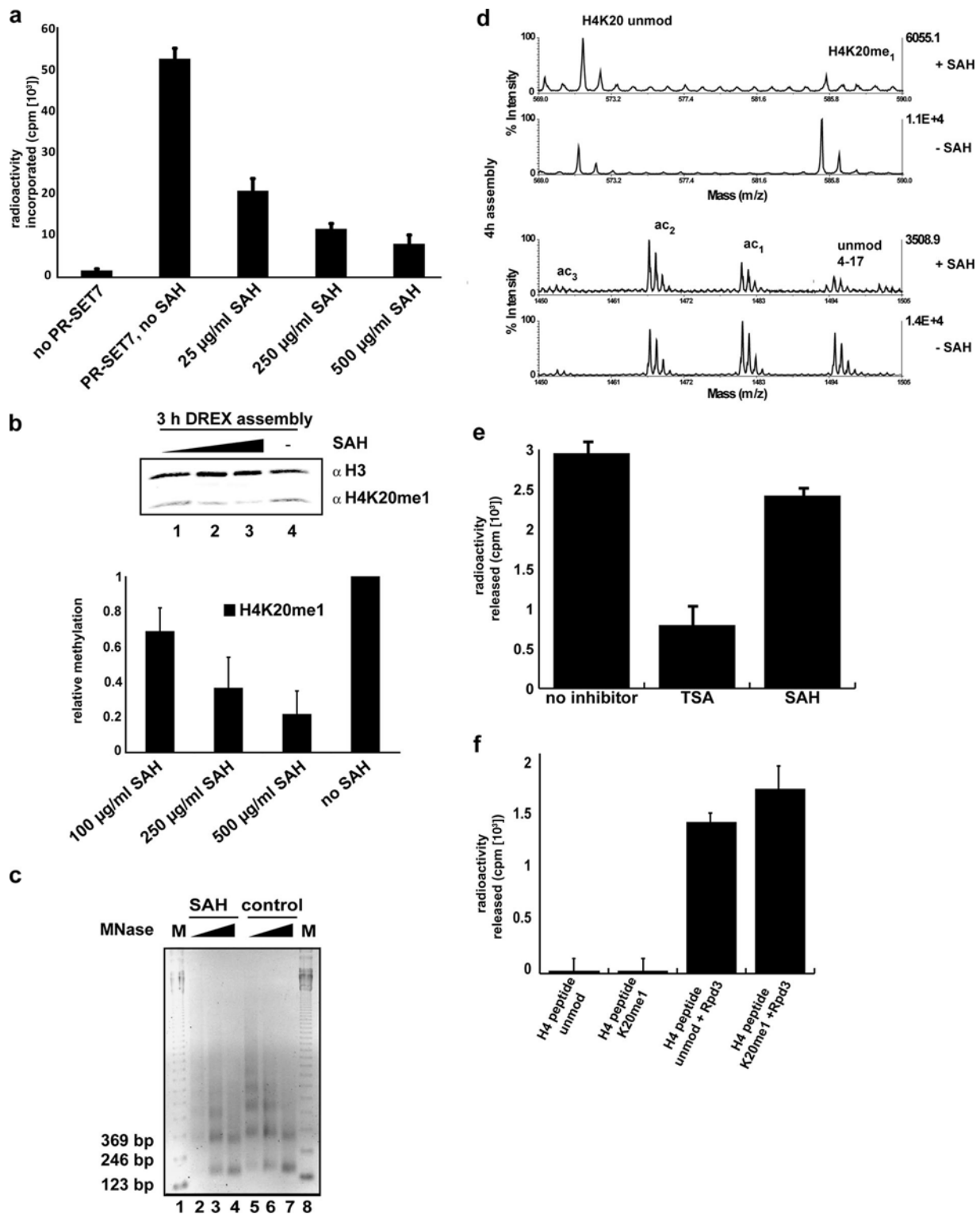


FIG. 5. Deacetylation of H4K5/K12 is dependent on H4K20 monomethylation. (a) A histone methyltransferase assay was performed in the presence and absence of SAH with and without PR-SET7. (b) Quantification of Western blot analysis. Chromatin was reconstituted for 3 h using DREX treated with and without SAH. Chromatin was washed, separated on an 18% protein gel, blotted to a nitrocellulose membrane, and detected with H4K20me₁ antibody. H3 was used as a loading control. (c) Micrococcal digestion pattern of the reconstituted chromatin incubated with or without SAH. M, lanes containing the 123-bp ladder as a molecular size marker. (d) Chromatin was assembled for 4 h. Histones were separated by 18% SDS-PAGE and then digested with trypsin prior to mass spectrometric analysis. Top two panels, comparison of unmodified H4K20 and monomethylated K20 peak of chromatin treated with or without SAH (shown is the peptide 20-23) (Fig. 3); bottom two panels, comparison of acetylation ratios of peptide 4-17 of chromatin that has been treated with and without SAH. (e) HDAC assay using 5 µl of chromatin assembly extract in the presence of either 500 µM TSA or 500 µg/ml SAH. (f) Deacetylation of an in vitro-acetylated peptide containing amino acids 9 to 29 of H4 carrying a methylation or no modification at K20.

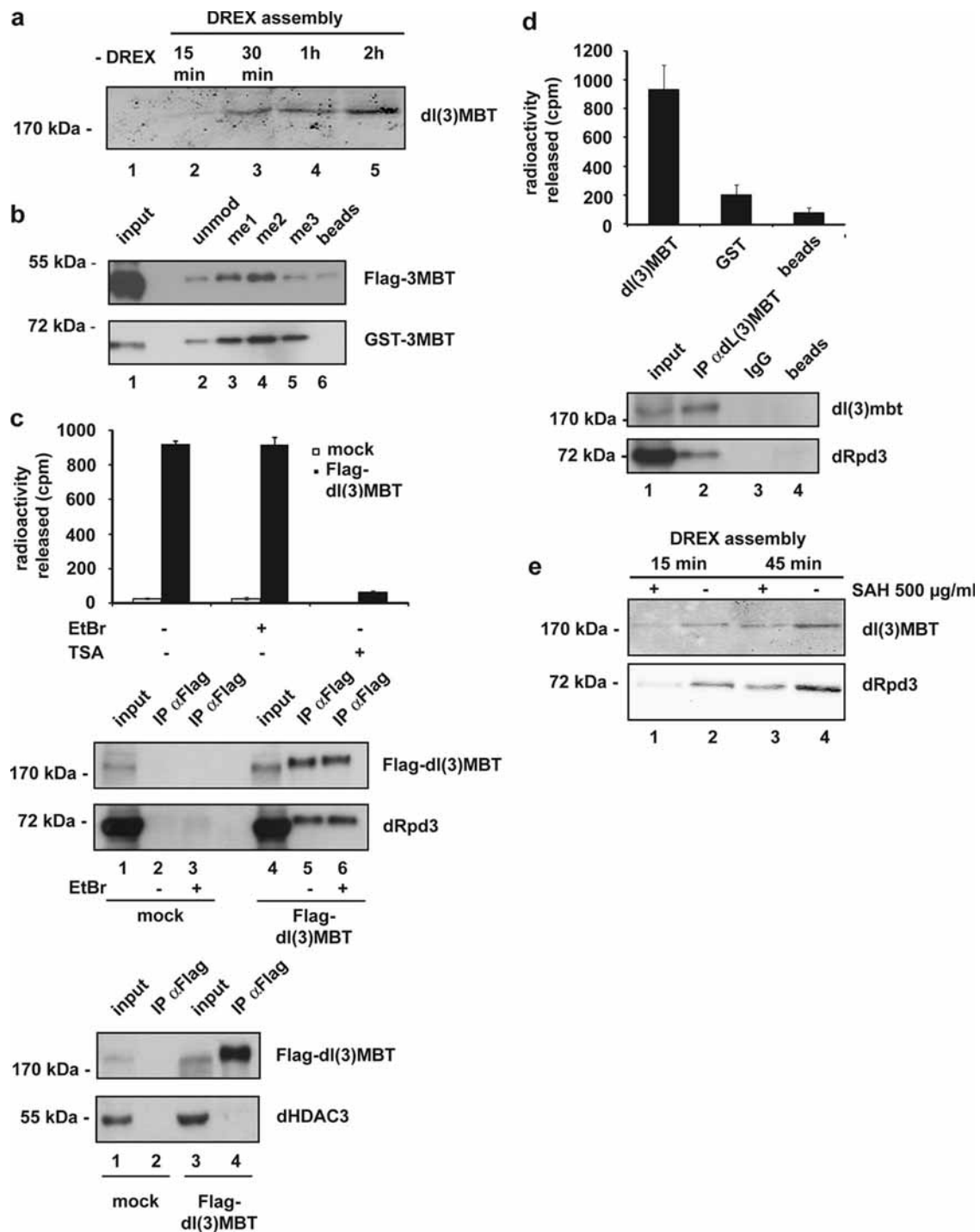


FIG. 6. Binding of dl(3)MBT to chromatin is inhibited by SAH, and dl(3)MBT is found in a complex with dRpd3. (a) After chromatin was reconstituted using DREX, bound dl(3)MBT was detected by Western blotting. (b) Immobilized H4 peptides (amino acids 16 to 25) were incubated with recombinant baculovirally expressed FLAG-3MBT (top) or recombinant GST-3MBT expressed in bacteria (bottom). Binding of GST- and FLAG-tagged proteins was analyzed by immunoblotting using anti-GST and anti-FLAG antibodies. unmod, unmodified H4 16-25 peptide; me1, me2, and me3, H4 peptide mono-, di-, and tri-methylated at K20; control, beads without peptide. (c, top) HDAC assays were performed with anti-FLAG immunoprecipitates (IP α Flag) from nuclear extracts of S2 cells (mock) and an S2 line stably expressing FLAG-tagged dl(3)MBT [Flag-dl(3)MBT]. Immunoprecipitations were carried out in the absence or presence of ethidium bromide (EtBr), and HDAC reactions were performed with or without TSA as indicated (middle and bottom). Anti-FLAG immunoprecipitates were analyzed by Western blotting for the presence of Flag-dl(3)MBT, dRpd3, and dHDAC3 as indicated. Ten percent of nuclear extracts were loaded as input. (d) HDAC assays were performed with immunoprecipitates obtained with a mixture of two monoclonal anti-dl(3)MBT antibodies (at a ratio of 1:1), anti-GST antibody, or no antibody (beads only) (top), and S2 nuclear extract was precipitated with dl(3)MBT antibody (bottom). Immunoprecipitations were subjected to Western blotting using anti-dRpd3 and anti-dl(3)MBT antibody as shown. (e) Chromatin was reconstituted for a specific time and treated with or without SAH (500 μ g/ml). The reconstitution was stopped after 15 and 45 min. Chromatin attached to beads was washed (100 mM NaCl) and separated by 18% SDS-PAGE. dl(3)MBT and dRPD3 were detected by a polyclonal antibody.

extracts had robust HDAC activity. To rule out that association of HDAC activity was a result of spurious coprecipitation of HDAC-containing chromatin fragments, immunoprecipitations were carried out in the presence of ethidium bromide to dissociate protein-DNA interactions. Ethidium bromide had no significant effect on dl(3)MBT-associated HDAC activity. Immunoprecipitated HDAC activity was sensitive to inhibition by TSA, suggesting that it was due to a class I HDAC. We therefore probed immunoprecipitates for the presence of the class I HDACs dRPD3 and dHDAC3 by Western blotting (Fig. 6c, middle and bottom). dRPD3 specifically coprecipitated with FLAG-tagged dl(3)MBT, and this interaction was not affected by the presence of ethidium bromide, confirming that it is due to a protein-protein interaction. In contrast, dHDAC3 could not be detected in the immunoprecipitates (Fig. 6c, bottom).

In order to verify that endogenous dl(3)MBT associates with HDAC activity (Fig. 6d, top), we immunoprecipitated S2 extracts with dl(3)MBT antibodies. Indeed, HDAC activity was precipitated by the dl(3)MBT but not by the control antibody. In addition, immunoprecipitation of dl(3)MBT coprecipitated endogenous dRPD3 (Fig. 6d, bottom).

Taken together, these results demonstrate that dl(3)MBT forms a complex with the HDAC dRPD3. In order to finally test whether this interaction and hence the recruitment might be responsible for the efficient deacetylation of newly assembled chromatin, we investigated the recruitment of dl(3)MBT and dRpd3 to chromatin during assembly. By using specific antibodies against dl(3)MBT and dRpd3, we could see an increase in dl(3)MBT and dRpd3 binding to chromatin with increasing assembly time (Fig. 6e, lanes 2 and 4). However, when the monomethylation of H4K20 was inhibited, this recruitment was greatly reduced (Fig. 6e, compare lanes 2 and 4 with lanes 1 and 3), suggesting a model in which the monomethylation of H4K20 indeed facilitates the recruitment of the deacetylase by virtue of its interaction with dl(3)MBT, thereby assisting the maturation of histone modifications during chromatin assembly.

DISCUSSION

In this work, we use an *in vitro* chromatin assembly system to recapitulate and dissect the changes in histone modifications during chromatin assembly. We find that H4 histone molecules carrying a diacetyl mark at K5 and K12 assemble onto DNA added to a *Drosophila* embryo extract. Histone H4 is monomethylated at K20 immediately after histone deposition. A candidate enzyme for carrying out this methylation is PR-SET7, which we show to (mono)methylate H4K20 within nucleosomal substrates. Concomitantly with H4K20 monomethylation, dl(3)MBT associates with chromatin. This is then followed by the removal of the two acetyl groups of H4. The three MBT domains of dl(3)MBT have the capacities to bind methylated H4K20 *in vitro*, and the full-length protein forms a complex with the HDAC dRPD3 *in vivo*. Our results strongly support a model of stepwise maturation of histone marks, which may help to guarantee the fidelity of chromatin assembly.

Lysine methylation within histone tails has been suggested to be a key player during epigenetic inheritance. However, in

contrast to the methylation of H3, methylation of H4 has not been so clearly associated with transcriptional regulation (30, 41, 60). The mapping of H4 species methylated at K20 gave somewhat confusing results. Whereas H4K20me₃ is a rare modification that has been clearly associated with transcriptionally silent chromatin (45), most H4 molecules carry a dimethyl mark in the model systems analyzed so far (7, 39, 40, 59). H4K20me₁, on the contrary, has been reported to be enriched within promoter and coding regions of active genes (52) as well as in inactive regions of the genome (47). Furthermore, the monomethyl mark has been suggested to play a role in chromatin assembly rather than transcriptional regulation, which is based mainly on observations made on PR-SET7, the methyltransferase that is responsible for H4K20 monomethylation in mammalian cells (57) and in *Drosophila* cells (27). The enzyme localizes to the replication fork (53) and is required for S-phase progression (24). Furthermore, H4K20me₁ levels have been shown to increase during late S- and G₂-phase (13, 40, 42). Recent findings also show that H4K20 (mono)methylation not only plays a role during chromatin assembly during S-phase but is also involved in the regulation of DNA repair. In the fission yeast *Schizosaccharomyces pombe*, the methyltransferase that methylates H4K20, SET9, is required for an efficient targeting of a known checkpoint protein *crb2* to sites of DNA damage, thereby mediating cell cycle arrest (44). A lack of H4K20me₁ also leads to the accumulation of DNA breaks and cell cycle arrest before the entry into mitosis in mammalian and *Drosophila* tissue culture cells (18, 43). The arrest seems to be initiated by a G₂/M checkpoint, as the lack of PR-SET7 induces the activation of the checkpoint kinase ATM (18). The role of H4K20me₁ in repair processes is further confirmed by the fact that the simultaneous mutation of the *Drosophila* checkpoint gene *ami1* strongly increases the survival rate of PR-SET7 mutant larvae (43).

Our results strongly support the idea that the monomethylation of K20 within H4 plays a crucial role during chromatin assembly by marking the fully assembled nucleosome after histone deposition. Recombinant dPR-SET7 methylates H4 only after it has been assembled into a nucleosome, which is consistent with the observations that have been made on mammalian PR-SET7 (13, 36). The fact that the enzymatic activity as well as the expression of PR-SET7 is highly regulated during different phases of the cell cycle (18, 53) suggests that the methylation of H4 after nucleosome assembly might have an important regulatory function that has to be tightly controlled.

The effects of histone methylations are thought to be mediated by Tudor domain-containing factors (33). One of these factors that has been shown to bind a peptide carrying H4K20me₁ is l(3)MBT, which has been suggested to act as a chromatin lock to stabilize a higher-order chromatin structure (25, 54). Other factors that bind to H4K20me are p53BP1 and *crb2*, which mediate key processes in DNA repair (8). Our findings that dl(3)MBT interacts with the HDAC and is recruited to newly assembled chromatin via a mechanism dependent on H4K20me₁ could explain why H4K20me₁ has been mapped to transcriptionally active as well as inactive regions. Both cellular processes, DNA synthesis and transcription, involve a disruption of chromatin structure and are often accompanied by a *de novo* histone assembly (1, 14, 17). We show that the monomethylation of H4K20 is a very early step after dep-

osition that stimulates the recruitment of a complex of dl(3)MBT and dRpd3 immediately after nucleosome formation. The association of the complex greatly facilitates the deacetylation of the newly deposited histones. The effect we observe is clearly a kinetic effect, as we eventually observe deacetylation even in the absence of any monomethylation, which is very likely due to the abundance of HDAC enzymes in the extract. In this light, it is interesting that the kinetics of K12 deacetylation after deposition have been shown to differ when comparing early and late-replicating chromatin (51). It will be interesting to investigate whether this is due to the different degrees of monomethylation of H4.

Chromatin has a very high rate of disruption and reassembly at transcriptionally active genes, which may explain the fact that the monomethyl mark can be found at transcriptionally active promoters (52). However, the HDAC recruitment after nucleosome assembly may at the same time lead to a removal of acetyl groups from histones at these promoters, leading to transcriptional repression (25) if the primary signal of gene activation (such as the binding of a transcription factor) is gone. This may explain the contradictory results of H4K20me₁ mapping data.

Given that we are using linear DNA fragments and a de novo assembly system, it may well be that our in vitro system mimics repair-coupled chromatin assembly and that the monomethylation is part of a mechanism that governs histone modifications during chromatin repair. Based on our in vitro observations and the reported in vivo data, we suggest that the monomethylation mark may indeed function as an important step to ensure the proper establishment of histone modification marks during and after assembly. In this light, it is also interesting that H4K20 monomethylated histones have been found in a non-chromatin-bound histone pool in *Drosophila* S2 cells (26), which may contain the H4 molecules that are ejected during RNA transcription and repair.

Based on our experiments, we would argue that, at least in the *Drosophila* system, the kinetics of H4K5ac and H4K12ac deacetylation are controlled by PR-SET7-mediated H4K20 methylation. It will be an interesting task for the future to analyze how the PR-SET7 activity is regulated in vivo in response to cellular stress and what downstream factors play a role in sensing improper chromatin assembly.

ACKNOWLEDGMENTS

We thank M. Parthun for the yHAT1 expression clone and R. Steward for the PR-SET7 antibody, and the anti-dRpd3 and anti-HDAC3 antibodies were generous gifts from J. Müller and B. Turner, respectively. We are also thankful to XinLin Zu, I. Vetter, and T. Schlunck for expert technical assistance and to P.B. Becker and A. Grothe for critical reading of the manuscript and helpful comments.

A.N.D.S. is sponsored by a Boehringer predoctoral fellowship, and A.I.'s lab is funded by a grant from the European Union (LSHG-CT2006-037415). K.M. is supported by DFG GRK 767, and work in A.B.'s lab is funded by the DFG Forschergruppe Chromatin-Mediated Biological Decisions.

REFERENCES

- Ahmad, K., and S. Henikoff. 2002. Histone H3 variants specify modes of chromatin assembly. *Proc. Natl. Acad. Sci. USA* **99**(Suppl. 4):16477–16484.
- Akey, C. W., and K. Luger. 2003. Histone chaperones and nucleosome assembly. *Curr. Opin. Struct. Biol.* **13**:6–14.
- Bannister, A. J., R. Schneider, and T. Kouzarides. 2002. Histone methylation: dynamic or static? *Cell* **109**:801–806.
- Becker, P. B., and C. Wu. 1992. Cell-free system for assembly of transcriptionally repressed chromatin from *Drosophila* embryos. *Mol. Cell. Biol.* **12**:2241–2249.
- Benson, L. J., Y. Gu, T. Yakovleva, K. Tong, C. Barrows, C. L. Strack, R. G. Cook, C. A. Mizzen, and A. T. Annunziato. 2006. Modifications of H3 and H4 during chromatin replication, nucleosome assembly, and histone exchange. *J. Biol. Chem.* **281**:9287–9296.
- Blank, T. A., R. Sandaltzopoulos, and P. B. Becker. 1997. Biochemical analysis of chromatin structure and function using *Drosophila* embryo extracts. *Methods* **12**:28–35.
- Bonaldi, T., A. Imhof, and J. T. Regula. 2004. A combination of different mass spectroscopic techniques for the analysis of dynamic changes of histone modifications. *Proteomics* **4**:1382–1396.
- Botuyan, M. V., J. Lee, I. M. Ward, J. E. Kim, J. R. Thompson, J. Chen, and G. Mer. 2006. Structural basis for the methylation state-specific recognition of histone H4-K20 by 53BP1 and Crb2 in DNA repair. *Cell* **127**:1361–1373.
- Bouazoune, K., A. Mitterweiger, G. Langst, A. Imhof, A. Akhtar, P. B. Becker, and A. Brehm. 2002. The dMi-2 chromodomains are DNA binding modules important for ATP-dependent nucleosome mobilization. *EMBO J.* **21**:2430–2440.
- Brehm, A., G. Langst, J. Kehle, C. R. Clapier, A. Imhof, A. Eberharther, J. Muller, and P. B. Becker. 2000. dMi-2 and ISWI chromatin remodelling factors have distinct nucleosome binding and mobilization properties. *EMBO J.* **19**:4332–4341.
- Dimitrov, S., G. Almouzni, M. Dasso, and A. P. Wolffe. 1993. Chromatin transitions during early *Xenopus* embryogenesis: changes in histone H4 acetylation and in linker histone type. *Dev. Biol.* **160**:214–227.
- Eskeland, R., A. Eberharther, and A. Imhof. 2007. HP1 binding to chromatin methylated at H3K9 is enhanced by auxiliary factors. *Mol. Cell. Biol.* **27**:453–465.
- Fang, J., Q. Feng, C. S. Ketel, H. Wang, R. Cao, L. Xia, H. Erdjument-Bromage, P. Tempst, J. A. Simon, and Y. Zhang. 2002. Purification and functional characterization of SET8, a nucleosomal histone H4-lysine 20-specific methyltransferase. *Curr. Biol.* **12**:1086–1099.
- Groth, A., W. Rocha, A. Verreault, and G. Almouzni. 2007. Chromatin challenges during DNA replication and repair. *Cell* **128**:721–733.
- Gruss, C., J. Wu, T. Koller, and J. M. Sogo. 1993. Disruption of the nucleosomes at the replication fork. *EMBO J.* **12**:4533–4545.
- Hansen, J. C., K. E. van Holde, and D. Lohr. 1991. The mechanism of nucleosome assembly onto oligomers of the sea urchin 5 S DNA positioning sequence. *J. Biol. Chem.* **266**:4276–4282.
- Henikoff, S., and K. Ahmad. 2005. Assembly of variant histones into chromatin. *Annu. Rev. Cell Dev. Biol.* **21**:133–153.
- Houston, S. L., K. J. McManus, M. M. Adams, J. K. Sims, P. B. Carpenter, M. J. Hendzel, and J. C. Rice. 2008. Catalytic function of the PR-Set7 histone H4 lysine 20 monomethyltransferase is essential for mitotic entry and genomic stability. *J. Biol. Chem.* **283**:19478–19488.
- Jackson, V. 1988. Deposition of newly synthesized histones: hybrid nucleosomes are not tandemly arranged on daughter DNA strands. *Biochemistry* **27**:2109–2120.
- Jackson, V., and R. Chalkley. 1985. Histone segregation on replicating chromatin. *Biochemistry* **24**:6930–6938.
- Jackson, V., D. Granner, and R. Chalkley. 1976. Deposition of histone onto the replicating chromosome: newly synthesized histone is not found near the replication fork. *Proc. Natl. Acad. Sci. USA* **73**:2266–2269.
- Jackson, V., D. K. Granner, and R. Chalkley. 1975. Deposition of histones onto replicating chromosomes. *Proc. Natl. Acad. Sci. USA* **72**:4440–4444.
- Jenuwein, T., and C. D. Allis. 2001. Translating the histone code. *Science* **293**:1074–1080.
- Jørgensen, S., I. Elvers, M. B. Trelle, T. Menzel, M. Eskildsen, O. N. Jensen, T. Helleday, K. Helin, and C. S. Sorensen. 2007. The histone methyltransferase SET8 is required for S-phase progression. *J. Cell Biol.* **179**:1337–1345.
- Kalakonda, N., W. Fischle, P. Boccuni, N. Gurchich, R. Hoya-Arias, X. Zhao, Y. Miyata, D. Macgrogan, J. Zhang, J. K. Sims, J. C. Rice, and S. D. Nimer. 2008. Histone H4 lysine 20 monomethylation promotes transcriptional repression by L3MBTL1. *Oncogene* **27**:4293–4304.
- Karachentsev, D., M. Druzhinina, and R. Steward. 2007. Free and chromatin-associated mono-, di-, and trimethylation of histone H4-lysine 20 during development and cell cycle progression. *Dev. Biol.* **304**:46–52.
- Karachentsev, D., K. Sarma, D. Reinberg, and R. Steward. 2005. PR-Set7-dependent methylation of histone H4 Lys 20 functions in repression of gene expression and is essential for mitosis. *Genes Dev.* **19**:431–435.
- Klymenko, T., B. Papp, W. Fischle, T. Kocher, M. Schelder, C. Fritsch, B. Wild, M. Wilm, and J. Muller. 2006. A polycomb group protein complex with sequence-specific DNA-binding and selective methyl-lysine-binding activities. *Genes Dev.* **20**:1110–1122.
- Kornberg, R. D., and Y. Lorch. 1999. Twenty-five years of the nucleosome, fundamental particle of the eukaryote chromosome. *Cell* **98**:285–294.
- Kouzarides, T. 2007. Chromatin modifications and their function. *Cell* **128**:693–705.
- Li, H., W. Fischle, W. Wang, E. M. Duncan, L. Liang, S. Murakami-Ishibe, C. D. Allis, and D. J. Patel. 2007. Structural basis for lower lysine methyl-

- ation state-specific readout by MBT repeats of L3MBTL1 and an engineered PHD finger. *Mol. Cell* **28**:677–691.
32. Loyola, A., T. Bonaldi, D. Roche, A. Imhof, and G. Almouzni. 2006. PTMs on H3 variants before chromatin assembly potentiate their final epigenetic state. *Mol. Cell* **24**:309–316.
 33. Maurer-Stroh, S., N. J. Dickens, L. Hughes-Davies, T. Kouzarides, F. Eisenhaber, and C. P. Ponting. 2003. The Tudor domain 'Royal Family': Tudor, plant Agenet, Chromo, PWWP and MBT domains. *Trends Biochem. Sci.* **28**:69–74.
 34. Mello, J. A., and G. Almouzni. 2001. The ins and outs of nucleosome assembly. *Curr. Opin. Genet. Dev.* **11**:136–141.
 35. Murawska, M., N. Kunert, J. van Vugt, G. Langst, E. Kremmer, C. Logie, and A. Brehm. 2008. dCHD3, a novel ATP-dependent chromatin remodeler associated with sites of active transcription. *Mol. Cell. Biol.* **28**:2745–2757.
 36. Nishioka, K., J. C. Rice, K. Sarma, H. Erdjument-Bromage, J. Werner, Y. Wang, S. Chuikov, P. Valenzuela, P. Tempst, R. Steward, J. T. Lis, C. D. Allis, and D. Reinberg. 2002. PR-Set7 is a nucleosome-specific methyltransferase that modifies lysine 20 of histone H4 and is associated with silent chromatin. *Mol. Cell* **9**:1201–1213.
 37. Osley, M. A. 1991. The regulation of histone synthesis in the cell cycle. *Annu. Rev. Biochem.* **60**:827–861.
 38. Parthun, M. R., J. Widom, and D. E. Gottschling. 1996. The major cytoplasmic histone acetyltransferase in yeast: links to chromatin replication and histone metabolism. *Cell* **87**:85–94.
 39. Pesavento, J. J., C. A. Mizzen, and N. L. Kelleher. 2006. Quantitative analysis of modified proteins and their positional isomers by tandem mass spectrometry: human histone H4. *Anal. Chem.* **78**:4271–4280.
 40. Pesavento, J. J., H. Yang, N. L. Kelleher, and C. A. Mizzen. 2008. Certain and progressive methylation of histone H4 at lysine 20 during the cell cycle. *Mol. Cell. Biol.* **28**:468–486.
 41. Reinberg, D., S. Chuikov, P. Farnham, D. Karachentsev, A. Kirmizis, A. Kuzmichev, R. Margueron, K. Nishioka, T. S. Preissner, K. Sarma, C. Abate-Shen, R. Steward, and A. Vaquero. 2004. Steps toward understanding the inheritance of repressive methyl-lysine marks in histones. *Cold Spring Harb. Symp. Quant. Biol.* **69**:171–182.
 42. Rice, J. C., K. Nishioka, K. Sarma, R. Steward, D. Reinberg, and C. D. Allis. 2002. Mitotic-specific methylation of histone H4 Lys 20 follows increased PR-Set7 expression and its localization to mitotic chromosomes. *Genes Dev.* **16**:2225–2230.
 43. Sakaguchi, A., and R. Steward. 2007. Aberrant monomethylation of histone H4 lysine 20 activates the DNA damage checkpoint in *Drosophila melanogaster*. *J. Cell Biol.* **176**:155–162.
 44. Sanders, S. L., M. Portoso, J. Mata, J. Bahler, R. C. Allshire, and T. Kouzarides. 2004. Methylation of histone H4 lysine 20 controls recruitment of Crb2 to sites of DNA damage. *Cell* **119**:603–614.
 45. Schotta, G., M. Lachner, K. Sarma, A. Ebert, R. Sengupta, G. Reuter, D. Reinberg, and T. Jenuwein. 2004. A silencing pathway to induce H3-K9 and H4-K20 trimethylation at constitutive heterochromatin. *Genes Dev.* **18**:1251–1262.
 46. Shimamura, A., and A. Worcel. 1989. The assembly of regularly spaced nucleosomes in the *Xenopus* oocyte S-150 extract is accompanied by deacetylation of histone H4. *J. Biol. Chem.* **264**:14524–14530.
 47. Sims, J. K., and J. C. Rice. 2008. PR-Set7 establishes a repressive trans-tail histone code that regulates differentiation. *Mol. Cell. Biol.* **28**:4459–4468.
 48. Smith, J. J., S. E. Torigoe, J. Maxson, L. C. Fish, and E. A. Wiley. 2008. A class II histone deacetylase acts on newly synthesized histones in *Tetrahymena*. *Eukaryot. Cell* **7**:471–482.
 49. Smith, P. A., V. Jackson, and R. Chalkley. 1984. Two-stage maturation process for newly replicated chromatin. *Biochemistry* **23**:1576–1581.
 50. Sobel, R. E., R. G. Cook, C. A. Perry, A. T. Annunziato, and C. D. Allis. 1995. Conservation of deposition-related acetylation sites in newly synthesized histones H3 and H4. *Proc. Natl. Acad. Sci. USA* **92**:1237–1241.
 51. Taddei, A., D. Roche, J. B. Sibarita, B. M. Turner, and G. Almouzni. 1999. Duplication and maintenance of heterochromatin domains. *J. Cell Biol.* **147**:1153–1166.
 52. Talasz, H., H. H. Lindner, B. Sarg, and W. Helliger. 2005. Histone H4-lysine 20 monomethylation is increased in promoter and coding regions of active genes and correlates with hyperacetylation. *J. Biol. Chem.* **280**:38814–38822.
 53. Tardat, M., R. Murr, Z. Herceg, C. Sardet, and E. Julien. 2007. PR-Set7-dependent lysine methylation ensures genome replication and stability through S phase. *J. Cell Biol.* **179**:1413–1426.
 54. Trojer, P., G. Li, R. J. Sims III, A. Vaquero, N. Kalakonda, P. Bocconi, D. Lee, H. Erdjument-Bromage, P. Tempst, S. D. Nimer, Y. H. Wang, and D. Reinberg. 2007. L3MBTL1, a histone-methylation-dependent chromatin lock. *Cell* **129**:915–928.
 55. Turner, B. M. 2000. Histone acetylation and an epigenetic code. *Bioessays* **22**:836–845.
 56. Wolffe, A. P. 1998. *Chromatin structure and function*, 3rd ed. Academic Press, San Diego, CA.
 57. Yang, H., J. J. Pesavento, T. W. Starnes, D. E. Cryderman, L. L. Wallrath, N. L. Kelleher, and C. A. Mizzen. 2008. Preferential dimethylation of histone H4 lysine 20 by Suv4-20. *J. Biol. Chem.* **283**:12085–12092.
 58. Yohn, C. B., L. Pusateri, V. Barbosa, and R. Lehmann. 2003. *l(3)malignant brain tumor* and three novel genes are required for *Drosophila* germ-cell formation. *Genetics* **165**:1889–1900.
 59. Zhang, K., K. E. Williams, L. Huang, P. Yau, J. S. Siino, E. M. Bradbury, P. R. Jones, M. J. Minch, and A. L. Burlingame. 2002. Histone acetylation and deacetylation: identification of acetylation and methylation sites of HeLa histone H4 by mass spectrometry. *Mol. Cell Proteomics* **1**:500–508.
 60. Zhang, Y., and D. Reinberg. 2001. Transcription regulation by histone methylation: interplay between different covalent modifications of the core histone tails. *Genes Dev.* **15**:2343–2360.

3.1.3 Histone modifications during chromatin assembly *in vivo*

When a cell replicates, not only the DNA must double but also the amount of histones. Each cell receives the identical sequence of DNA reflecting the genetic code. A second code, the epigenetic code is thought to be established by epigenetic regulators such as histone modifications. Therefore, it is essential to copy the histone modifications from the parental cell to the daughter cell. Newly synthesized histones carry specific predeposition patterns that are subjected to fundamental changes after chromatin is reassembled behind the replication fork. Different ways of depositing new and old histones after replication have been described in the introduction. But independent of how deposition is conducted, the timeframe is restricted to one cell cycle. So before the next cell cycle starts the entire information encoded in posttranslational histone modifications has to be transferred to the daughter cell. Given the number of modification sites it is very likely that not all modifications are inherited immediately after chromatin assembly. It is of great interest to study the kinetics how new histones adjust to the modifications of the old histones. Here, we analyzed old and new modification patterns by applying a newly established technique (pSILAC) and it resulted in a detailed map of the individual steps of chromatin maturation.

Annette N.D. Scharf*, Teresa Barth*, Axel Imhof. Establishment of Histone Modifications after Chromatin Assembly *NAR*, Advance Access published on June 18, 2009 (*equally contributed)

Declaration of contribution to “Establishment of histone modifications after chromatin assembly measured by pulsed SILAC labeling”: The project was conceived by Axel Imhof and me. Experiments were equally performed by Teresa Barth and me. I prepared all the figures, legends and material and methods. I wrote the manuscript with the help of Axel Imhof

Establishment of Histone Modifications after Chromatin Assembly

Annette N. D. Scharf, Teresa K. Barth and Axel Imhof*

Munich Center of Integrated Protein Science and Adolf-Butenandt Institute, Ludwig Maximilians University of Munich, Schillerstr. 44, 80336 Munich, Germany

Received April 17, 2009; Revised May 29, 2009; Accepted June 1, 2009

ABSTRACT

Every cell has to duplicate its entire genome during S-phase of the cell cycle. After replication, the newly synthesized DNA is rapidly assembled into chromatin. The newly assembled chromatin ‘matures’ and adopts a variety of different conformations. This differential packaging of DNA plays an important role for the maintenance of gene expression patterns and has to be reliably copied in each cell division. Posttranslational histone modifications are prime candidates for the regulation of the chromatin structure. In order to understand the maintenance of chromatin structures, it is crucial to understand the replication of histone modification patterns. To study the kinetics of histone modifications *in vivo*, we have pulse-labeled synchronized cells with an isotopically labeled arginine ($^{15}\text{N}_4$) that is 4 Da heavier than the naturally occurring $^{14}\text{N}_4$ isoform. As most of the histone synthesis is coupled with replication, the cells were arrested at the G1/S boundary, released into S-phase and simultaneously incubated in the medium containing heavy arginine, thus labeling all newly synthesized proteins. This method allows a comparison of modification patterns on parental versus newly deposited histones. Experiments using various pulse/chase times show that particular modifications have considerably different kinetics until they have acquired a modification pattern indistinguishable from the parental histones.

INTRODUCTION

The packaging of DNA into chromatin plays a crucial role in regulating its accessibility for RNA polymerases and transcription factors. The level of chromatin condensation is dependent on the differentiation state of a cell, ranging from a hyper-dynamic, highly accessible structure in

embryonic stem cells (1,2) to a less accessible more condensed form in senescent cells (3). The posttranslational modification of histones can alter the properties of chromatin fibers and is therefore a prime candidate to mediate the stable inheritance of chromatin structures. The histone code hypothesis (4,5) is further supported by genome-wide mapping studies of histone modifications (6,7), which show a high degree of correlation between particular histone modifications and RNA–Pol II occupancy. Based on these data, a complex set of modifications has been postulated to stably mark specific regions of the genome with regard to their further activity. Experiments in yeast (8), however, suggest that a putative histone code may reflect a relatively simple binary signal (9). An alternative model to explain the generation of complex histone modification patterns has been put forward by Schreiber and Bernstein who suggested that histone modifications function similar to modification networks involving receptor tyrosine kinases (10).

In order to distinguish between an inheritable histone code and the generation of modification patterns in response to external signals, it is crucial to investigate the histone modifications that occur during and immediately after histone deposition. During S-phase, newly synthesized and parental histones are distributed randomly on the two daughter strands (11,12) resulting in a dispersive replication of histone modification patterns (13). Newly synthesized histones have a distinct modification pattern (14,15) that matures after assembly into a pattern similar to the one observed on parental histones (16–18). As the histone modifications are considered to be causal for the maintenance of particular chromatin structures (5), mechanisms have to exist that allow a faithful copying of modification patterns from ‘old’ paternal histones to new ones. It is striking that many enzymes that catalyze a posttranslational modification of histones also carry domains known to bind to modified histone molecules or interact with factors containing such a domain (19–24). These domains could target histone-modifying or demodifying enzymes to particular regions within the

*To whom correspondence should be addressed. Tel: +49 89 2180 75420; Fax: +49 89 2180 75440; E-mail: imhof@lmu.de

The authors wish it to be known that, in their opinion, the first two authors should be regarded as joint First Authors.

© 2009 The Author(s)

This is an Open Access article distributed under the terms of the Creative Commons Attribution Non-Commercial License (<http://creativecommons.org/licenses/by-nc/2.0/uk/>) which permits unrestricted non-commercial use, distribution, and reproduction in any medium, provided the original work is properly cited.

genome by recognizing a modification pattern on the 'old' histones and copying it to the new ones.

The kinetics with which the modifications are copied from old histones to the new ones may define the time frame during which a given cell is susceptible for incoming signals and therefore its epigenetic plasticity. We investigated the kinetics of how fast modification patterns on new histones resemble the one on old ones by pulsed stable isotope labeling with amino acids in cell culture (pSILAC) and mass spectrometric analysis of histones. In accordance with previously published work, we observed a rapid adjustment of lysine acetylation patterns within the first 2 h after deposition (14,25,26). In contrast to this rapid acetylation and deacetylation, the methylation of lysine residues requires much more time to become indistinguishable from the old histones. In fact some of the modification patterns on newly incorporated histones remain different through most of the next cell cycle after deposition indicating that the histone code needs one full cell cycle in order to become fully re-established. Our findings have a major implication in our view for how histone modification marks may mediate epigenetic inheritance.

EXPERIMENTAL PROCEDURES

Synchronization of HeLa cells

For G1/S-phase synchronization, a double thymidine block was used. Therefore, HeLa cells were seeded and cultured for 24 h at 37°C in the R⁰ SILAC medium (Invitrogen). Thymidine (Sigma) was added to a final concentration of 2 mM and incubation was maintained for 16 h. The block was released by exchanging the thymidine-containing medium with the R⁰ culture medium. The cells were grown for 9 h before adding thymidine again to 2 mM final concentration for further 16 h to synchronize the HeLa cells at the G1/S border. The arrest was finally released by refeeding the cells with the thymidine-free R⁴ SILAC medium (Invitrogen) to allow cell cycle progression. Whenever indicated, 10 mM NaBu was added directly into the medium and the cells were washed twice with PBS before transferring them into the medium without NaBu. The cells were maintained in a 37°C incubator with a humidified atmosphere of 5% CO₂.

SILAC labeling

We used three different SILAC DMEM media: R⁰ SILAC (L-arginine), R⁴ (L-¹²C₆ ¹⁵N₄-arginine) and R¹⁰ (L-¹³C₆ ¹⁵N₄-arginine). HeLa cells were synchronized at the G1/S border in the R⁰ SILAC medium and released into the cell cycle in the R⁴ SILAC medium in order to label all newly synthesized histones. For all pulse-chase experiments, we fed the synchronized cells with the R⁴ SILAC medium for 6 h and chased with the R¹⁰ SILAC medium. All materials for SILAC labeling were purchased from Invitrogen and prepared according to the manufacturer's instructions.

Flow cytometric analysis of the cell cycle

For fluorescence activated cell sorting (FACS) analysis, the cells (1 × 10⁶) were harvested, washed twice in PBS followed by fixation in 70% ethanol at -20°C for a

minimum of 1 h. Fixed cells were washed in PBS and incubated with 100 µg/ml of RNase A in PBS for 30 min at 37°C. Afterward, propidium iodide (Sigma) to a final concentration of 50 µg/ml was added and the cells were incubated at 37°C for 30 min. The samples were stored at 4°C in the dark until analysis on BD Biosciences FACSCanto. A minimum of 10 000 cells were counted, and the raw data were analyzed and histograms plotted using the FlowJo software.

RT-PCR

RNA was extracted from snap-frozen HeLa cell pellets using the RNeasy kit (Qiagen) according to the manufacturer's manual and dissolved in RNase-free water. Total RNA concentration was quantified using a spectrophotometer (Peqlab, Nanodrop). Reverse transcription was primed with 250 µg of random primers (Promega) with 1 µg of total RNA per sample at 70°C for 5 min. The samples were then incubated with 20 U MuLV in 20 µl of buffer containing 1000 µM dNTP and manufacturer's RT buffer for 10 min at 25°C, then heated up to 37°C for 1 h, 70°C for 10 min, chilled on ice and frozen at -20°C. PCR reaction was conducted with the following primers: H3.2 (5'-GCTACCAGAAGTCCACGGAG, 5'-GATGTCCTTGGGCATAATGG) and 18S (5'-TTGTGGTTTTTCGGAAGTGG, 5'-CATCGTTTATGGT CGGAAGTACG).

Histone extraction

The cell pellets were redissolved in 0.4 N HCl in a total volume of 0.5 ml per 1 × 10⁶ cells and centrifuged for a minimum of 1 h at 4°C. After centrifugation at 13 000 rpm for 30 min, the supernatant was dialyzed at 4°C against 100 mM ice-cold acetic acid for three times for 1 h using 6–8000 MWCO. The sample was concentrated using a speed vac and redissolved in SDS-loading buffer and applied to a SDS-PAGE gel for further analysis.

MALDI-TOF analysis

Histones were separated by 18% SDS-PAGE. G-250 Coomassie blue stained bands were excised and destained with 50 mM ammonium bicarbonate in 50% ACN (Sigma) for 30 min at 37°C. After washing the gel pieces with HPLC grade water, histones were chemically modified by treating with 2 µl propionic anhydride (Sigma) and 48 µl of ammonium bicarbonate (1M) at 37°C. After 1 h, the modified histones were washed with HPLC grade water and digestions were carried out at 37°C overnight with 200 ng of sequencing grade trypsin (Promega) according to the manufacturer's manual. Digestion products were collected and the gel pieces were acid extracted in addition with 25 mM ammonium bicarbonate and afterward with 5% formic acid. The pooled digestions were concentrated using a speed vac and redissolved in 0.1% TFA. Afterward, the samples were desalted with ziptip µc18 (Millipore) according to the manufacturer's instructions and directly eluted onto the target plate with a saturated solution of α-cinnamic acid in 0.3% TFA and 50% ACN. The target plate was loaded into the Voyager DE STR spectrometer (Applied

Biosystems) and analyzed. Peptide mass fingerprint covered the mass range from 500–2000 amu.

Quantification of MALDI signals

To determine all modifications occurring on histones, the Manuelito software was used. Spectra were processed and analyzed with the Data Explorer software (Applied Biosystems). For quantification, the integrated area of the peaks was used with a signal-to-noise ratio of 2. The sum of the area from all peaks derived from a single peptide was defined as 100%. Charts were drawn in Excel.

RESULTS

Pulse labeling can be used to mark newly synthesized histones

Most of the new histones that are incorporated during replication are synthesized during S-phase [(27) and Figure 1B and C]. To study the dynamics of histone modifications on the newly synthesized histones in comparison to the parental histones, we designed a method to selectively label new histones by isotopic labeling (Figure 1A). To do this, we arrested HeLa cells at the G1/S boundary using a double thymidine block (28) and verified the cell cycle arrest using fluorescence-activated cytometry (Figure 1B). After removal of the block, the cells were placed into the labeling medium containing isotopically labeled arginine ($^{15}\text{N}_4$). To control the correct replication-dependent synthesis of histone mRNA, we analyzed RNA at different times after removal of the cell cycle block (Figure 1C). As cells went into S-phase, the amount of histone H3.2 mRNA (29) increased substantially indicating that the histone mRNA synthesis is not affected by the heavy medium. Isotopically labeled histones also accumulate with a kinetic similar to the mRNA (Figure 1D). We measured the total level of incorporation by comparing the integrated peak areas of H3 and H4 peptides that were not modified in our samples [H3 64–69, $m/z = 844.5$ (light) or 848.5 (heavy) and H4 68–78, $m/z = 1346.7$ (light) or 1350.7 (heavy)]. A continuous labeling during the first 8-h postrelease resulted in a continuous increase in the histone synthesis. Theoretically, one would expect the level of incorporation to be 50% assuming that the total amount of histones is doubled and that all newly synthesized histones incorporate exclusively labeled arginine. In our experiments, the labeling efficiency is ~40% of all H3 and H4 molecules (Figure 1D). This discrepancy may either be due to the fact that (i) not all cells enter S-phase after synchronization (Figure 1B), (ii) not all histones are incorporated into chromatin or that (iii) residual pools of light arginine are used in HeLa cells to synthesize new histone molecules. To quantify the latter, we measured the incorporation of heavy arginine in the H3 peptide containing amino acids 41–49. This peptide has the sequence YRPGTVLR, which is not cleaved by trypsin after R42 and therefore contains two arginines. It can get singly or doubly labeled depending on the amount of light arginine still present in the cell (Supplemental Figure S1). We do get a low level of singly labeled peptide of ~5%, suggesting that

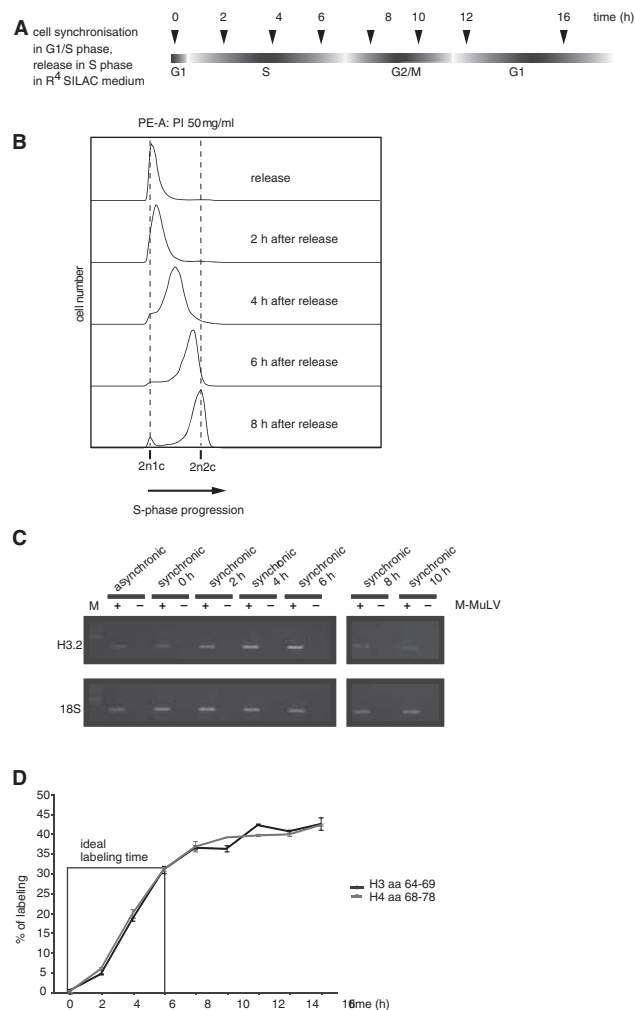


Figure 1. pSILAC can be used to distinguish old from newly synthesized histones. (A) Schematic experimental overview. HeLa cells were synchronized using a double thymidine block. Cells were released into S-phase and simultaneously grown in the R⁴ SILAC medium in order to label all newly synthesized proteins. The cells were harvested at indicated time points. (B) DNA content of synchronized HeLa cells after different time points of release into S-phase using FACS analysis. The fluorescence intensity (DNA content) is depicted on the abscissa. (C) mRNA amount of H3.2 for asynchronous and synchronic cells detected by reverse transcriptase PCR. 18S serves as a loading control. M, marker. (D) Labeling efficiency when using the SILAC medium (R⁴). Two peptides H3 aa 64–69 and H4 aa 68–78 are analyzed by MALDI-TOF from 0 h to 16 h after release into S-phase. Error bars indicate the standard error of the mean (SEM) from three independent biological replicates.

~5% of all arginines used for the histone synthesis are in fact derived from endogenous amino-acid pools.

Histone acetylation

One of the best-known modifications on histones is the acetylation of lysines, which is considered to lead to a more open and hence to a more active chromatin structure (30). Histones are acetylated at specific sites before deposition (14,15), which get deacetylated after histone assembly (16,18,25). We wanted to determine, whether our analysis would allow us to dissect the process of acetylation and deacetylation coupled with histone deposition *in vivo*.

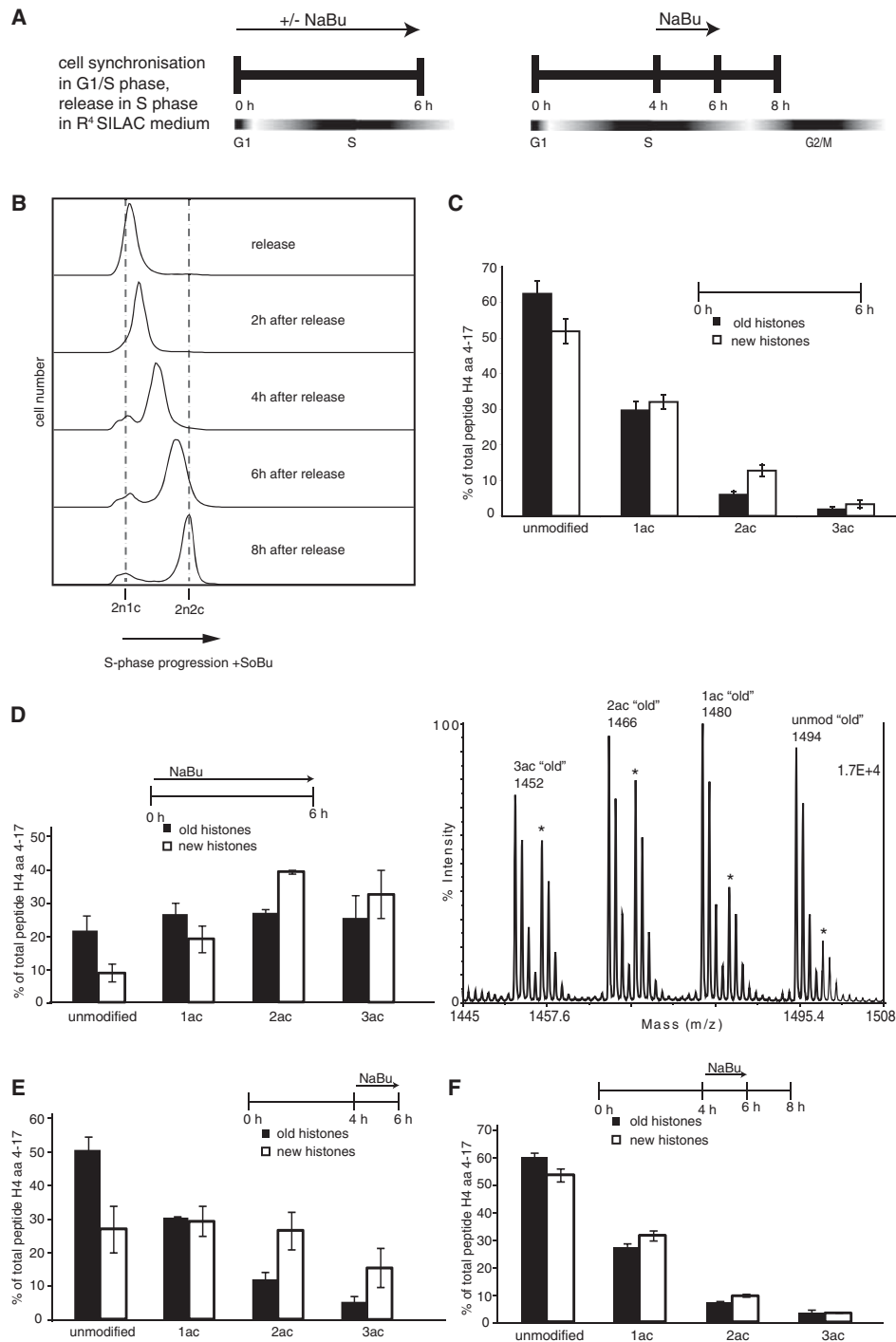


Figure 2. Deacetylation of H4 peptide 4–17 happens fast. (A) Scheme of pulse-chase experiments including 10 mM sodium butyrate treatment. Sodium butyrate (NaBu) was added either at the time of release for 6 h or for a shorter period of time (2 h) during S-phase. (B) FACS analysis of synchronized HeLa cells treated with sodium butyrate harvested at 0, 2, 4, 6 and 8 h after release. (C) Acetylation patterns of H4 peptide 4–17 (GKGGKGLGKGGAKR) of ‘old’ (R⁰) and ‘new’ (R⁴) histones after 6 h after a release into G1/S-phase. Error bars indicate the SEM from three independent biological experiments. 1ac, monoacetylation; 2ac, diacetylation; 3ac, triacetylation. (D) Comparison of acetylation patterns of ‘old’ and ‘new’ histones after 6 h of NaBu treatment. Left: quantification; right: MALDI-TOF spectrum; asterisk indicates peaks of ‘new’ histones. (E) Comparing acetylation patterns of ‘old’ and ‘new’ histones when treating for 2 h with NaBu without additional chase or with an additional 2 h chase (F).

Therefore, we compared the levels of lysine acetylation on newly synthesized histones with that on old histones. When histones were analyzed 6 h after the release into S-phase, we observed a small but reproducibly an increased proportion

of the diacetylated isoform in the new histones (Figure 2C). As free H4 is exclusively diacetylated before deposition (14,15,25), this increased level of diacetylated H4 reflects the higher percentage of pre-deposition forms with the pool

of new histones. In order to get an estimate of how quickly the pre-deposition markers disappear, we used the broad-range deacetylase inhibitor sodium butyrate (NaBu) (Figure 2A). When treating the cells with NaBu throughout the labeling period, we observed an increase in acetylation on the old as well as on the new histones, suggesting that histone acetyltransferases as well as histone deacetylases do not distinguish between old and new histones. However, whereas NaBu treatment leads to similar amounts of all acetylated isoforms among old histones [mono-, di- and triacetylated; tetraacetylated H4 could not be analyzed by MALDI-TOF due to an overlap of the heavy peptide H4_{ac4} (4–17) with an unmodified H4 peptide], in the case of the new histones, H4_{ac2} is the most abundant isoform (Figure 2D). This was not due to a NaBu-induced delay of the cell cycle, as treated cells entered S-phase approximately at the same rate as untreated ones (compare Figures 1B and 2B). Besides the enrichment of the diacetylated H4, we also saw a strong increase in the triacetylated form of the new H4 molecules, suggesting that a subsequent acetylation that follows incorporation is independent of a deacetylation event at the other residues (Figure 2D). This acetylation occurs very likely at K16, as this is the major acetylation site in human cells (31), and the diacetylated deposition form of H4 is acetylated at K5 and K12 (14–17). When NaBu was added 4 h after the start of the histone synthesis, we observed a substantial increase in the monoacetylated and the unmodified forms of new H4 suggesting that the pre-deposition modifications are removed within <2 h after assembly (Figure 2E). The higher percentage of diacetylated H4 on the new histones compared to the old ones is very likely due to the ongoing assembly at 4–6 h, after the beginning of S-phase. If, after treatment, the histones were incubated for another 2 h in the absence of NaBu, the acetylation patterns become indistinguishable between the old and new histones (Figure 2F). In summary, we conclude from the analysis of acetylation kinetics of new and old histones that the acetylation is rapidly adjusted to equalize the modification patterns between old and new histones. Due to the high turnover of acetyl groups (32), the pattern of acetylation does not seem to be well suited to confer stable epigenetic memory. Moreover, as acetylation events occur independent from each other, we have no evidence for a regulated establishment of a specific modification pattern that is based on distinct pre-existing modifications. This is in agreement with what has been previously described in yeast (33) and human cells (8).

Histone methylation

In contrast to acetylation, the methylation of lysine residues on histone tails has been suggested to constitute a major factor in the establishment and inheritance of stable chromatin states (4,5,34). We therefore wondered whether the methylation of histones might show a different behavior than acetylation. We focused our studies mainly on the most prominent methylations on H3 and H4 (K4, 9, 27, 36 and 79 on H3 and K20 on H4). In contrast to the highly dynamic lysine acetylation, lysines on the histone tails of newly synthesized histones are methylated with a much slower kinetic. When we compared the methylation

levels of H3 and H4 after 6 h of pSILAC labeling, we observed a striking difference in modification patterns between old and new histones (Figure 3). As the cells progress through the cell cycle, methylation patterns on new histones gradually adopt those on the old histones. This is most obvious for the methylation of lysine 20 within histone H4 (Figure 3A). On newly synthesized H4 molecules, K20 is usually not modified (15,16) and becomes monomethylated after incorporation into chromatin (16,26). This is in sharp contrast to the methylation pattern on the pre-existing H4 molecules that are mainly dimethylated at K20 (Figure 3A).

We observed a similar difference for the methylation on the H3 tail. Like in the H4 molecule, the replication-dependent H3 variants are not methylated to a measurable extent before incorporation (15,16). We concentrated our analysis on K9, K27, K36 and K79, as these have been suggested to play important roles during the inheritance of epigenetic states (5,34). In contrast to yeast cells, most of the H3 molecules remain unmodified at K79 in human cells (35,36). This makes it difficult to quantitatively compare the methylation levels of K79 on old and new histones. However, we observed a small but discernible difference between old and new histones with regard to K79 methylation. Interestingly, we saw more dimethylation of K79 on the new histones at 6 h after synthesis, whereas the old histones contain a higher percentage of monomethylated K79 (Figure 3B). The other lysines that carry methyl groups within H3 are K4, K9, K27 and K36. We limited our analysis on K9, K27 and K36, as the peptide containing K4 (3–8) gave only a very weak signal and appeared to be mostly unmodified in new as well as in old histones. Like H4K20me, the differences in methylation levels between old and new histones 6 h after the release into S-phase were clearly visible (Figure 3C and D). In the case of H3K9, the degree of mono- or dimethylation was considerably lower in the new histones when compared to the old ones and a large percentage of the new H3 molecules were still unmodified at that time point (Figure 3D). As we used MALDI-TOF for quantification, we could not distinguish between trimethylation and acetylation of the peptide, but based on earlier experiments (15) we suggest that most of the peptides contributing to this mass carry an acetyl group at K14. The methylation profiles of the peptides carrying K27 and K36 that were derived from the old and new histones are shown in Figure 3D and also show a marked difference between the two histone types. In contrast to the methylation at K9, we observed a higher percentage of monomethylation of this peptide, which was predominantly due to monomethylation at K27 (data not shown). Interestingly, within the first 6 h after release, this monomethylation does not seem to get further methylated to the trimethyl state on the new histones, and we do not observe a strong trimethylated peptide, which is the predominant one in the pre-existing histones (Figure 3D). In light of recent reports that show a localization of the main H3K27-specific histone methyltransferase EZH2 to sites of replication (37), the rapid monomethylation of H3K27 is very likely a product of the enzyme bound to replication foci.

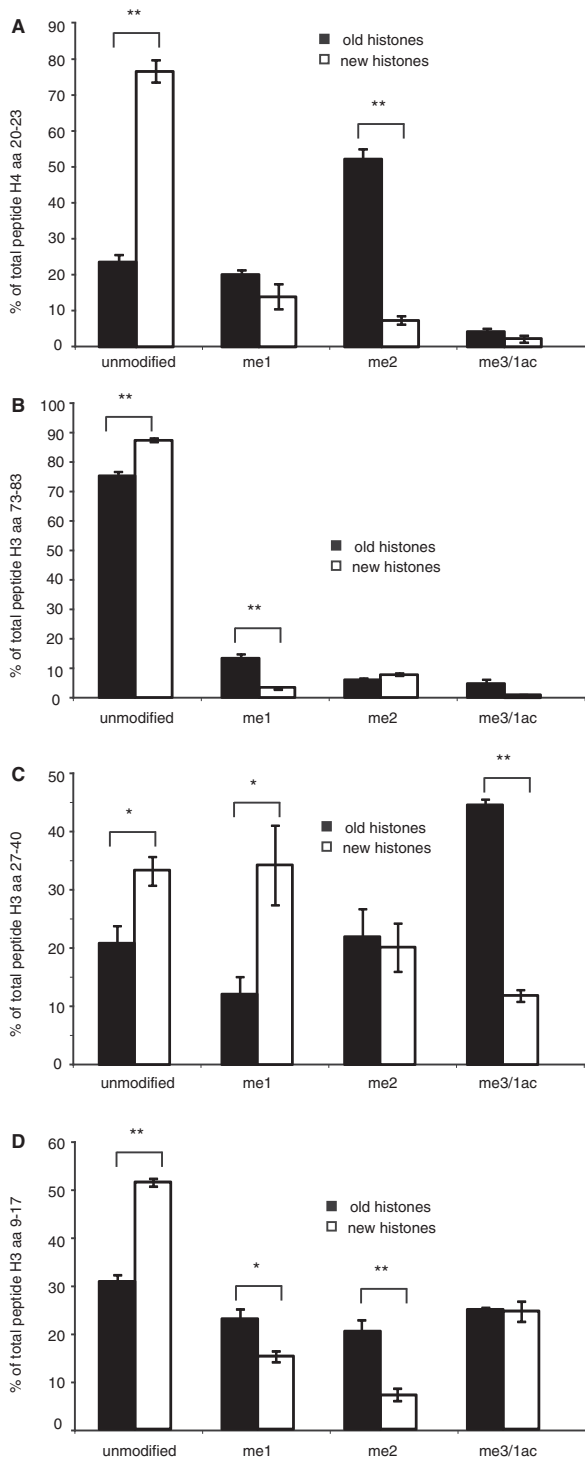


Figure 3. Differences in methylation patterns of 'old' and 'new' histones 6 h after release in G1/S-phase. (A) Methylation patterns of H4 peptide 20–23 of 'old' and 'new' histones analyzed by MALDI-TOF. lac, monoacetylation; me1, monomethylation; me2, dimethylation; me3, trimethylation. (B) H3 73–83 (C) H3 27–40 (D) H3 9–17. Error bars indicate the SEM of three independent biological replicates. The *P*-values are calculated using Student's unpaired *t*-test. The significance of the differences in methylation levels were assessed by unpaired Student's *t*-tests and indicated on the top of the bars ***P* < 0.01: a highly significant difference; **P* < 0.05: a significant difference; and no bracket means no significant difference.

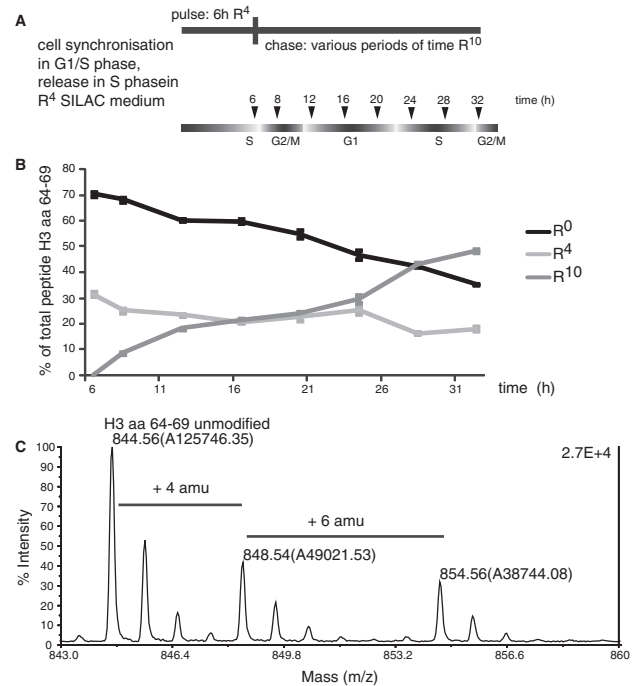


Figure 4. Double labeling using different SILAC media allows to follow histones for a period longer than one cell cycle. (A) Experimental scheme. After synchronization, HeLa cells are released into S-phase under the R⁴-medium conditions. After 6 h, the cells were transferred into a medium containing R¹⁰ and then harvested at indicated time points. time (h); time after release. (B) Incorporation efficiency of double-labeled histones for R⁴ and R¹⁰ showing H3 peptide aa 64–69. Error bars indicate the SEM of three independent biological replicates. (C) MALDI-TOF spectrum of H3 aa 64–69 from HeLa cells that were R⁴ labeled for 6 h and afterward R¹⁰ labeled for additional 6 h.

Pulse chase labeling to follow histone modifications over one cell cycle

Our findings that the methylation patterns of lysine residues does not adopt the identical modification patterns immediately after deposition prompted us to ask how long it would take until the two modification patterns become indistinguishable. To do this, we pulse labeled the newly synthesized histones for 6 h using heavy arginine (R⁴) and subsequently chased the culture using super-heavy arginine (R¹⁰). This procedure is crucial for the analysis as it prevents the interference of histones incorporated at late S-phase, outside S-phase or during the next S-phase. As for R⁴ labeling, we measured incorporation by quantifying the peptides H3_{64–69} and H4_{68–78} (Figure 4 shows only the quantification of the H3 peptide; a representative spectrum is shown in Figure 4C). As the HeLa cells partly lost their synchrony during the second cell cycle, the incorporation of R¹⁰ into histones is not as clearly restricted to a defined time window but increases over the whole analysis time (Figure 4B). Therefore, we focused our analysis on the comparison between the old pre-existing histones and the ones incorporated during the first 6 h of S-phase. The samples were taken every 4 h after the end of the labeling period until the end of the following S-phase as judged by FACS analysis (~30 h after

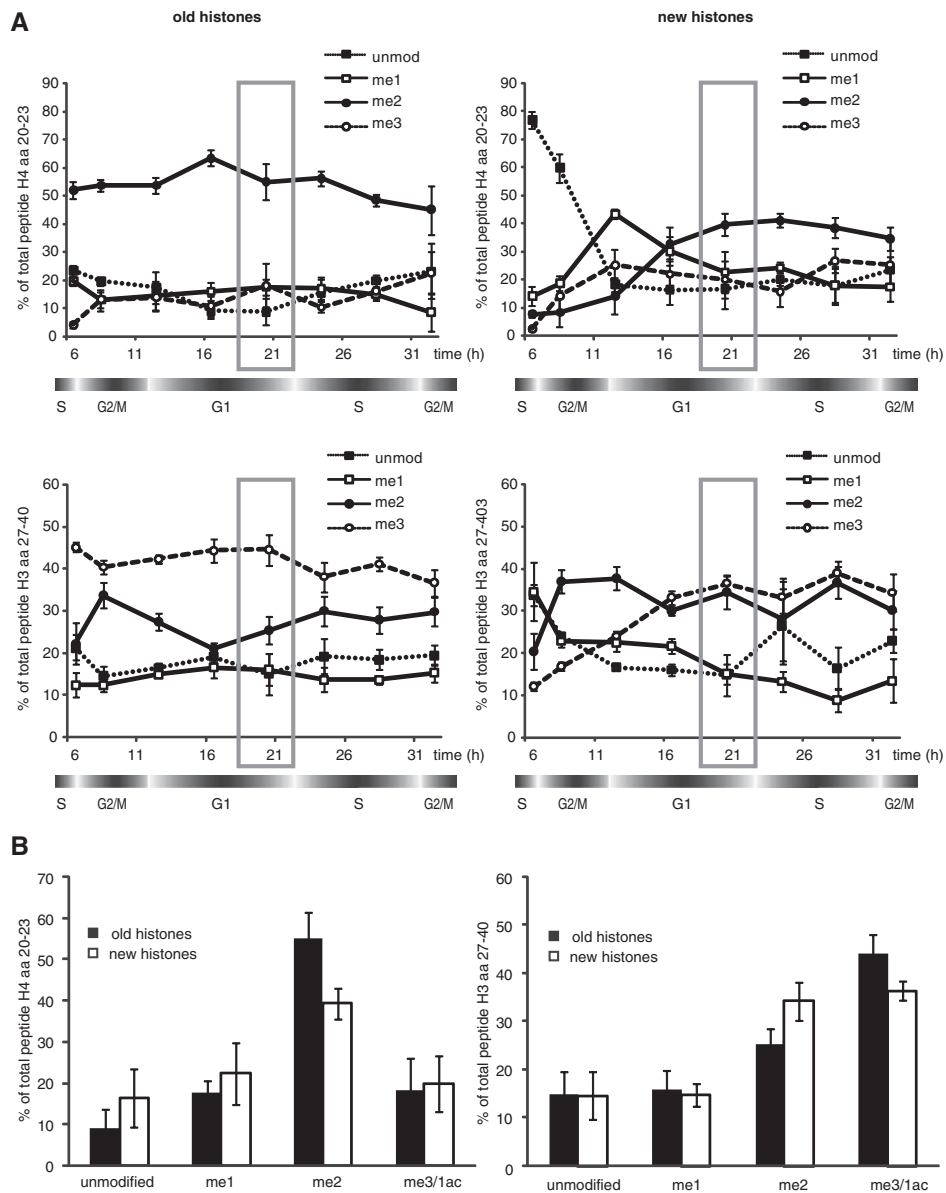


Figure 5. Establishment of posttranslational modification patterns of histones differ in their kinetics. Pulse-chase experiments as described in Figure 4A. Underneath the charts, a cell cycle scheme is depicted. time (h); time after release. Three independent biological experiments are shown and analyzed by MALDI-TOF. Error bars indicate standard deviation of a mean. Grey square indicates 20 h after release (A) top left: H4 peptide aa 20–23 is shown of the ‘old’ histones. Top right: H4 peptide aa 20–23 is shown of the ‘new’ histones. Bottom left: R⁰ (‘old’)-labeled histones showing H3 peptide 27–40. Bottom right: R⁴ (‘new’)-labeled histones showing H3 peptide 27–40. (B) Methylation patterns after 20-h release of H4 peptide 20–23 (left) and H3 peptide 27–40 (right) of ‘old’ and ‘new’ histones analyzed by MALDI-TOF. lac, monoacetylation; me1, monomethylation; me2, dimethylation; me3, trimethylation. Error bars indicate the SEM from three independent biological replicates.

release from the G1/S block). During this time, we only see minor changes in the global methylation patterns of the old histones arguing for a relatively stable marking system (Figure 5A, left panels). The methylation patterns of the newly synthesized histones on the contrary change slowly during the course of one cell cycle (Figure 5A, right panels). Similar to what had been reported before (26), H4K20 gets transiently monomethylated after deposition and subsequently dimethylated. At the beginning of the next S-phase, the H4K20 methylation levels of the new

histones are very similar to the old ones (Figure 5B). This situation is slightly different in the case of the peptide containing H3K27 and K36, where a dimethylation transiently peaks during G2/M after which the amount of K27/36me2 declines and the trimethylated peak increases (Figure 5A, bottom right panel). As in the case of H4K20me, the methylation of K27/36 is adjusted to the pattern of the parental histones during the following G1, such that it is very similar to the parental one at the beginning of the next S-Phase (Figure 5B).

DISCUSSION

Histone modifications are considered to constitute a second (epi)genetic code that operates to establish distinct chromatin structures and maintain them throughout several cell divisions. In order for this to happen, the histone modifications on the pre-existing old histones have to be copied on the newly deposited histones, which have a fundamentally different modification pattern when placed onto DNA (15,18). It has been shown that histone modifications indeed change during the cell cycle (38). However, no distinction has been made with regard to modifications present on old and new histones except for H4 (26). In order to investigate the mechanisms and the kinetics of modification pattern inheritance, we used a pulsed SILAC labeling technique that enabled us to selectively label the newly synthesized histones and subsequently compare modifications on old and new histones. In agreement with previous results (32), we found that the acetylation of histones is highly dynamic and regulated by a tight equilibrium of acetyltransferases and deacetylases. The situation is different in the case of the observed methylations. For all lysines investigated (except H3K79), we observed a transient peak in the monomethylated isoform, suggesting that the monomethylation is put onto the histones either at or immediately after histone deposition. Several histone methyltransferases have been shown to interact with the replication machinery (37,39,40) where they probably catalyze the monomethylation of histones (41,42). This early burst of monomethylation is followed by a relatively slow progression to higher levels of methylation. This is in accordance with earlier observations, which suggest that monomethylation occurs first and may indeed be a prerequisite for further methylations (16,43). This is especially interesting in the case of H3K27, where the methylase EZH2 is responsible for all degrees of methylation. The stepwise methylation suggests a highly regulated progression from lower to higher methylated forms. Such a regulation of the generation of higher methylation states has been reported for several HMT complexes, where histone-binding subunits are required to achieve these states (44,45). The trimethylated forms are much better binding partners for the structural proteins HP1 and Polycomb (46–48) that are thought to condense chromatin by preventing nucleosome remodelers from acting on them (49). It is therefore tempting to speculate that the slow trimethylation on newly deposited histones prevents a premature chromatin condensation and allows chromatin to adopt a structure that is more susceptible for external signals. This window of opportunity could allow cells to stably shift their gene expression profile when they are exposed to changing external signals, such as stem cells leaving their specific niche. On the other hand, the methylation state could also provide a means for the cell to detect the cellular age, as trimethylated isoforms will increase when senescent cells do not undergo continuous cell division (3,50). Especially, as no demethylase has been characterized so far that is able to remove methyl groups from H4, H4K20 may have an exquisite function in measuring cellular age (26).

We and others (26) have analyzed the modification kinetics in immortalized human cells (HeLa) of a tumorigenic origin. Many tumor cells have a markedly different histone modification pattern when compared to normal cells (51). This has to be taken into account when interpreting our data. It will be interesting to see whether primary cells have a similar kinetic or whether the fast replication of tumor cells may in fact prevent the cells from fully replicating the epigenome, which could in fact explain the epigenetic instability that is frequently observed in tumors.

SUPPLEMENTARY DATA

Supplementary Data are available at NAR Online.

ACKNOWLEDGEMENTS

We would like to thank S. Hake for the primer pair to study H3.2 mRNA synthesis. We are grateful to L. Israel and I. Forne-Ferrer for expert technical assistance and to A. Villar-Garea, P.B. Becker and Richard Page for critical reading of the manuscript and helpful comments. We also would like to thank the whole Imhof lab for constant support during the progress of the work.

FUNDING

Boehringer predoctoral fellowship to A.N.D.S.; European Union LSHG-CT2006-037415 grants and the Deutsche Forschungsgemeinschaft (SFB/TR5, M4). Funding for open access charge: LSHG-CT2006-037415.

Conflict of interest statement. None declared.

REFERENCES

- Meshorer,E., Yellajoshula,D., George,E., Scambler,P.J., Brown,D.T. and Misteli,T. (2006) Hyperdynamic plasticity of chromatin proteins in pluripotent embryonic stem cells. *Dev. Cell*, **10**, 105–116.
- Bernstein,B.E., Mikkelsen,T.S., Xie,X., Kamal,M., Huebert,D.J., Cuff,J., Fry,B., Meissner,A., Wernig,M., Plath,K. *et al.* (2006) A bivalent chromatin structure marks key developmental genes in embryonic stem cells. *Cell*, **125**, 315–326.
- Narita,M., Nunez,S., Heard,E., Lin,A.W., Hearn,S.A., Spector,D.L., Hannon,G.J. and Lowe,S.W. (2003) Rb-mediated heterochromatin formation and silencing of E2F target genes during cellular senescence. *Cell*, **113**, 703–716.
- Turner,B.M. (2000) Histone acetylation and an epigenetic code. *BioEssays*, **22**, 836–845.
- Jenuwein,T. and Allis,C.D. (2001) Translating the histone code. *Science*, **293**, 1074–1080.
- Rando,O.J. (2007) Global patterns of histone modifications. *Curr. Opin. Genet. Dev.*, **17**, 94–99.
- Barski,A., Cuddapah,S., Cui,K., Roh,T.Y., Schones,D.E., Wang,Z., Wei,G., Chepelev,I. and Zhao,K. (2007) High-resolution profiling of histone methylations in the human genome. *Cell*, **129**, 823–837.
- Dion,M.F., Altschuler,S.J., Wu,L.F. and Rando,O.J. (2005) Genomic characterization reveals a simple histone H4 acetylation code. *Proc. Natl Acad. Sci. USA*, **102**, 5501–5506.
- Henikoff,S. (2005) Histone modifications: combinatorial complexity or cumulative simplicity? *Proc. Natl Acad. Sci. USA*, **102**, 5308–5309.
- Schreiber,S.L. and Bernstein,B.E. (2002) Signaling network model of chromatin. *Cell*, **111**, 771–778.
- Jackson,V. and Chalkley,R. (1985) Histone segregation on replicating chromatin. *Biochemistry*, **24**, 6930–6938.

12. Sogo, J.M., Stahl, H., Koller, T. and Knippers, R. (1986) Structure of replicating simian virus 40 minichromosomes. The replication fork, core histone segregation and terminal structures. *J. Mol. Biol.*, **189**, 189–204.
13. Groth, A., Rocha, W., Verreault, A. and Almouzni, G. (2007) Chromatin challenges during DNA replication and repair. *Cell*, **128**, 721–733.
14. Sobel, R.E., Cook, R.G., Perry, C.A., Annunziato, A.T. and Allis, C.D. (1995) Conservation of deposition-related acetylation sites in newly synthesized histones H3 and H4. *Proc. Natl Acad. Sci. USA*, **92**, 1237–1241.
15. Loyola, A., Bonaldi, T., Roche, D., Imhof, A. and Almouzni, G. (2006) PTMs on H3 variants before chromatin assembly potentiate their final epigenetic state. *Mol. Cell*, **24**, 309–316.
16. Scharf, A.N., Meier, K., Seitz, V., Kremmer, E., Brehm, A. and Imhof, A. (2009) Monomethylation of lysine 20 on histone H4 facilitates chromatin maturation. *Mol. Cell Biol.*, **29**, 57–67.
17. Shimamura, A. and Worcel, A. (1989) The assembly of regularly spaced nucleosomes in the *Xenopus* oocyte S-150 extract is accompanied by deacetylation of histone H4. *J. Biol. Chem.*, **264**, 14524–14530.
18. Benson, L.J., Gu, Y., Yakovleva, T., Tong, K., Barrows, C., Strack, C.L., Cook, R.G., Mizzen, C.A. and Annunziato, A.T. (2006) Modifications of H3 and H4 during chromatin replication, nucleosome assembly, and histone exchange. *J. Biol. Chem.*, **281**, 9287–9296.
19. Carre, C., Szymczak, D., Pidoux, J. and Antoniewski, C. (2005) The histone H3 acetylase dGcn5 is a key player in *Drosophila* melanogaster metamorphosis. *Mol. Cell Biol.*, **25**, 8228–8238.
20. Hassan, A.H., Prochasson, P., Neely, K.E., Galasinski, S.C., Chandry, M., Carozza, M.J. and Workman, J.L. (2002) Function and selectivity of bromodomains in anchoring chromatin-modifying complexes to promoter nucleosomes. *Cell*, **111**, 369–379.
21. Syntichaki, P., Topalidou, I. and Thireos, G. (2000) The Gcn5 bromodomain co-ordinates nucleosome remodelling. *Nature*, **404**, 414–417.
22. Melcher, M., Schmid, M., Aagaard, L., Selenko, P., Laible, G. and Jenuwein, T. (2000) Structure-function analysis of SUV39H1 reveals a dominant role in heterochromatin organization, chromosome segregation, and mitotic progression. *Mol. Cell Biol.*, **20**, 3728–3741.
23. Lee, J., Thompson, J.R., Botuyan, M.V. and Mer, G. (2008) Distinct binding modes specify the recognition of methylated histones H3K4 and H4K20 by JMJD2A-tudor. *Nat. Struct. Mol. Biol.*, **15**, 109–111.
24. Huang, Y., Fang, J., Bedford, M.T., Zhang, Y. and Xu, R.M. (2006) Recognition of histone H3 lysine-4 methylation by the double tudor domain of JMJD2A. *Science*, **312**, 748–751.
25. Annunziato, A.T. and Seale, R.L. (1983) Histone deacetylation is required for the maturation of newly replicated chromatin. *J. Biol. Chem.*, **258**, 12675–12684.
26. Pesavento, J.J., Yang, H., Kelleher, N.L. and Mizzen, C.A. (2008) Certain and progressive methylation of histone H4 at lysine 20 during the cell cycle. *Mol. Cell Biol.*, **28**, 468–486.
27. Osley, M.A. (1991) The regulation of histone synthesis in the cell cycle. *Annu. Rev. Biochem.*, **60**, 827–861.
28. Xeros, N. (1962) Deoxyriboside control and synchronization of mitosis. *Nature*, **194**, 682–683.
29. Hake, S.B., Garcia, B.A., Duncan, E.M., Kauer, M., Dellaire, G., Shabanowitz, J., Bazett-Jones, D.P., Allis, C.D. and Hunt, D.F. (2006) Expression patterns and post-translational modifications associated with mammalian histone H3 variants. *J. Biol. Chem.*, **281**, 559–568.
30. Wolffe, A.P. (1998) *Chromatin Structure and Function*, 3rd edn. Academic Press, San Diego, CA.
31. Taipale, M., Rea, S., Richter, K., Vilar, A., Lichter, P., Imhof, A. and Akhtar, A. (2005) hMOF Histone Acetyltransferase Is Required for Histone H4 Lysine 16 Acetylation in Mammalian Cells. *Mol. Cell Biol.*, **25**, 6798–6810.
32. Chestier, A. and Yaniv, M. (1979) Rapid turnover of acetyl groups in the four core histones of simian virus 40 minichromosomes. *Proc. Natl Acad. Sci. USA*, **76**, 46–50.
33. Pesavento, J.J., Bullock, C.R., Leduc, R.D., Mizzen, C.A. and Kelleher, N.L. (2008) Combinatorial modification of human histone H4 quantitated by two-dimensional liquid chromatography coupled with top down mass spectrometry. *J. Biol. Chem.*, **283**, 468–486.
34. Sims, R.J. III, Nishioka, K. and Reinberg, D. (2003) Histone lysine methylation: a signature for chromatin function. *Trends Genet.*, **19**, 629–639.
35. Garcia, B.A., Barber, C.M., Hake, S.B., Ptak, C., Turner, F.B., Busby, S.A., Shabanowitz, J., Moran, R.G., Allis, C.D. and Hunt, D.F. (2005) Modifications of human histone H3 variants during mitosis. *Biochemistry*, **44**, 13202–13213.
36. Thomas, C.E., Kelleher, N.L. and Mizzen, C.A. (2006) Mass spectrometric characterization of human histone H3: a bird's eye view. *J. Proteome Res.*, **5**, 240–247.
37. Hansen, K.H., Bracken, A.P., Pasini, D., Dietrich, N., Gehani, S.S., Monrad, A., Rappsilber, J., Lerdrup, M. and Helin, K. (2008) A model for transmission of the H3K27me3 epigenetic mark. *Nat. Cell Biol.*, **10**, 1291–1300.
38. Bonenfant, D., Towbin, H., Coulot, M., Schindler, P., Mueller, D.R. and van Oostrum, J. (2007) Analysis of dynamic changes in post-translational modifications of human histones during cell cycle by mass spectrometry. *Mol. Cell Proteomics*, **6**, 1917–1932.
39. Sarraf, S.A. and Stancheva, I. (2004) Methyl-CpG binding protein MBD1 couples histone H3 methylation at lysine 9 by SETDB1 to DNA replication and chromatin assembly. *Mol. Cell*, **15**, 595–605.
40. Huen, M.S., Sy, S.M., van Deursen, J.M. and Chen, J. (2008) Direct interaction between SET8 and proliferating cell nuclear antigen couples H4-K20 methylation with DNA replication. *J. Biol. Chem.*, **283**, 11073–11077.
41. Rice, J.C., Briggs, S.D., Ueberheide, B., Barber, C.M., Shabanowitz, J., Hunt, D.F., Shinkai, Y. and Allis, C.D. (2003) Histone methyltransferases direct different degrees of methylation to define distinct chromatin domains. *Mol. Cell*, **12**, 1591–1598.
42. Nishioka, K., Rice, J.C., Sarma, K., Erdjument-Bromage, H., Werner, J., Wang, Y., Chuikov, S., Valenzuela, P., Tempst, P., Steward, R. et al. (2002) PR-Set7 is a nucleosome-specific methyltransferase that modifies lysine 20 of histone H4 and is associated with silent chromatin. *Mol. Cell*, **9**, 1201–1213.
43. Schotta, G., Lachner, M., Sarma, K., Ebert, A., Sengupta, R., Reuter, G., Reinberg, D. and Jenuwein, T. (2004) A silencing pathway to induce H3-K9 and H4-K20 trimethylation at constitutive heterochromatin. *Genes Dev.*, **18**, 1251–1262.
44. Wang, H., An, W., Cao, R., Xia, L., Erdjument-Bromage, H., Chatton, B., Tempst, P., Roeder, R.G. and Zhang, Y. (2003) mAM facilitates conversion by ESET of dimethyl to trimethyl lysine 9 of histone H3 to cause transcriptional repression. *Mol. Cell*, **12**, 475–487.
45. Wysocka, J., Swigut, T., Milne, T.A., Dou, Y., Zhang, X., Burlingame, A.L., Roeder, R.G., Brivanlou, A.H. and Allis, C.D. (2005) WDR5 associates with histone H3 methylated at K4 and is essential for H3 K4 methylation and vertebrate development. *Cell*, **121**, 859–872.
46. Nielsen, P.R., Nietlispach, D., Mott, H.R., Callaghan, J., Bannister, A., Kouzarides, T., Murzin, A.G., Murzina, N.V. and Laue, E.D. (2002) Structure of the HP1 chromodomain bound to histone H3 methylated at lysine 9. *Nature*, **416**, 103–107.
47. Lachner, M., O'Carroll, D., Rea, S., Mechtler, K. and Jenuwein, T. (2001) Methylation of histone H3 lysine 9 creates a binding site for HP1 proteins. *Nature*, **410**, 116–120.
48. Fischle, W., Wang, Y., Jacobs, S.A., Kim, Y., Allis, C.D. and Khorasanizadeh, S. (2003) Molecular basis for the discrimination of repressive methyl-lysine marks in histone H3 by Polycomb and HP1 chromodomains. *Genes Dev.*, **17**, 1870–1881.
49. Narlikar, G.J., Fan, H.Y. and Kingston, R.E. (2002) Cooperation between complexes that regulate chromatin structure and transcription. *Cell*, **108**, 475–487.
50. Sarg, B., Koutzamani, E., Helliger, W., Rundquist, I. and Lindner, H.H. (2002) Postsynthetic trimethylation of histone H4 at lysine 20 in mammalian tissues is associated with aging. *J. Biol. Chem.*, **277**, 39195–39201.
51. Fraga, M.F., Ballestar, E., Villar-Garea, A., Boix-Chornet, M., Espada, J., Schotta, G., Bonaldi, T., Haydon, C., Ropero, S., Petrie, K. et al. (2005) Loss of acetylation at Lys16 and trimethylation at Lys20 of histone H4 is a common hallmark of human cancer. *Nat. Genet.*, **37**, 391–400.

3.2 Discussion

3.2.1 H3K36 methylation during transcription

Stepwise regulation has been described before for H3K76 (K76 equates to K79 in other organisms) in *Trypanosoma brucei* (Janzen et al. 2006). This unicellular parasitic protozoan has two homologs of DOT1 (A and B) that catalyzes di- and trimethylation of H3K76, respectively. DOT1A is essential for viability and dimethylation occurs only in mitosis. Whereas trimethylation is detected throughout the cell cycle and the absence of DOT1B does not affect viability (Janzen et al. 2006). Moreover, H4K20 methylation is also regulated in a stepwise manner. Monomethylation is catalyzed by Pr-Set7/Set8 exclusively and Suv4-20h1 and Suv4-20h2 are the methyltransferases for H4K20 di- and trimethylation (Schotta et al. 2004; Pesavento et al. 2008). Increasing the methylation degree in a stepwise manner adds additional regulation possibilities. Only when reaching a specific condition the next methyl group is added or removed. However, when the cascade of methylation is disrupted the final cell fate cannot be obtained.

The H3K36 specific methyltransferase dMes-4 is required for dimethylation whereas trimethylation is mediated by dHypb. Knockdowns of dMes-4 and dHypb affected the global methylation levels of H3K36. Specifically, reduction of dHypb resulted in a decrease of H3K36 trimethylation and at the same time in an increase of dimethylation. Knockdown of dMes-4 reduced the levels of di- as well as trimethylation of H3K36. This was shown by Western blot analysis and confirmed by mass spectrometry using MS/MS analysis in order to determine specifically the modified residue and exclude antibody cross reactivity when Western blotting.

One way how histone modifications can convey their biological signal is by recruiting specific binding factors. Several proteins binding to methylated histone tails containing the chromodomain as a binding motif (Daniel et al. 2005). MSL3, a component of the MSL (male specific lethal) complex, also contains a chromodomain. The MSL complex is required for dosage compensation of the X chromosome in *Drosophila*. The MSL3 homolog in yeast is the Eaf3 protein and it was identified to interact via its chromodomain with H3K36 trimethylation (Joshi et al. 2005). The *Drosophila*

MSL3 protein is highly conserved and also contains an N-terminal chromodomain (Koonin et al. 1995). A recent study by Larschan et al. demonstrated that the MSL complex is recruited to active genes on the X chromosome by the interaction of H3K36 trimethylation and MSL3 (Larschan et al. 2007). For a comparative ChIP-chip analysis chromodomain deletion mutants as well as targeted point mutation mutants were created. The results of the high resolution analysis revealed that the chromodomain mutants fail to bind most of the genes on the X chromosome (Sural et al. 2008). Sural et al also suggest that the spreading of dosage compensation is mediated by the MSL3 chromodomain.

Different methylation states of H3K36 lead to either increasing or decreasing levels of H4K16 acetylation on autosomes. Dimethylation of H3K36 increases H4K16 acetylation whereas trimethylation is associated with reduction of H4K16 acetylation levels. A speculative scenario would be that dimethylation is recruiting MOF, a H4K16 HAT activity (Akhtar et al. 2000; Taipale et al. 2005) to the region. This would fit to previous described studies where MOF interacts with MLL, a H3K4 methyltransferase (Dou et al. 2005). By controlling hyperacetylation di- and trimethylation states of H3K36 possess opposing effects towards chromatin accessibility. Open and closed chromatin structures are needed during cycles of transcription (Gregory et al. 1998). Especially acetylation of H4K16 is known to have an impact on higher order chromatin structure and to influence the binding of non-histone proteins. Interestingly, chromatin compaction by ISWI, a remodeling ATPase is restricted by H4K16 acetylation, as well as the remodeling ability of ACF is inhibited when H4K16 acetylation is present (Corona et al. 2002; Clapier et al. 2002; Shogren-Knaak et al. 2006). This site specific function of H4K16 acetylation to counteract chromatin compaction in combination with its dependency of a specific H3K36 methylation state supports the histone code hypothesis. It would be of great interest to investigate further mechanisms by which acetylation in combination with methylation exerts its role in transcription.

3.2.2 H4K20 monomethylation during chromatin assembly

To study chromatin assembly a cell free extract was used that derived from early *D. melanogaster* embryos. Embryogenesis in *Drosophila* is unique since cleavage results in a syncytium. First cells surrounded by plasma membranes are formed after an approximate accumulation of 5000 nuclei. At the end of embryogenesis heterochromatin becomes strongly visible at the apical pole of early blastoderm nuclei (Rudolph et al. 2007). An extract from preblastoderm embryos contains the maternal pool of histones and assembly factors that assembly DNA into nucleosomal arrays. This very stable and efficient system is particularly useful to investigate chromatin assembly mechanism *in vitro* (Becker et al. 1992; Eskeland et al. 2007). However, the reconstituted chromatin lacks linker histone H1 (Becker et al. 1992). Therefore, in early *Drosophila* development H1 is not involved in chromatin condensation. But studies from early embryogenesis suggest that HMG-D (high mobility group proteins), an abundant chromosomal protein, serves as substitute for linker histone H1 (Ner et al. 2001). Maybe also other essential factors are substituted or even missing since the analysis of histone modifications on H3 and H4 unveiled only H4K20 to be methylated. Previous studies using HeLa cells have revealed that also H3K9 methylation exists prior to deposition (Loyola et al. 2006). It is difficult to compare organisms since the profiles of histone modifications differ significantly from unicellular eukaryotes to mammals (Garcia et al. 2007). In contrast to HeLa cells this present study detected no H3K9 methylation, neither before assembly nor after assembly. Possibly, methylation on H3K9 is needed prior to deposition in order to spread the mark during chromatin maturation. Another explanation could be that targeting of Su(var)3-9 to chromatin is inactive or inhibited in the extract. To address these questions further experiments could include adding candidate targeting factors to the assembly reaction or add premethylated nucleosomes.

In contrast to methylation, acetylation patterns obtained before and after assembly are in agreement with previous studies. H4 is deposited in a diacetylated form (Sobel et al. 1995; Chang et al. 1997) and the removal of the acetyl marks starts after assembly in a constant manner. Taddei and colleagues suggest that deacetylation takes less than one hour (Taddei et al. 1999) but the results of this study observe a gradual deacetylation at least over six hours. We conclude that the *in vitro* system is reliable in terms of what happens but the kinetics is shifted.

In this work and also in other studies (Pesavento et al. 2008) it was demonstrated that H4K20

is monomethylated right after chromatin assembly (Figure 6). The functions of H4K20 monomethylation are still vague. Studies on H4K20 reported monomethylation associated with the promoter region of a repressed reporter system (Vaquero et al. 2004) and also with *Xist* expression in ES cells and labels the initiation of X inactivation (Kohlmaier et al. 2004). On the contrary H4K20 monomethylation is also found at promoter and coding regions of active gene and complies with hyperacetylation (Talasz et al. 2005). This present work suggests H4K20 monomethylation to have a role in chromatin assembly.

Pr-Set7, the monomethyltransferase of H4K20 (Nishioka et al. 2002; Xiao et al. 2005) localizes to the replication fork and is essential for S phase progression (Tardat et al. 2007; Jørgensen et al. 2007). Together with the fact that Pr-Set7 only acts on nucleosomal substrates, being consistent with studies in mammalian (Fang et al. 2002), this also supports the assumption that at least one function of H4K20 monomethylation is to label newly synthesized H4 immediately after chromatin assembly. With this mark one could distinguish between old and new H4 since old histones H4 are predominantly dimethylated and no demethylase found so far impacts on H4K20. This mark could then be important for assembly and coordinated chromatin maturation during cell cycle. Previous studies also observe a cell cycle dependent change in Pr-Set7 expression and also in the corresponding histone mark with an increase at late S/G₂ and a peak in M phase (Houston et al. 2008; Pesavento et al. 2008; Oda et al. 2009). To summarize this, newly synthesized H4 is deposited onto chromatin during S phase and becomes monomethylated at lysine 20 at late S/G₂ phase. During G₁ phase levels drop due to a conversion to di- or trimethylation.

Methylation marks recruit a diverse array of proteins such as Tudor domain containing factors classified as the “Royal family” (Maurer-Stroh et al. 2003). One of these factors is l(3)MBT that has been shown to bind, via a conserved malignant brain tumor motif, H4K20 monomethylated peptides (Li et al. 2007) and compacts nucleosomal arrays to promote a higher order chromatin structure (Trojer et al. 2007). This present study describes the interaction of dl(3)MBT and dRpd3. The recruited HDAC may also assist in establishing higher order chromatin by the removal of acetyl groups.

The importance of Pr-Set7 and thus H4K20 monomethylation is stressed by recent mouse studies where embryonic lethality is observed in Pr-Set7/Set8 knockout mice (Oda et al. 2009). Oda and

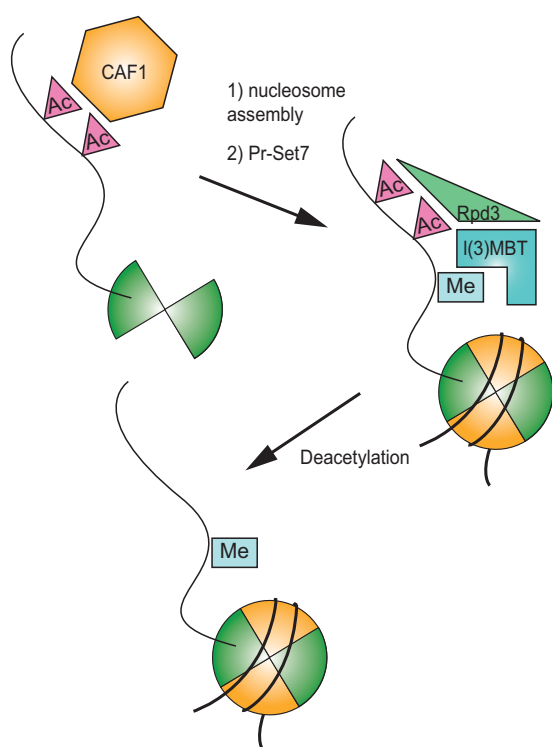


Figure 6: Chromatin maturation. Newly synthesized H4 is acetylated at K5 and K12 and associated with the histone chaperone CAF-1. Upon nucleosome assembly, H4 is monomethylated at K20, that serves as a binding site for I(3)MBT. Rpd3 is in a complex with I(3)MBT and deacetylates H4K5 and K12.

al. 2009). The authors conclude that Pr-Set7/Set8 coordinately regulates adipocyte differentiation through histone modifications. This finding provides yet another role of H4K20 monomethylation *in vivo*.

Preliminary studies have shown in the context of DREX assembly that inhibition of H4K20 monomethylation by SAH not only inhibits the deacetylation of the predeposition marks but also the dissociation kinetic of CAF1 is altered (Figure 7). Without inhibitor CAF1 stays associated with chromatin for less than 60 minutes but under addition of SAH CAF1 remains bound to chromatin for more than three hours. It would be interesting to investigate which mechanisms trigger the chaperone to abide with chromatin or to dissociate from chromatin.

colleagues can link DNA damage and cell cycle delay to the lack of Pr-Set7. Pr-Set7 RNAi cells show an increase in DNA damage as well as aberrant centrosomes (Houston et al. 2008). However, it was recently shown that Pr-Set7 is also able to methylate p53. So it can be assumed that the association with DNA damage is due to altered functions of p53 (Shi et al. 2007). So it will be to further studies to discover the still unknown proteins that can be methylated by Pr-Set7.

Cell differentiation is controlled by transcriptional mechanisms and epigenetic modifications. A recent study revealed a link between H4K20 monomethylation and adipocyte differentiation. Pr-Set7/Set8 is upregulated thus increasing H4K20 monomethylation levels during adipogenesis and the knockdown of Pr-Set7/Set8 represses adipocyte differentiation (Wakabayashi et

Preliminary proteomics experiments were done, analyzing all proteins bound to chromatin again with or without treating the samples with SAH after three hours of assembly. Upon inhibition with SAH Pr-Set7 was found whereas in the control no Pr-Set7 was identified. This suggests that Pr-Set7 briefly interacts with chromatin and can only be trapped to chromatin when monomethylation of H4K20 is inhibited. However, these proteomics experiments need to be repeated and analysis of chromatin of different time points after assembly could reveal additional information about the dynamics of chromatin assembly factors.

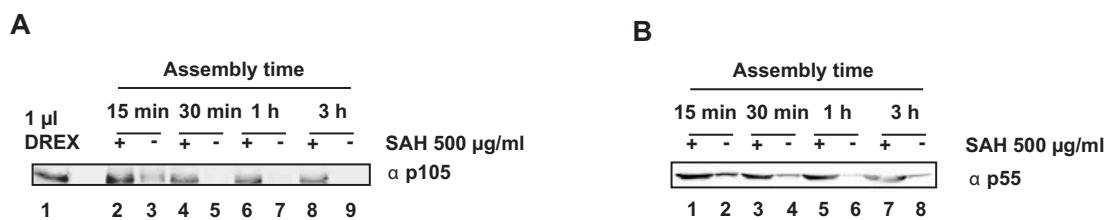


Figure 7: Monomethylation of H4K20 triggers dissociation of CAF1. Western blot analysis of kinetics of CAF1 subunit p105 (A) and subunit p55 (B) with and without inhibition of H4K20 monomethylation by SAH.

3.2.3 Histone modifications during chromatin assembly *in vivo*

To be able to compare old and new histones and its associated modifications a pulsed SILAC labeling technique was used that selectively labeled new histones (Scharf, Barth, et al. 2009). Analysis by means of mass spectrometry (Bonaldi et al. 2004) made it possible to compare modification pattern from old versus new histones in the same spectrum. Using pulsed SILAC for investigating the inheritance of histones has several advantages. First no radioactive material is needed as it was for the pulse chase experiments from Jackson (Jackson et al. 1975). These studies were also not powerful enough to analyze individual histone modification patterns and no direct comparison old versus new histones was possible. In the recent years genomewide arrays revealed valuable information about histone modification patterns however a direct comparison old versus new histones is not feasible (Robyr et al. 2003). Thus pulsed SILAC is an elegant method to use when comparing the modification patterns of old and new histones.

The amount of DNA and tightly coupled the amount of histones (Marzluff et al. 2002) doubles during S phase expecting 50% old and 50% new histones after one round of S phase. To test this, tumor cells (HeLa) were synchronized and labeled during S phase and further on. RT PCR results as well as MALDI TOF results showed preferential labeling between two and six hours post release into S phase. A total maximum of 43% incorporation efficiency is reached after 12 hours of labeling. Reasons for the discrepancy between expected and observed incorporation may be due to an endogenous stored pool of R⁰ arginine that is incorporated before the exogenous supply. To test the amount of endogenously stored R⁰ arginine, peptide aa41 to 49 of histone H3 was analyzed since it contained two arginines resulting from the lacking ability of trypsin to digest before a proline. The amount of peptides containing one R⁰ and one R⁴ labeled arginines reflects the amount of the stored pool. Only six percent of the total peptides show a combination of R⁰ and R⁴ labeled arginines arguing for a low abundance of stored arginine within the cell. But these six percent explain part of the difference between measured and calculated incorporation efficiency. Another possible explanation for not reaching the expected 50% is that upon the release of the thymidine block not all cells recover and thus hesitate to start into S phase. In the FACS profiles a very small pool of cells arrest in G1 phase and do not enter S phase as it was also observed in previous studies (Bostock et al. 1971).

Analysis of histone modifications was solely performed using MALDI TOF. This technique allows determining the mass of a peptide and conclusion can be drawn about the modification state of the peptide. However, from the mass alone the exact position of the modification cannot be deduced. For peptides containing multiple modifiable residues tandem MS is suggested to map the specific site of the modification (Villar-Garea et al. 2008).

Furthermore propionic anhydride treatment was used for the analysis. This chemical modification procedure is needed to achieve analyzable peptide fragment after the tryptic digest. However, when using the anhydride treatment it cannot be distinguished between acetylation and trimethylation as both masses create overlapping peaks. To assign a mass to either acetylation or trimethylation tandem MS should be used in further experimental analysis.

When using SILAC additional overlapping peaks were created. Therefore it was not possible to analyze the four times acetylation state of peptide aa4 to 17 of the newly synthesized histones as this peak overlaps with the unmodified peptide aa56 to 67 of H4. However, the incidence that all four lysines (K5, 8, 12, 16) are acetylated at the very same time is rare.

Consistent with previous studies (Chestier et al. 1979) a highly dynamic acetylation pattern was detected thus proofing the experimental setup to be correct. In this study peptide aa4 to 17 on H4 was analyzed. Six hours post release the modification pattern of old and new histones are indistinguishable and most peptides are unmodified. However, it is known that lysine 5 and 12 on H4 are acetylated prior to chromatin assembly (Sobel et al. 1995) and the deacetylation is important for chromatin maturation (Annunziato et al. 1983). Taddei and colleagues defined a time window of 20 to 60 minutes where deacetylation occurs (Taddei et al. 1999). To omit deacetylation a deacetylase inhibitor sodium butyrate was applied. The diacetylated form can be visualized when sodium butyrate is applied simultaneously with the release. Further experiments using sodium butyrate at different time points and for different duration revealed a dynamic equilibrium of acetylation and deacetylation. Also the fact that deacetylation occurs fast was verified with pulsed SILAC.

On the contrary methylation patterns show slow dynamics. It takes longer than the 60 minutes shown for deacetylation until the new histones resemble old histones in terms of modification marks. After six hours post release methylation on H4K20 is strikingly different when comparing old and new histones. Old histones are mainly dimethylated but new histones preferentially show

the monomethylated mark. Previous studies have shown a cell cycle regulated manner of H4K20 methylation starting in an unmethylated state prior to deposition, followed by an immediate increase of monomethylation and then ending in a dimethylated form rather than the rare trimethylated state (Pesavento et al. 2008; Scharf, Meier, et al. 2009). Judging from the pulsed SILAC results H4K20 requires more than 20 hours in a stepwise manner to adjust the modification patterns from old to new. The kinetics for the individual methylation states differ so that monomethylation is observed very rapidly whereas further methylation states require more time. It was also shown that monomethylation is needed as a substrate for the enzymes responsible for setting the di- and trimethylation mark (Schotta et al. 2008). In the line with methylation kinetics on K20 the establishment of K27/K36 and K9/16 methylation on the new histones is also observed in a stepwise manner and also requires almost one entire cell cycle. For K36 on H3 a stepwise methylation manner involving different enzymes has also been shown in the study by Bell et al. (Bell et al. 2007). It is tempting to speculate that the stepwise methylation and its different kinetics are caused by the different recruitment manners of the appropriate methyltransferase. So is Pr-Set7/Set8 the monomethylase of H4K20 brought by PCNA to the replication fork and is able immediately after chromatin assembly to set the methylation mark thus supporting the fact that monomethylation occurs fast on K20. The recruitment of the enzymes mediating di- and trimethylation seem to be obtained outside S phase. However, this argument holds not true for H3K27 methylation as the same enzyme EZH2 is responsible for all three methylation states. Another possibility to explain the stepwise methylation and the long methylation process is that the cell creates a window of opportunity. During this window only histone modifications are set that allow an accessible chromatin structure. The cell is now able to easily process external signals and just before the start of the next cell cycle further methylation degrees are added allowing chromatin to mature to its condensed state. Interestingly, no demethylase for H4K20 is found so far. Therefore it would be an advantage for the cell to postpone permanent marks as long as possible in order to be flexible to the environment as long as possible.

For future experiments changing the synchronization technique should be considered. The common method of a double thymidine block is a simple way to synchronize cells but it may lead to metabolism perturbation and may affect the progression through the cell cycle. A more elaborate method is counterflow centrifugal elutriation, where cells are separated according to their cell size and sedimentation density thus resulting in different pools of cells in different cell cycle stages.

This method is devoid from external supplementation thereby adding no additional stress on the individual cells (Banfalvi 2008).

In this study HeLa cells were used as the only cell line to be analyzed. However, many tumor cells carry abnormal modification pattern (Fraga et al. 2005). It would be of great interest to explore the modification behavior in a non tumor derived cells such as primary cell lines and compare the results with the obtained in this study. Maybe inaccurate inheritance of histone modification pattern as a consequence of a rapid replication time in tumor cells is responsible for genomic and epigenetic instability typically considered as a hallmark of cancer (Sieber et al. 2003).

The timing of DNA replication during S phase of the cell cycle and gene transcription is coordinated and replication timing, histone acetylation and transcription was profiled throughout the *Drosophila* genome by a recent study of Schwaiger et al. H4K16 acetylation was shown to be enriched at initiation zones (Schwaiger et al. 2009). Since now the technique of pulsed SILAC is established for comparing old and new histones, it would be interesting to alter labeling times. By shortening the labeling time to less than 6 h one could dissect modifications associated with early replicating chromatin. Also interesting would be the labeling of late replicating chromatin solely and of course the comparison of late versus early replicating chromatin whether and how the establishment of histone modifications are different.

3.2.4 General outlook

All DNA mediated processes have to cope with chromatin and given the fact that histone modifications are key players in controlling the structure and function of the chromatin fiber, it is of great importance to understand how histone modifications are regulated and organized. Especially interesting is the inheritance of histone modifications since defined patterns of gene expression and silencing, are needed for cell survival. To ensure such epigenetic inheritance, it is clear that complex mechanisms operate during replication. Besides histone modifications there are also other factors involved in epigenetic inheritance that can be found in early replicating chromatin. An elegant technique to specifically investigate newly replicated chromatin is “click chemistry”. When using click chemistry, a base analog is incorporated during replication similar to BrdU labeling. But instead of using an antibody for further processing, the modified base is “clicked” to a linker that can be coupled to either a fluorophor or biotin. The latter can then be isolated with streptavidin coated beads (Salic et al. 2008; Speers et al. 2004). This technique of labeling newly replicated chromatin and the possibility to isolate associated chromatin binding proteins could shed more light in the mechanisms of epigenetic inheritance. Even more powerful could be the combination of click chemistry and thus labeling newly replicated chromatin and pSILAC that allows specific labeling of newly synthesized histones to discover the mechanisms by which the cells identity is defined.

Annette N.D. Scharf und Axel Imhof. Replikation des Chromatins-dispersiv statt semi-konservativ? *BIOspektrum*, September 2007.

Declaration of contribution to “Replikation des Chromatins –dispersiv statt semikonservativ?”: The first draft of the manuscript was composed by me and the final version was written with Axel Imhof.

Histonmodifikationen

Replikation des Chromatins – dispersiv statt semikonservativ?

ANNETTE N. D. SCHARF UND AXEL IMHOF
BIOMEDIZINISCHES ZENTRUM DER LUDWIG-MAXIMILIANS-UNIVERSITÄT, MÜNCHEN

Vergleicht man eine menschliche Leberzelle mit einer Muskelzelle, so ist die gespeicherte Erbinformation in Form von DNA bei beiden Zelltypen identisch. Dennoch erfüllen Leber- und Muskelzelle unterschiedliche Aufgaben im Körper und exprimieren dazu unterschiedliche Gene. Wie kann man sich dieses Phänomen erklären?

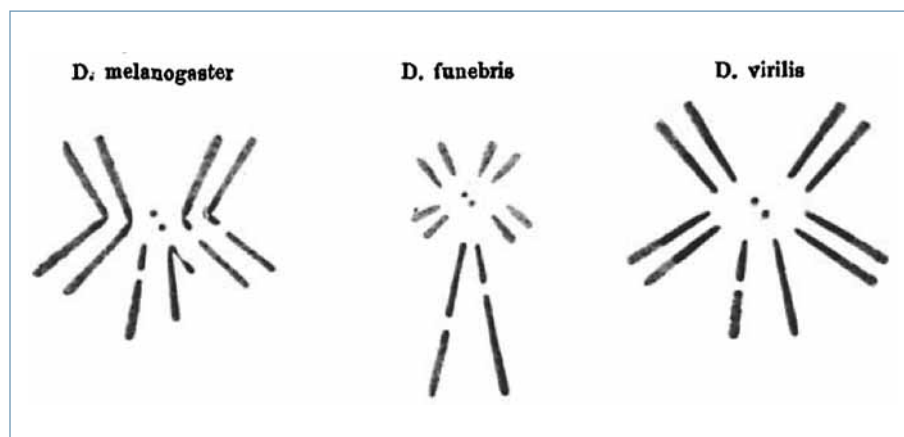
■ Schon seit Anfang des letzten Jahrhunderts wurde der Verpackung der DNA eine wichtige regulatorische Rolle zugeschrieben. Bereits vor fast 80 Jahren hat Emil Heitz auf eine Diskrepanz zwischen der physikalischen und der genetischen Karte von Chromosomen der Taufliege *Drosophila melanogaster* hingewiesen (Abb. 1). Heitz konnte in Moosen zeigen, dass sich unterschiedliche Bereiche des Chromatins während des Zellzyklus unterschiedlich verhalten, was zur Etablierung der Begriffe Euchromatin für das sich verändernde und Heterochromatin für das stets kondensiert bleibende Chromatin führte. Bereits damals hat Heitz auf die, wie er es nannte, genetische Passivität des Heterochromatins hingewiesen^[1]. Nach den Beobachtungen von Heitz dauerte es jedoch noch weitere 40 Jahre, bis die molekulare Grundstruktur des Chromatins, das Nukleosom, charakterisiert werden konnte^[2]. Dieser fundamentale Baustein beinhaltet doppelsträngige DNA mit einer Länge von 147 Basenpaaren, die um ein Oktamer aus Proteinen, die Histone, gewunden ist. Ein Oktamer besteht aus jeweils zwei Molekülen der Kernhistone H2A, H2B, H3 und H4^[3]. Nukleosomen, die durch den fortlaufenden DNA-Faden miteinander verbunden sind, werden oft als „Perlenkette“ mit einer Größe von 11 nm dargestellt, die sich erst durch den Einbau des Linker-Histons H1 sowie die posttranslationalen Modifikationen von Kernhistonen zu einer spiralförmigen Struktur mit einem Durchmesser von 30 nm faltet. Höhere Stufen der Kompaktierung bis hin zum mitotischen Chromosom unterliegen dem Zusammenspiel weiterer Proteine.

Wie werden nun bestimmte Chromatinstrukturen, wie das Heitz'sche Euchromatin oder das inaktive X-Chromosom in weiblichen Säugetieren, etabliert? Die vollständige Sequenzierung von ganzen Genomen und die damit einhergehenden Möglichkeiten, die Eigenschaften bestimmter Bereiche des Chromatins „genomweit“ zu untersuchen, erlaubten eine sehr viel genauere und detailliertere Charakterisierung des Chromatins, als dies noch zu Zeiten von Emil Heitz der Fall war. So stellte sich heraus, dass z. B. große Bereiche im Genom durch DNA-Methylierung stillgelegt werden können^[4], was durch bestimmte posttranslationale Modifikationen von Histonen^[5] oder den Einbau von Histonvarianten^[6] und Chromatin-bindenden Proteinen noch weiter verstärkt wird.

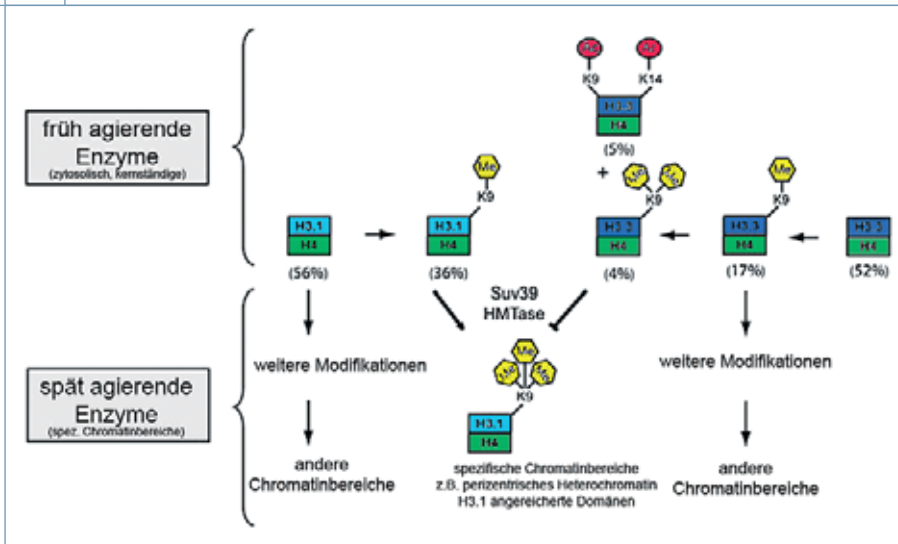
Histon-Modifikationen, Bausteine des Zellgedächtnisses

Besonders den Histon-Modifikationen wird derzeit große Bedeutung bei der Ausbildung von definierten Chromatinstrukturen zugemessen. Viele sequenzspezifisch DNA-bindende Faktoren sind in der Lage, Chromatin-modifizierende Enzyme an dem jeweiligen Genlokus zu rekrutieren und dort ein spezifisches Modifikationsmuster, einen Histon-Code^[7], zu etablieren. Dieses Muster kann dann, so die Hypothese, von Chromatin-assoziierten Proteinen ausgelesen werden, die ihrerseits wiederum eine typische Chromatinstruktur induzieren. Acetylierte Nukleosomen kennzeichnen so zum Beispiel offene Chromatinstrukturen, die von der Transkriptionsmaschinerie abgelesen werden können, während Histone, die an bestimmten Lysinresten mehrfach methyliert sind, stillgelegte Chromatinbereiche zu markieren scheinen.

Die Verteilung von Heterochromatin und Euchromatin wird klonal vererbt, das heißt, dass eine bestimmte Struktur, nachdem sie einmal gebildet wurde, über mehrere Zellgenerationen hinweg vererbt werden muss. Während jedoch über die Erzeugung von komplexen Histon-Modifikationen schon relativ viel bekannt ist, wird die Aufrechterhaltung



▲ **Abb. 1:** Zeichnungen von E. Heitz von Chromosomensätzen unterschiedlicher *Drosophila*-Unterarten (nach^[1]). Besonders auffällig sind das Vorhandensein jeweils eines stark verkürzten Chromosoms in der Mitte sowie die unterschiedliche Dicke innerhalb eines Chromosoms (chromosomale Längsdifferenzierung).



▲ **Abb. 2:** Stufenmodell der Etablierung und Vererbung posttranslationaler Histon-Modifikationen am Beispiel von H3K9. Monomethyliertes H3.1 ist sensitiv für Suv39 und kann an K9 (Lysin 9) trimethyliert werden. Im Gegensatz dazu ist H3.3 auf K9 acetyliert beziehungsweise dimethyliert und kann nicht weiter methyliert werden (Copyright Elsevier).

von definierten Modifikationsmustern auf den Histonen bei der Verdopplung des Chromatins noch wenig verstanden. Während der Replikation muss sich eine einmal etablierte Chromatinstruktur mitsamt ihren teilweise hochkomplexen Modifikationen der Herausforderung zweier elementarer Prozesse stellen. Zum einen müssen die bereits auf der DNA existierenden Nukleosomen auf die neu entstandene DNA transferiert werden, zum anderen muss der aufgrund der Replikation erhöhte Bedarf an Nukleosomen durch neu synthetisierte Histone gedeckt werden. Während der S-Phase besteht also die Gefahr, dass bereits etablierte Chromatinstrukturen entweder durch den Einbau neu synthetisierter Histone oder durch die Entfernung von strukturbildenden Nicht-Histon-Proteinen des Chromatins verändert wird. Viele experimentelle Beobachtungen zeigen jedoch, dass genau das nicht der Fall ist und die Unterschiede im Chromatin erstaunlich präzise epigenetisch, also nicht an die DNA-Sequenz gekoppelt, vererbt werden. Um diesem Phänomen der Vererbung von Chromatinstrukturen auf den Grund zu gehen, haben wir uns mit den Histon-Modifikationen während des Zusammenbaus von Chromatin aus neu synthetisierten Histonen und DNA genauer beschäftigt.

Einbau neu synthetisierter Histone

Mit Fortschreiten der Replikationsgabel werden die bereits vorhandenen Nukleosomen von der DNA entfernt. Allerdings ist es unklar, ob die Bewegung der DNA-Synthesemaschine alleine für diesen Vorgang ausreichend ist oder ob zusätzliche Faktoren eine Rolle

spielen. RNAi-Experimente zeigten, dass ATP-abhängige Chromatin-remodelers für die DNA-Replikation unerlässlich sind^[8]. Zur Wiederverwertung der bereits vorher vorhandenen Histone werden Histon-Chaperone benötigt^[9]. Solche Hilfsproteine interagieren mit Histonen, fördern den langsamen Transfer der basischen Histone auf die DNA und verhindern damit die Bildung eines Histon-DNA-Aggregats. H2A-H2B-Dimere assoziieren zum Beispiel mit FACT¹, einem hoch konservierten Histon-Chaperon, welches interessanterweise auch die Transkription stimuliert. Das Histon-Chaperon CAF-1², bestehend aus drei Untereinheiten, ist mit den Histonen H3 und H4 assoziiert und erleichtert den Einbau dieser Histone in das Chromatin. Die bestehenden Histone werden in zufälliger Art und Weise hinter der Replikationsgabel verteilt und neu synthetisierte Nukleosomen füllen die Lücken auf^[10]. Die Replikation des Chromatins oder zumindest der Histone und der Information, die sie tragen, erfolgt also im Gegensatz zur DNA-Replikation dispersiv statt semikonservativ.

Es stellt sich nun die Frage, wie die epigenetische Information bei der Verdopplung der DNA vererbt wird. Theoretisch können die bereits vorher vorhandenen Histone und ihre Modifikationen als Blaupause dienen und somit die Information auf die neu synthetisierten Histone kopieren.

1 Facilitates chromatin transcription
2 Chromatin assembly factor 1

Bestimmen bestehende Histon-Modifikationen das Schicksal des neu synthetisierten Chromatins?

In Zusammenarbeit mit der Arbeitsgruppe von Genevieve Almouzni am Institut Pasteur in Paris konnten wir zeigen, dass neu synthetisierte Histone H3 und H4 sich durch ein spezifisches Modifikationsmuster auszeichnen, das sich deutlich von dem der elterlichen Histone unterscheidet^[11]. Neu synthetisiertes H4 besitzt evolutionär konservierte Acetylierungen an Lysin 5 und 12, die von der Histon-Acetyl-Transferase HAT1 übertragen und zeitnah nach Replikationsende von Histon-Deacetylasen wieder entfernt werden. Verglichen mit der transienten Acetylierung ist die Halbwertszeit der Histon-Methylierung deutlich länger^[12]. Jedoch hat die Isolierung von mehreren Histon-Demethylasen die bisherige Ansicht, dass Histon-Methylierung eine irreversible und damit hervorragend zur Vererbung von Chromatinstrukturen geeignete Modifikation ist, zunichte gemacht. Die einzige Methylierung an neu synthetisierten Histonen scheint eine Methylierung am Lysin 9 im H3-Molekül zu sein. Alle weiteren Methylierungen von Histonen finden erst nach Einbau in das Chromatin statt. Es ist gut möglich, dass diese ursprünglichen Modifikationen von Enzymen erkannt werden, die auf dem Level der Nukleosomen ihre Aktivität ausüben und dadurch das endgültige Modifikationsstadium beeinflussen. Bereits beim Einbau der Histone während der Replikation scheinen also schon die Weichen für bestimmte Chromatinstrukturen gelegt zu werden. So ist es zum Beispiel schon seit längerem bekannt, dass Histon-H3-Varianten in unterschiedlichen Bereichen des Chromatins zu finden sind. Während das replikationsabhängig exprimierte H3.1-Molekül in allen Bereichen des Chromatins, also auch dem Heterochromatin, zu finden ist, haben wir die replikationsunabhängig synthetisierte Variante H3.3 hauptsächlich in aktiv transkribierten Bereichen gefunden. Die beiden Varianten unterscheiden sich jedoch nur in wenigen Aminosäuren und das für die Synthese von stillgelegtem Heterochromatin so wichtige Lysin 9 (K 9) wird in beiden Varianten gefunden. Wir stellten uns daher die Frage, warum die Trimethylierung von Lysin 9 als Signatur des Heterochromatins fast nie in Nukleosomen, die H3.3 enthalten, nachweisbar ist, oft jedoch in H3.1-Nukleosomen. Die Enzyme, die für die Methylierung von Lysin 9 in Säugerzellen verantwortlich sind – SETDB1³, SUV3-9H1 und -H2⁴, G9a⁵, ESET⁶ –

sind alle *in vitro* in der Lage, sowohl H3.1 als auch H3.3 zu methylieren. Eine mögliche Erklärung für diese Beobachtung liefert jedoch ein Vergleich der verschiedenen H3-Varianten, jeweils vor und nach dem Einbau in Chromatin. So findet man, dass H3.1 am Lysin 9 zunächst nur monomethyliert ist, dann von der Heterochromatin-spezifischen Methyltransferase SUV39H1 trimethyliert wird und somit vermutlich zur Bildung des Heterochromatins beiträgt. Dagegen wird H3.3 bereits vor dem Einbau an Lysin 9 acetyliert und dimethyliert, was eine nachfolgende Trimethylierung von Lysin 9 verhindert und somit schon frühzeitig die Ausbildung von Heterochromatin in den H3.3-enhaltenden Bereichen unterbindet^[11].

Epigenetische Lesezeichen

Epigenetische Ereignisse ermöglichen es, über die Ebene der DNA hinaus zusätzliche Informationen zu kodieren. Wenn man den DNA-Code mit den Buchstaben eines Buchs vergleicht, dann würde dem Chromatin die Rolle der Inhaltsangabe und des Registers zukommen. In vielen Nachschlagewerken ist eine gute Gliederung der Schlüssel für das Auffinden von Informationen und bestimmt daher den Nutzwert des Werks. Die derzeitige Forschung steht noch an den Anfängen, die genauen Vorgänge wäh-

rend der Chromatin-Assemblierung zu verstehen. Wir hoffen, dass unsere Arbeiten einen Beitrag zum Verständnis des Kopiermechanismus der Chromatinstruktur und damit zur epigenetischen Vererbung liefern können. ■

Literatur

- [1] Heitz, E. (1935): Chromosomenstruktur und Gene. *Mol. Gen. Genet.* 70, 402-447.
- [2] Kornberg, R. D. (1974): Chromatin structure: a repeating unit of histones and DNA. *Science* 184: 868-871.
- [3] Luger, K., Mader, A. W., Richmond, R. K., Sargent, D. F., Richmond, T. J. (1997): Crystal structure of the nucleosome core particle at 2.8 Å resolution. *Nature* 389: 251-260.
- [4] Razin, A., Riggs, A. D. (1980): DNA methylation and gene function. *Science* 210: 604-610.
- [5] Kouzarides, T. (2007): Chromatin modifications and their function. *Cell* 128: 693-705.
- [6] Kamakaka, R. T., Biggins, S. (2005): Histone variants: deviants? *Genes Dev.* 19: 295-310.
- [7] Jenuwein, T., Allis, C. D. (2001): Translating the histone code. *Science* 293: 1074-1080.
- [8] Poot, R. A., Bozhenok, L., van den Berg, D. L., Steffensen, S., Ferreira, F., Grimaldi, M., Gilbert, N., Ferreira, J., Varga-Weisz, P. D. (2004): The Williams syndrome transcription factor interacts with PCNA to target chromatin remodelling by ISWI to replication foci. *Nat. Cell Biol.* 6: 1236-1244.
- [9] Loyola, A., Almouzni, G. (2004): Histone chaperones, a supporting role in the limelight. *Biochim. Biophys. Acta* 1677: 3-11.
- [10] Jackson, V., Chalkley, R. (1985): Histone segregation on replicating chromatin. *Biochemistry* 24: 6930-6938.
- [11] Loyola, A., Bonaldi, T., Roche, D., Imhof, A., Almouzni, G. (2006): PTMs on H3 variants before chromatin assembly potentiate their final epigenetic state. *Mol. Cell.* 24: 309-316.
- [12] Waterborg, J. H. (1993): Dynamic methylation of alfalfa histone H3. *J. Biol. Chem.* 268: 4918-4921.

Korrespondenzadresse:

Prof. Dr. Axel Imhof
 Histone Modifications Group
 Biomedical Center
 Ludwig-Maximilians-Universität München
 Schillerstraße 44
 D-80336 München
 Tel.: 089-2180-75435
 Fax: 089-2180-75425
 imhof@lmu.de
<http://proteinanalytik.web.med.uni-muenchen.de>

- 3 set domain bifurcated 1
- 4 Suppressor of position effect variegation human orthologue 1 and 2
- 5 cDNA-Klon-Nummer (Spies *et al.*, *PNAS* 86 (1989) 8955) Heute ist das offizielle Gensymbol der Maus *Ehmt2* und steht für euchromatic histone lysine-N-methyltransferase (www.informatics.jax.org).
- 6 Erg associated protein with a SET domain

AUTOREN



Annette Nicole Daniela Scharf
 2000-2005 Biologiestudium an der LMU, München. 2005 Diplomarbeit, seit 2006 Promotionsstudium am Adolf-Butenandt-Institut, Abteilung Molekularbiologie, LMU.



Axel Imhof
 1987-1992 Biologiestudium an der Universität Regensburg. 1993 Diplomarbeit am Institut für Pathologie der Universität Regensburg. 1993-1995 Dissertation am Institut für Pathologie der Universität Regensburg. 1996-1999 Gastwissenschaftler im Labor von Dr. Alan P. Wolffe, Laboratory of Molecular Embryology, NIH, USA. 1999-2005 Gruppenleiter (C1) am Adolf-Butenandt-Institut, LMU München. Seit 2006 W2-Professor für Proteinanalytik an der LMU, München.

REFERENCES

ABBREVIATIONS

CURRICULUM VITAE

References

- Akhtar, A., and Becker, P. B. (2000). Activation of transcription through histone H4 acetylation by MOF, an acetyltransferase essential for dosage compensation in *Drosophila*. *Mol. Cell* 5, 367-375.
- Annunziato, A. T., and Seale, R. L. (1983). Histone deacetylation is required for the maturation of newly replicated chromatin. *J. Biol. Chem* 258, 12675-12684.
- Arents, G., and Moudrianakis, E. N. (1995). The histone fold: a ubiquitous architectural motif utilized in DNA compaction and protein dimerization. *Proc Natl Acad Sci U S A* 92, 11170-4.
- Banfalvi, G. (2008). Cell cycle synchronization of animal cells and nuclei by centrifugal elutriation. *Nat Protoc* 3, 663-673.
- Bannister, A. J., and Kouzarides, T. (1996). The CBP co-activator is a histone acetyltransferase. *Nature* 384, 641-643.
- Bannister, A. J., Zegerman, P., Partridge, J. F., Miska, E. A., Thomas, J. O., Allshire, R. C., and Kouzarides, T. (2001). Selective recognition of methylated lysine 9 on histone H3 by the HP1 chromo domain. *Nature* 410, 120-124.
- Bannister, A. J., Schneider, R., Myers, F. A., Thorne, A. W., Crane-Robinson, C., and Kouzarides, T. (2005). Spatial distribution of di- and tri-methyl lysine 36 of histone H3 at active genes. *J Biol Chem* 280, 17732-6.
- Barski, A., Cuddapah, S., Cui, K., Roh, T., Schones, D. E., Wang, Z., Wei, G., Chepelev, I., and Zhao, K. (2007). High-resolution profiling of histone methylations in the human genome. *Cell* 129, 823-37.
- Becker, P. B., and Wu, C. (1992). Cell-free system for assembly of transcriptionally repressed chromatin from *Drosophila* embryos. *Mol. Cell. Biol* 12, 2241-2249.
- Bednar, J., Horowitz, R. A., Grigoryev, S. A., Carruthers, L. M., Hansen, J. C., Koster, A. J., and Woodcock, C. L. (1998). Nucleosomes, linker DNA, and linker histone form a unique structural motif that directs the higher-order folding and compaction of chromatin. *Proc Natl Acad Sci U S A* 95, 14173-8.
- Bell, O. et al. (2007). Localized H3K36 methylation states define histone H4K16 acetylation during transcriptional elongation in *Drosophila*. *EMBO J* 26, 4974-84.
- Belmont, A. S. (2006). Mitotic chromosome structure and condensation. *Curr. Opin. Cell Biol* 18, 632-638.
- Benson, L. J., Gu, Y., Yakovleva, T., Tong, K., Barrows, C., Strack, C. L., Cook, R. G., Mizzen, C. A., and Annunziato, A. T. (2006). Modifications of H3 and H4 during chromatin replication, nucleosome assembly, and histone exchange. *J Biol Chem* 281, 9287-96.
- Birnboim, H. C., and Doly, J. (1979). A rapid alkaline extraction procedure for screening recombinant plasmid DNA. *Nucleic Acids Res* 7, 1513-1523.
- Bonaldi, T., Imhof, A., and Regula, J. T. (2004). A combination of different mass spectroscopic techniques for the analysis of dynamic changes of histone modifications. *Proteomics* 4, 1382-1396.
- Bostock, C. J., Prescott, D. M., and Kirkpatrick, J. B. (1971). An evaluation of the double thymidine block for synchronizing mammalian cells at the G1-S border. *Exp. Cell Res* 68, 163-168.

- Botuyan, M. V., Lee, J., Ward, I. M., Kim, J., Thompson, J. R., Chen, J., and Mer, G. (2006). Structural basis for the methylation state-specific recognition of histone H4-K20 by 53BP1 and Crb2 in DNA repair. *Cell* 127, 1361-73.
- Boyer, L. A., Mathur, D., and Jaenisch, R. (2006). Molecular control of pluripotency. *Curr. Opin. Genet. Dev* 16, 455-462.
- Boyer, L. A., Plath, K., et al. (2006). Polycomb complexes repress developmental regulators in murine embryonic stem cells. *Nature* 441, 349-353.
- Bracken, A. P., Dietrich, N., Pasini, D., Hansen, K. H., and Helin, K. (2006). Genome-wide mapping of Polycomb target genes unravels their roles in cell fate transitions. *Genes Dev* 20, 1123-1136.
- Bradford, M. M. (1976). A rapid and sensitive method for the quantitation of microgram quantities of protein utilizing the principle of protein-dye binding. *Anal. Biochem* 72, 248-254.
- Brownell, J. E., Zhou, J., Ranalli, T., Kobayashi, R., Edmondson, D. G., Roth, S. Y., and Allis, C. D. (1996). Tetrahymena histone acetyltransferase A: a homolog to yeast Gcn5p linking histone acetylation to gene activation. *Cell* 84, 843-51.
- Cao, R., Wang, L., Wang, H., Xia, L., Erdjument-Bromage, H., Tempst, P., Jones, R. S., and Zhang, Y. (2002). Role of histone H3 lysine 27 methylation in Polycomb-group silencing. *Science* 298, 1039-1043.
- Carrozza, M. J. et al. (2005). Histone H3 methylation by Set2 directs deacetylation of coding regions by Rpd3S to suppress spurious intragenic transcription. *Cell* 123, 581-92.
- Chang, L., Loranger, S. S., Mizzen, C., Ernst, S. G., Allis, C. D., and Annunziato, A. T. (1997). Histones in transit: cytosolic histone complexes and diacetylation of H4 during nucleosome assembly in human cells. *Biochemistry* 36, 469-480.
- Chestier, A., and Yaniv, M. (1979). Rapid turnover of acetyl groups in the four core histones of simian virus 40 minichromosomes. *Proc. Natl. Acad. Sci. U.S.A* 76, 46-50.
- Chuang, L. S., Ian, H. I., Koh, T. W., Ng, H. H., Xu, G., and Li, B. F. (1997). Human DNA-(cytosine-5) methyltransferase-PCNA complex as a target for p21WAF1. *Science* 277, 1996-2000.
- Clapier, C. R., Nightingale, K. P., and Becker, P. B. (2002). A critical epitope for substrate recognition by the nucleosome remodeling ATPase ISWI. *Nucleic Acids Res* 30, 649-655.
- Corona, D. F. V., Clapier, C. R., Becker, P. B., and Tamkun, J. W. (2002). Modulation of ISWI function by site-specific histone acetylation. *EMBO Rep* 3, 242-247.
- Corpet, A., and Almouzni, G. (2009). Making copies of chromatin: the challenge of nucleosomal organization and epigenetic information. *Trends Cell Biol* 19, 29-41.
- Craig, J. M. (2005). Heterochromatin--many flavours, common themes. *Bioessays* 27, 17-28.
- Cremer, T., and Cremer, C. (2001). Chromosome territories, nuclear architecture and gene regulation in mammalian cells. *Nat Rev Genet* 2, 292-301.
- Cremer, T., Cremer, M., Dietzel, S., Müller, S., Solovei, I., and Fakan, S. (2006). Chromosome territories--a functional nuclear landscape. *Curr Opin Cell Biol* 18, 307-16.

References

- Czermin, B., Melfi, R., McCabe, D., Seitz, V., Imhof, A., and Pirrotta, V. (2002). Drosophila enhancer of Zeste/ESC complexes have a histone H3 methyltransferase activity that marks chromosomal Polycomb sites. *Cell* 111, 185-196.
- Daniel, J. A., Pray-Grant, M. G., and Grant, P. A. (2005). Effector proteins for methylated histones: an expanding family. *Cell Cycle* 4, 919-926.
- Das, C., Lucia, M. S., Hansen, K. C., and Tyler, J. K. (2009). CBP/p300-mediated acetylation of histone H3 on lysine 56. *Nature* 459, 113-117.
- Dorigo, B., Schalch, T., Kulangara, A., Duda, S., Schroeder, R. R., and Richmond, T. J. (2004). Nucleosome arrays reveal the two-start organization of the chromatin fiber. *Science* 306, 1571-3.
- Dou, Y. et al. (2005). Physical association and coordinate function of the H3 K4 methyltransferase MLL1 and the H4 K16 acetyltransferase MOF. *Cell* 121, 873-885.
- Durrin, L. K., Mann, R. K., Kayne, P. S., and Grunstein, M. (1991). Yeast histone H4 N-terminal sequence is required for promoter activation in vivo. *Cell* 65, 1023-31.
- Dyda, F., Klein, D. C., and Hickman, A. B. (2000). GCN5-related N-acetyltransferases: a structural overview. *Annu Rev Biophys Biomol Struct* 29, 81-103.
- Ebert, A., Lein, S., Schotta, G., and Reuter, G. (2006). Histone modification and the control of heterochromatic gene silencing in Drosophila. *Chromosome Res* 14, 377-392.
- Ebert, A., Schotta, G., Lein, S., Kubicek, S., Krauss, V., Jenuwein, T., and Reuter, G. (2004). Su(var) genes regulate the balance between euchromatin and heterochromatin in Drosophila. *Genes Dev* 18, 2973-83.
- Elgin, S. C. R., and Grewal, S. I. S. (2003). Heterochromatin: silence is golden. *Curr. Biol* 13, R895-898.
- Eskeland, R., Eberharter, A., and Imhof, A. (2007). HP1 binding to chromatin methylated at H3K9 is enhanced by auxiliary factors. *Mol. Cell. Biol* 27, 453-465.
- Fang, J. et al. (2002). Purification and functional characterization of SET8, a nucleosomal histone H4-lysine 20-specific methyltransferase. *Curr Biol* 12, 1086-99.
- Felsenfeld, G., and Groudine, M. (2003). Controlling the double helix. *Nature* 421, 448-53.
- Fischle, W., Tseng, B. S., Dormann, H. L., Ueberheide, B. M., Garcia, B. A., Shabanowitz, J., Hunt, D. F., Funabiki, H., and Allis, C. D. (2005). Regulation of HP1-chromatin binding by histone H3 methylation and phosphorylation. *Nature* 438, 1116-1122.
- Fischle, W., Wang, Y., and Allis, C. D. (2003a). Binary switches and modification cassettes in histone biology and beyond. *Nature* 425, 475-479.
- Fischle, W., Wang, Y., and Allis, C. D. (2003b). Histone and chromatin cross-talk. *Curr Opin Cell Biol* 15, 172-83.
- Fischle, W., Wang, Y., Jacobs, S. A., Kim, Y., Allis, C. D., and Khorasanizadeh, S. (2003). Molecular basis for the discrimination of repressive methyl-lysine marks in histone H3 by Polycomb and HP1 chromodomains. *Genes Dev* 17, 1870-1881.

- Fouse, S. D., Shen, Y., Pellegrini, M., Cole, S., Meissner, A., Van Neste, L., Jaenisch, R., and Fan, G. (2008). Promoter CpG methylation contributes to ES cell gene regulation in parallel with Oct4/Nanog, PcG complex, and histone H3 K4/K27 trimethylation. *Cell Stem Cell* 2, 160-169.
- Fraga, M. F. et al. (2005). Loss of acetylation at Lys16 and trimethylation at Lys20 of histone H4 is a common hallmark of human cancer. *Nat. Genet* 37, 391-400.
- Gallinari, P., Di Marco, S., Jones, P., Pallaoro, M., and Steinkühler, C. (2007). HDACs, histone deacetylation and gene transcription: from molecular biology to cancer therapeutics. *Cell Res* 17, 195-211.
- Gambus, A., Jones, R. C., Sanchez-Diaz, A., Kanemaki, M., van Deursen, F., Edmondson, R. D., and Labib, K. (2006). GINS maintains association of Cdc45 with MCM in replisome progression complexes at eukaryotic DNA replication forks. *Nat. Cell Biol* 8, 358-366.
- Garcia, B. A. et al. (2007). Organismal differences in post-translational modifications in histones H3 and H4. *J. Biol. Chem* 282, 7641-7655.
- Gargiulo, G., and Minucci, S. (2009). Epigenomic profiling of cancer cells. *Int. J. Biochem. Cell Biol* 41, 127-135.
- Giordano, A., and Avantaggiati, M. L. (1999). p300 and CBP: partners for life and death. *J. Cell. Physiol* 181, 218-230.
- Goldberg, A. D., Allis, C. D., and Bernstein, E. (2007). Epigenetics: a landscape takes shape. *Cell* 128, 635-8.
- Gregory, P. D., and Hörz, W. (1998). Chromatin and transcription--how transcription factors battle with a repressive chromatin environment. *Eur. J. Biochem* 251, 9-18.
- Grewal, S. I. S., and Elgin, S. C. R. (2002). Heterochromatin: new possibilities for the inheritance of structure. *Curr. Opin. Genet. Dev* 12, 178-187.
- Grewal, S. I. S., and Jia, S. (2007). Heterochromatin revisited. *Nat Rev Genet* 8, 35-46.
- Grimaud, C., Nègre, N., and Cavalli, G. (2006). From genetics to epigenetics: the tale of Polycomb group and trithorax group genes. *Chromosome Res* 14, 363-375.
- Grønbaek, K., Hother, C., and Jones, P. A. (2007). Epigenetic changes in cancer. *APMIS* 115, 1039-1059.
- Groth, A. (2009). Replicating chromatin: a tale of histones. *Biochem Cell Biol* 87, 51-63.
- Groth, A., Corpet, A., Cook, A. J. L., Roche, D., Bartek, J., Lukas, J., and Almouzni, G. (2007). Regulation of replication fork progression through histone supply and demand. *Science* 318, 1928-1931.
- Groth, A., Ray-Gallet, D., Quivy, J., Lukas, J., Bartek, J., and Almouzni, G. (2005). Human Asf1 regulates the flow of S phase histones during replicational stress. *Mol. Cell* 17, 301-311.
- Groth, A., Rocha, W., Verreault, A., and Almouzni, G. (2007). Chromatin challenges during DNA replication and repair. *Cell* 128, 721-33.
- Heard, E. (2005). Delving into the diversity of facultative heterochromatin: the epigenetics of the inactive X chromosome. *Curr. Opin. Genet. Dev* 15, 482-489.

References

- Hebbes, T. R., Clayton, A. L., Thorne, A. W., and Crane-Robinson, C. (1994). Core histone hyperacetylation co-maps with generalized DNase I sensitivity in the chicken beta-globin chromosomal domain. *EMBO J* 13, 1823-30.
- Henikoff, S., Furuyama, T., and Ahmad, K. (2004). Histone variants, nucleosome assembly and epigenetic inheritance. *Trends Genet* 20, 320-326.
- Holdeman, R., Nehrt, S., and Strome, S. (1998). MES-2, a maternal protein essential for viability of the germline in *Caenorhabditis elegans*, is homologous to a *Drosophila* Polycomb group protein. *Development* 125, 2457-2467.
- Holliday, R. (2006). Epigenetics: a historical overview. *Epigenetics* 1, 76-80.
- Houston, S. I., McManus, K. J., Adams, M. M., Sims, J. K., Carpenter, P. B., Hendzel, M. J., and Rice, J. C. (2008). Catalytic function of the PR-Set7 histone H4 lysine 20 monomethyltransferase is essential for mitotic entry and genomic stability. *J Biol Chem* 283, 19478-88.
- Huen, M. S. Y., Sy, S. M., van Deursen, J. M., and Chen, J. (2008). Direct interaction between SET8 and proliferating cell nuclear antigen couples H4-K20 methylation with DNA replication. *J. Biol. Chem* 283, 11073-11077.
- Imhof, A., Yang, X. J., Ogryzko, V. V., Nakatani, Y., Wolffe, A. P., and Ge, H. (1997). Acetylation of general transcription factors by histone acetyltransferases. *Curr. Biol* 7, 689-692.
- Imhof, A. (2003). Histone modifications: an assembly line for active chromatin? *Curr. Biol* 13, R22-24.
- Jackson, V., and Chalkley, R. (1985). Histone segregation on replicating chromatin. *Biochemistry* 24, 6930-6938.
- Jackson, V., Granner, D. K., and Chalkley, R. (1975). Deposition of histones onto replicating chromosomes. *Proc Natl Acad Sci U S A* 72, 4440-4.
- Janzen, C. J., Hake, S. B., Lowell, J. E., and Cross, G. A. M. (2006). Selective di- or trimethylation of histone H3 lysine 76 by two DOT1 homologs is important for cell cycle regulation in *Trypanosoma brucei*. *Mol. Cell* 23, 497-507.
- Jenuwein, T., and Allis, C. D. (2001). Translating the histone code. *Science* 293, 1074-80.
- Johansen, K. M., and Johansen, J. (2006). Regulation of chromatin structure by histone H3S10 phosphorylation. *Chromosome Res* 14, 393-404.
- Jones, R. S., and Gelbart, W. M. (1993). The *Drosophila* Polycomb-group gene Enhancer of zeste contains a region with sequence similarity to trithorax. *Mol. Cell. Biol* 13, 6357-6366.
- Jørgensen, S., Elvers, I., Trelle, M. B., Menzel, T., Eskildsen, M., Jensen, O. N., Helleday, T., Helin, K., and Sørensen, C. S. (2007). The histone methyltransferase SET8 is required for S-phase progression. *J. Cell Biol* 179, 1337-1345.
- Joshi, A. A., and Struhl, K. (2005). Eaf3 chromodomain interaction with methylated H3-K36 links histone deacetylation to Pol II elongation. *Mol. Cell* 20, 971-978.
- Karachentsev, D., Sarma, K., Reinberg, D., and Steward, R. (2005). PR-Set7-dependent methylation of histone H4 Lys 20 functions in repression of gene expression and is essential for mitosis. *Genes Dev* 19, 431-5.

- Kim, J., Daniel, J., Espejo, A., Lake, A., Krishna, M., Xia, L., Zhang, Y., and Bedford, M. T. (2006). Tudor, MBT and chromo domains gauge the degree of lysine methylation. *EMBO Rep* 7, 397-403.
- Kleff, S., Andrulis, E. D., Anderson, C. W., and Sternglanz, R. (1995). Identification of a gene encoding a yeast histone H4 acetyltransferase. *J. Biol. Chem* 270, 24674-24677.
- Klose, R. J., Kallin, E. M., and Zhang, Y. (2006). JmjC-domain-containing proteins and histone demethylation. *Nat. Rev. Genet* 7, 715-727.
- Klose, R. J., Yamane, K., Bae, Y., Zhang, D., Erdjument-Bromage, H., Tempst, P., Wong, J., and Zhang, Y. (2006). The transcriptional repressor JHDM3A demethylates trimethyl histone H3 lysine 9 and lysine 36. *Nature* 442, 312-316.
- Kohlmaier, A., Savarese, F., Lachner, M., Martens, J., Jenuwein, T., and Wutz, A. (2004). A chromosomal memory triggered by Xist regulates histone methylation in X inactivation. *PLoS Biol* 2, E171.
- Koonin, E. V., Zhou, S., and Lucchesi, J. C. (1995). The chromo superfamily: new members, duplication of the chromo domain and possible role in delivering transcription regulators to chromatin. *Nucleic Acids Res* 23, 4229-4233.
- Kornberg, R. D. (1974). Chromatin structure: a repeating unit of histones and DNA. *Science* 184, 868-71.
- Kotake, Y., Cao, R., Viatour, P., Sage, J., Zhang, Y., and Xiong, Y. (2007). pRB family proteins are required for H3K27 trimethylation and Polycomb repression complexes binding to and silencing p16INK4alpha tumor suppressor gene. *Genes Dev* 21, 49-54.
- Kouzarides, T. (2007). Chromatin modifications and their function. *Cell* 128, 693-705.
- Krogan, N. J. et al. (2003). Methylation of histone H3 by Set2 in *Saccharomyces cerevisiae* is linked to transcriptional elongation by RNA polymerase II. *Mol. Cell. Biol* 23, 4207-4218.
- Lachner, M., O'Carroll, D., Rea, S., Mechtler, K., and Jenuwein, T. (2001). Methylation of histone H3 lysine 9 creates a binding site for HP1 proteins. *Nature* 410, 116-120.
- Larschan, E., Alekseyenko, A. A., Gortchakov, A. A., Peng, S., Li, B., Yang, P., Workman, J. L., Park, P. J., and Kuroda, M. I. (2007). MSL complex is attracted to genes marked by H3K36 trimethylation using a sequence-independent mechanism. *Mol. Cell* 28, 121-133.
- Lee, J., and Shilatifard, A. (2007). A site to remember: H3K36 methylation a mark for histone deacetylation. *Mutat Res* 618, 130-4.
- Lee, M. G., Wynder, C., Bochar, D. A., Hakimi, M., Cooch, N., and Shiekhhattar, R. (2006). Functional interplay between histone demethylase and deacetylase enzymes. *Mol. Cell. Biol* 26, 6395-6402.
- Li, B., Howe, L., Anderson, S., Yates, J. R., and Workman, J. L. (2003). The Set2 histone methyltransferase functions through the phosphorylated carboxyl-terminal domain of RNA polymerase II. *J. Biol. Chem* 278, 8897-8903.
- Li, H., Fischle, W., Wang, W., Duncan, E. M., Liang, L., Murakami-Ishibe, S., Allis, C. D., and Patel, D. J. (2007). Structural basis for lower lysine methylation state-specific readout by MBT repeats of L3MBTL1 and an engineered PHD finger. *Mol. Cell* 28, 677-691.

References

- Loyola, A., Bonaldi, T., Roche, D., Imhof, A., and Almouzni, G. (2006). PTMs on H3 variants before chromatin assembly potentiate their final epigenetic state. *Mol. Cell* 24, 309-316.
- Luger, K., Mäder, A. W., Richmond, R. K., Sargent, D. F., and Richmond, T. J. (1997). Crystal structure of the nucleosome core particle at 2.8 Å resolution. *Nature* 389, 251-260.
- Luger, K., Rechsteiner, T. J., and Richmond, T. J. (1999). Expression and purification of recombinant histones and nucleosome reconstitution. *Methods Mol. Biol* 119, 1-16.
- Maier, V. K., Chioda, M., and Becker, P. B. (2008). ATP-dependent chromatin remodeling. *Biol Chem* 389, 345-52.
- Maison, C., and Almouzni, G. (2004). HP1 and the dynamics of heterochromatin maintenance. *Nat Rev Mol Cell Biol* 5, 296-304.
- Marsden, M. P., and Laemmli, U. K. (1979). Metaphase chromosome structure: evidence for a radial loop model. *Cell* 17, 849-858.
- Martin, C., and Zhang, Y. (2005). The diverse functions of histone lysine methylation. *Nat Rev Mol Cell Biol* 6, 838-49.
- Marzluff, W. F., and Duronio, R. J. (2002). Histone mRNA expression: multiple levels of cell cycle regulation and important developmental consequences. *Curr Opin Cell Biol* 14, 692-9.
- Masumoto, H., Hawke, D., Kobayashi, R., and Verreault, A. (2005). A role for cell-cycle-regulated histone H3 lysine 56 acetylation in the DNA damage response. *Nature* 436, 294-298.
- Maurer-Stroh, S., Dickens, N. J., Hughes-Davies, L., Kouzarides, T., Eisenhaber, F., and Ponting, C. P. (2003). The Tudor domain 'Royal Family': Tudor, plant Agenet, Chromo, PWWP and MBT domains. *Trends Biochem. Sci* 28, 69-74.
- Meinhart, A., Kamenski, T., Hoepfner, S., Baumli, S., and Cramer, P. (2005). A structural perspective of CTD function. *Genes Dev* 19, 1401-1415.
- Mello, J. A., and Almouzni, G. (2001). The ins and outs of nucleosome assembly. *Curr Opin Genet Dev* 11, 136-41.
- Mello, J. A., Silljé, H. H. W., Roche, D. M. J., Kirschner, D. B., Nigg, E. A., and Almouzni, G. (2002). Human Asf1 and CAF-1 interact and synergize in a repair-coupled nucleosome assembly pathway. *EMBO Rep* 3, 329-334.
- Metzger, E., Wissmann, M., Yin, N., Müller, J. M., Schneider, R., Peters, A. H. F. M., Günther, T., Buettner, R., and Schüle, R. (2005). LSD1 demethylates repressive histone marks to promote androgen-receptor-dependent transcription. *Nature* 437, 436-439.
- Milutinovic, S., Zhuang, Q., and Szyf, M. (2002). Proliferating cell nuclear antigen associates with histone deacetylase activity, integrating DNA replication and chromatin modification. *J. Biol. Chem* 277, 20974-20978.
- Min, J., Zhang, Y., and Xu, R. (2003). Structural basis for specific binding of Polycomb chromodomain to histone H3 methylated at Lys 27. *Genes Dev* 17, 1823-1828.
- Moggs, J. G., Grandi, P., Quivy, J. P., Jónsson, Z. O., Hübscher, U., Becker, P. B., and Almouzni, G. (2000). A CAF-1-PCNA-mediated chromatin assembly pathway triggered by sensing DNA damage. *Mol. Cell. Biol* 20, 1206-1218.

- Moldovan, G., Pfander, B., and Jentsch, S. (2007). PCNA, the maestro of the replication fork. *Cell* 129, 665-679.
- Morales, V., Straub, T., Neumann, M. F., Mengus, G., Akhtar, A., and Becker, P. B. (2004). Functional integration of the histone acetyltransferase MOF into the dosage compensation complex. *EMBO J* 23, 2258-2268.
- Morgan, H. D., Santos, F., Green, K., Dean, W., and Reik, W. (2005). Epigenetic reprogramming in mammals. *Hum. Mol. Genet* 14 Spec No 1, R47-58.
- Nakatani, Y., Tagami, H., and Shestakova, E. (2006). How is epigenetic information on chromatin inherited after DNA replication? *Ernst Schering Res. Found. Workshop*, 89-96.
- Ner, S. S., Blank, T., Pérez-Paralle, M. L., Grigliatti, T. A., Becker, P. B., and Travers, A. A. (2001). HMG-D and histone H1 interplay during chromatin assembly and early embryogenesis. *J. Biol. Chem* 276, 37569-37576.
- Ng, H. H., Feng, Q., Wang, H., Erdjument-Bromage, H., Tempst, P., Zhang, Y., and Struhl, K. (2002). Lysine methylation within the globular domain of histone H3 by Dot1 is important for telomeric silencing and Sir protein association. *Genes Dev* 16, 1518-1527.
- Ng, R. K., and Gurdon, J. B. (2008). Epigenetic inheritance of cell differentiation status. *Cell Cycle* 7, 1173-1177.
- Nishioka, K. et al. (2002). PR-Set7 is a nucleosome-specific methyltransferase that modifies lysine 20 of histone H4 and is associated with silent chromatin. *Mol Cell* 9, 1201-13.
- Oda, H., Okamoto, I., Murphy, N., Chu, J., Price, S. M., Shen, M. M., Torres-Padilla, M. E., Heard, E., and Reinberg, D. (2009). Monomethylation of histone H4-lysine 20 is involved in chromosome structure and stability and is essential for mouse development. *Mol Cell Biol* 29, 2278-95.
- Parthun, M. R. (2007). Hat1: the emerging cellular roles of a type B histone acetyltransferase. *Oncogene* 26, 5319-5328.
- Parthun, M. R., Widom, J., and Gottschling, D. E. (1996). The major cytoplasmic histone acetyltransferase in yeast: links to chromatin replication and histone metabolism. *Cell* 87, 85-94.
- Pesavento, J. J., Yang, H., Kelleher, N. L., and Mizzen, C. A. (2008). Certain and progressive methylation of histone H4 at lysine 20 during the cell cycle. *Mol Cell Biol* 28, 468-86.
- Peters, A. H. F. M. et al. (2003). Partitioning and plasticity of repressive histone methylation states in mammalian chromatin. *Mol. Cell* 12, 1577-1589.
- Poot, R. A., Bozhenok, L., van den Berg, D. L. C., Steffensen, S., Ferreira, F., Grimaldi, M., Gilbert, N., Ferreira, J., and Varga-Weisz, P. D. (2004). The Williams syndrome transcription factor interacts with PCNA to target chromatin remodelling by ISWI to replication foci. *Nat. Cell Biol* 6, 1236-1244.
- Probst, A. V., Dunleavy, E., and Almouzni, G. (2009). Epigenetic inheritance during the cell cycle. *Nat Rev Mol Cell Biol* 10, 192-206.
- Ramakrishnan, V. (1997). Histone structure and the organization of the nucleosome. *Annu Rev Biophys Biomol Struct* 26, 83-112.

References

- Rea, S. et al. (2000). Regulation of chromatin structure by site-specific histone H3 methyltransferases. *Nature* 406, 593-9.
- Reid, J. L., Moqtaderi, Z., and Struhl, K. (2004). Eaf3 regulates the global pattern of histone acetylation in *Saccharomyces cerevisiae*. *Mol. Cell. Biol* 24, 757-764.
- Ridgway, P., and Almouzni, G. (2000). CAF-1 and the inheritance of chromatin states: at the crossroads of DNA replication and repair. *J. Cell. Sci* 113 (Pt 15), 2647-2658.
- Robinson, P. J. J., and Rhodes, D. (2006). Structure of the ,30 nm² chromatin fibre: a key role for the linker histone. *Curr Opin Struct Biol* 16, 336-43.
- Roby, D., and Grunstein, M. (2003). Genomewide histone acetylation microarrays. *Methods* 31, 83-89.
- Routh, A., Sandin, S., and Rhodes, D. (2008). Nucleosome repeat length and linker histone stoichiometry determine chromatin fiber structure. *Proc. Natl. Acad. Sci. U.S.A* 105, 8872-8877.
- Rudolph, T. et al. (2007). Heterochromatin formation in *Drosophila* is initiated through active removal of H3K4 methylation by the LSD1 homolog SU(VAR)3-3. *Mol. Cell* 26, 103-115.
- Russev, G., and Hancock, R. (1982). Assembly of new histones into nucleosomes and their distribution in replicating chromatin. *Proc. Natl. Acad. Sci. U.S.A* 79, 3143-3147.
- Ruthenburg, A. J., Allis, C. D., and Wysocka, J. (2007). Methylation of lysine 4 on histone H3: intricacy of writing and reading a single epigenetic mark. *Mol. Cell* 25, 15-30.
- Salic, A., and Mitchison, T. J. (2008). A chemical method for fast and sensitive detection of DNA synthesis in vivo. *Proc. Natl. Acad. Sci. U.S.A* 105, 2415-2420.
- Sambrook, J., and Russell, D. W. (2000). *Molecular Cloning: A Laboratory Manual*, 3 Vol. 0003rd ed. (Cold Spring Harbor Laboratory).
- Sandaltzopoulos, R., and Becker, P. B. (1994). Solid phase DNase I footprinting: quick and versatile. *Nucleic Acids Res* 22, 1511-1512.
- Schaft, D., Roguev, A., Kotovic, K. M., Shevchenko, A., Sarov, M., Shevchenko, A., Neugebauer, K. M., and Stewart, A. F. (2003). The histone 3 lysine 36 methyltransferase, SET2, is involved in transcriptional elongation. *Nucleic Acids Res* 31, 2475-2482.
- Schalch, T., Duda, S., Sargent, D. F., and Richmond, T. J. (2005). X-ray structure of a tetranucleosome and its implications for the chromatin fibre. *Nature* 436, 138-41.
- Scharf, A. N. D., Barth, T. K., and Imhof, A. (2009). Establishment of Histone Modifications after Chromatin Assembly. *Nucleic Acids Res*. Available at: <http://www.ncbi.nlm.nih.gov/pubmed/19541851> [Accessed July 18, 2009].
- Scharf, A. N. D., Meier, K., Seitz, V., Kremmer, E., Brehm, A., and Imhof, A. (2009). Monomethylation of lysine 20 on histone H4 facilitates chromatin maturation. *Mol Cell Biol* 29, 57-67.

- Schotta, G., Ebert, A., Krauss, V., Fischer, A., Hoffmann, J., Rea, S., Jenuwein, T., Dorn, R., and Reuter, G. (2002). Central role of *Drosophila* SU(VAR)3-9 in histone H3-K9 methylation and heterochromatic gene silencing. *EMBO J* 21, 1121-31.
- Schotta, G., Lachner, M., Sarma, K., Ebert, A., Sengupta, R., Reuter, G., Reinberg, D., and Jenuwein, T. (2004). A silencing pathway to induce H3-K9 and H4-K20 trimethylation at constitutive heterochromatin. *Genes Dev* 18, 1251-62.
- Schotta, G. et al. (2008). A chromatin-wide transition to H4K20 monomethylation impairs genome integrity and programmed DNA rearrangements in the mouse. *Genes Dev* 22, 2048-61.
- Schreiber, S. L., and Bernstein, B. E. (2002). Signaling network model of chromatin. *Cell* 111, 771-778.
- Schwaiger, M., Stadler, M. B., Bell, O., Kohler, H., Oakeley, E. J., and Schübeler, D. (2009). Chromatin state marks cell-type- and gender-specific replication of the *Drosophila* genome. *Genes Dev* 23, 589-601.
- Shi, X., Kachirskaja, I., Yamaguchi, H., West, L. E., Wen, H., Wang, E. W., Dutta, S., Appella, E., and Gozani, O. (2007). Modulation of p53 function by SET8-mediated methylation at lysine 382. *Mol. Cell* 27, 636-646.
- Shi, Y., Lan, F., Matson, C., Mulligan, P., Whetstone, J. R., Cole, P. A., Casero, R. A., and Shi, Y. (2004). Histone demethylation mediated by the nuclear amine oxidase homolog LSD1. *Cell* 119, 941-953.
- Shogren-Knaak, M., Ishii, H., Sun, J., Pazin, M. J., Davie, J. R., and Peterson, C. L. (2006). Histone H4-K16 acetylation controls chromatin structure and protein interactions. *Science* 311, 844-847.
- Sieber, O. M., Heinemann, K., and Tomlinson, I. P. M. (2003). Genomic instability--the engine of tumorigenesis? *Nat. Rev. Cancer* 3, 701-708.
- Sobel, R. E., Cook, R. G., Perry, C. A., Annunziato, A. T., and Allis, C. D. (1995). Conservation of deposition-related acetylation sites in newly synthesized histones H3 and H4. *Proc. Natl. Acad. Sci. U.S.A* 92, 1237-1241.
- Song, Y. et al. (2007). CAF-1 is essential for *Drosophila* development and involved in the maintenance of epigenetic memory. *Dev. Biol* 311, 213-222.
- Speers, A. E., and Cravatt, B. F. (2004). Profiling enzyme activities in vivo using click chemistry methods. *Chem. Biol* 11, 535-546.
- Stassen, M. J., Bailey, D., Nelson, S., Chinwalla, V., and Harte, P. J. (1995). The *Drosophila* trithorax proteins contain a novel variant of the nuclear receptor type DNA binding domain and an ancient conserved motif found in other chromosomal proteins. *Mech. Dev* 52, 209-223.
- Steger, D. J. et al. (2008). DOT1L/KMT4 recruitment and H3K79 methylation are ubiquitously coupled with gene transcription in mammalian cells. *Mol. Cell. Biol* 28, 2825-2839.
- Sural, T. H., Peng, S., Li, B., Workman, J. L., Park, P. J., and Kuroda, M. I. (2008). The MSL3 chromodomain directs a key targeting step for dosage compensation of the *Drosophila melanogaster* X chromosome. *Nat. Struct. Mol. Biol* 15, 1318-1325.
- Swedlow, J. R., and Hirano, T. (2003). The making of the mitotic chromosome: modern insights into classical questions. *Mol. Cell* 11, 557-569.

References

- Taddei, A., Roche, D., Sibarita, J. B., Turner, B. M., and Almouzni, G. (1999). Duplication and maintenance of heterochromatin domains. *J. Cell Biol* 147, 1153-1166.
- Tagami, H., Ray-Gallet, D., Almouzni, G., and Nakatani, Y. (2004). Histone H3.1 and H3.3 complexes mediate nucleosome assembly pathways dependent or independent of DNA synthesis. *Cell* 116, 51-61.
- Taipale, M., Rea, S., Richter, K., Vilar, A., Lichter, P., Imhof, A., and Akhtar, A. (2005). hMOF histone acetyltransferase is required for histone H4 lysine 16 acetylation in mammalian cells. *Mol. Cell. Biol* 25, 6798-6810.
- Talasz, H., Lindner, H. H., Sarg, B., and Helliger, W. (2005). Histone H4-lysine 20 monomethylation is increased in promoter and coding regions of active genes and correlates with hyperacetylation. *J. Biol. Chem* 280, 38814-38822.
- Tan, B. C., Chien, C., Hirose, S., and Lee, S. (2006). Functional cooperation between FACT and MCM helicase facilitates initiation of chromatin DNA replication. *EMBO J* 25, 3975-3985.
- Tardat, M., Murr, R., Herceg, Z., Sardet, C., and Julien, E. (2007). PR-Set7-dependent lysine methylation ensures genome replication and stability through S phase. *J Cell Biol* 179, 1413-26.
- Taunton, J., Hassig, C. A., and Schreiber, S. L. (1996). A mammalian histone deacetylase related to the yeast transcriptional regulator Rpd3p. *Science* 272, 408-11.
- Thomas, J. O. (1999). Histone H1: location and role. *Curr. Opin. Cell Biol* 11, 312-317.
- Towbin, H., Staehelin, T., and Gordon, J. (1979). Electrophoretic transfer of proteins from polyacrylamide gels to nitrocellulose sheets: procedure and some applications. *Proc. Natl. Acad. Sci. U.S.A* 76, 4350-4354.
- Trojer, P. et al. (2007). L3MBTL1, a histone-methylation-dependent chromatin lock. *Cell* 129, 915-28.
- Tschiersch, B., Hofmann, A., Krauss, V., Dorn, R., Korge, G., and Reuter, G. (1994). The protein encoded by the *Drosophila* position-effect variegation suppressor gene *Su(var)3-9* combines domains of antagonistic regulators of homeotic gene complexes. *EMBO J* 13, 3822-3831.
- Turner, B. M. (2002). Cellular memory and the histone code. *Cell* 111, 285-91.
- Utey, R. T., and Côté, J. (2003). The MYST family of histone acetyltransferases. *Curr. Top. Microbiol. Immunol* 274, 203-236.
- Vakoc, C. R., Mandat, S. A., Olenchok, B. A., and Blobel, G. A. (2005). Histone H3 lysine 9 methylation and HP1gamma are associated with transcription elongation through mammalian chromatin. *Mol Cell* 19, 381-91.
- Vaquero, A., Scher, M., Lee, D., Erdjument-Bromage, H., Tempst, P., and Reinberg, D. (2004). Human SirT1 interacts with histone H1 and promotes formation of facultative heterochromatin. *Mol. Cell* 16, 93-105.
- Verreault, A., Kaufman, P. D., Kobayashi, R., and Stillman, B. (1996). Nucleosome assembly by a complex of CAF-1 and acetylated histones H3/H4. *Cell* 87, 95-104.
- Villar-Garea, A., Israel, L., and Imhof, A. (2008). Analysis of histone modifications by mass spectrometry. *Curr Protoc Protein Sci* Chapter 14, Unit 14.10.

- Waddington, C. (1942). *Endeavour* 1, 18-20.
- Wakabayashi, K. et al. (2009). The peroxisome proliferator-activated receptor gamma/retinoid X receptor alpha heterodimer targets the histone modification enzyme PR-Set7/Setd8 gene and regulates adipogenesis through a positive feedback loop. *Mol. Cell. Biol* 29, 3544-3555.
- Wang, X., and Hayes, J. J. (2006). Physical methods used to study core histone tail structures and interactions in solution. *Biochem Cell Biol* 84, 578-88.
- Welstead, G. G., Schorderet, P., and Boyer, L. A. (2008). The reprogramming language of pluripotency. *Curr. Opin. Genet. Dev* 18, 123-129.
- Widom, J. (1998). Chromatin structure: linking structure to function with histone H1. *Curr. Biol* 8, R788-791.
- Wysocka, J. et al. (2006). A PHD finger of NURF couples histone H3 lysine 4 trimethylation with chromatin remodelling. *Nature* 442, 86-90.
- Xiang, Y., Zhu, Z., Han, G., Lin, H., Xu, L., and Chen, C. D. (2007). JMJD3 is a histone H3K27 demethylase. *Cell Res* 17, 850-857.
- Xiao, B. et al. (2005). Specificity and mechanism of the histone methyltransferase Pr-Set7. *Genes Dev* 19, 1444-1454.
- Xu, C., Cui, G., Botuyan, M. V., and Mer, G. (2008). Structural basis for the recognition of methylated histone H3K36 by the Eaf3 subunit of histone deacetylase complex Rpd3S. *Structure* 16, 1740-1750.
- Yang, X., and Seto, E. (2008). The Rpd3/Hda1 family of lysine deacetylases: from bacteria and yeast to mice and men. *Nat Rev Mol Cell Biol* 9, 206-18.
- Yoshida, M., Kijima, M., Akita, M., and Beppu, T. (1990). Potent and specific inhibition of mammalian histone deacetylase both in vivo and in vitro by trichostatin A. *J Biol Chem* 265, 17174-9.
- Zeng, L., and Zhou, M. M. (2002). Bromodomain: an acetyl-lysine binding domain. *FEBS Lett* 513, 124-128.
- Zhang, Y., and Reinberg, D. (2001). Transcription regulation by histone methylation: interplay between different covalent modifications of the core histone tails. *Genes Dev* 15, 2343-60.
- Zheng, C., and Hayes, J. J. (2003). Intra- and inter-nucleosomal protein-DNA interactions of the core histone tail domains in a model system. *J Biol Chem* 278, 24217-24.

Ac	Acetylation
ACN	Acetonitrile
ADP	Adenosindiphosphate
ASF1	Antisilencing function 1
ATP	Adenosintriphosphate
bp	Basepairs
BSA	Bovine serum albumin
CAF1	Chromatin assembly factor 1
Co-REST	Corepressor to REST
CTD	C-terminal domain
DMSO	Dimethylsulfoxide
DNA	Desoxyribonucleic acid
dNTP	Desoxyribonucleotidetriphosphate
DREX	Drosophila embryonic extract
<i>Drosophila</i>	<i>Drosophila melanogaster</i>
DTT	Dithiothreitol
E(Z)	Enhancer of zeste
<i>E.coli</i>	<i>Echerichia coli</i>
EDTA	Ethylendiamintetraacetate
EGTA	Ethylenglycol-bis(2-aminoethyl)-N,N,N',N'-tetraacetic acid
ES cells	Embryonic stem cells
EtBr	Ethidiumbromide
EtOH	Ethanol
EW	Embryo wash
EX	Extraction buffer
EZH2	Enhancer of Zeste homolog 2
FACS	Fluorescence activated cell sorting
FACT	Facilitates chromatin transcription
FAD	Flavin adenine dinucleotide
Fe	Ferrum
FPLC	Fast protein liquid chromatography
Gcn5	General control non-derepressible
GNAT	Gcn5 related N-acetyltransferase
H3, H4, H2A, H2B, H1	Histones
HAT	Histone acetyltransferase
HDAC	Histone deacetylase

Abbreviations

HeLa cells	Henrietta Lacks cells
HEPES	(N-(2-Hydroxyethyl)piperazine-H ⁺)-(2-ethanesulfonic acid)
HMG	High mobility group proteins
HMT	Histone methyltransferase
HP1	Heterochromatin protein 1
IPTG	1-isopropyl- β -D-1-thiogalacto-pyranoside
JmjC	Jumonji C
K	Lysine
kb	Kilobase
l(3)MBT	Lethal(3)malignant brain tumor-like 3
LSD1	Lysine-specific demethylase 1
MALDI-TOF	Matrix Assisted Laser Desorption/Ionisation
MCM	Mini-Chromosome Maintenance
Me	Methylation
Mi-2/NuRD	Mi-2/nucleosome remodeling and deacetylase
MNase	Micrococcal nuclease
MW	Molecular weight
MWCO	Molecular weight cut off
MYST	<u>M</u> orf, <u>Y</u> bf2, <u>S</u> as2 and <u>T</u> ip60
NaBu	Sodiumbutyrate
NAD	Nicotinamid-adenin-dinucleotid
NSD1	Nuclear receptor-binding, su(var), enhancer-of-zeste and tritho- rax domain-containing protein 1
NuA4	nucleosome acetyltransferase of histone H4
OD	Optical density
P	Phosphorylation
PADI	Peptidylarginine deiminase
PAGE	Polyacrylamide gel electrophoresis
PBS	Phosphate buffered saline
PCAF	p300/CBP-associated Factor
PCNA	Proliferating cell nuclear antigen
PCR	Polymerase chain reaction
PHD	Plant homeodomain
PMSF	Phenylmethanesulfonyl fluoride
PRC1/2	Polycomb repressive complex 1/2
PRMT1	Protein arginine methyltransferase 1

PTM	Posttranslational modification
R	Arginine
RNA	Ribonucleic acid
Rpd3	Reduced potassium dependency
rpm	Revolutions per minute
RT	Room temperature
S	Serine
<i>S. cerevisiae</i>	<i>Saccharomyces cerevisiae</i>
SAH	S-Adenosyl-L-homocysteine
SAM	S-Adenosyl methionine
SDS	Sodiumdodecylsulfate
SILAC	Stable isotope labeling with amino acids in cell culture
Su(var)	Suppressor of position-effect variegation
SUMO	Small ubiquitin-related modifier
TC	Tissue culture
TEMED	N,N,N',N'-Tetramethylethylenediamine
TFA	Trifluor acetic acid
Tris	Tris(hydroxymethyl)aminomethane
Trx	Trithorax
TSA	Trichostatin A
v/v	Volume per volume
w/v	Weight per volume
α	Anti, alpha

Annette N.D. Scharf

Date of birth: November 16th 1978

Place of birth: Offenburg

EDUCATION

- 01/2006-present **PhD thesis at the Ludwig-Maximilians-University of Munich, Prof. Axel Imhof**
Project: Dynamics of histone modifications
PhD scholarship: Boehringer Ingelheim Fonds
- 1/2000 - 11/2005 **Diploma thesis at the Ludwig-Maximilians-University of Munich, Prof. Axel Imhof**
Project: Analyzing HP1 binding to chromatin with chromatin immunocleavage (ChIC).
- 10/2000 - 11/2005 **Studies of Biology at the Ludwig-Maximilians-University of Munich**

PUBLICATIONS

Annette N.D. Scharf*, Teresa Barth*, Axel Imhof. Establishment of Histone Modifications after Chromatin Assembly *NAR*, Advance Access published on June 18, 2009 (*equally contributed)

Annette N.D. Scharf, Karin Meier, Volker Seitz, Alexander Brehm, Axel Imhof. Monomethylation of lysine 20 on histone H4 facilitates chromatin maturation. *MCB*, 2009 Jan; 29 (1): 57-67.

Oliver Bell, Christiane Wirbelauer, Marc Hild, **Annette N.D. Scharf**, Michaela Schwaiger, David M. MacAlpine, Frederic Zilberman, Stephen P. Bell, Axel Imhof, Dan Garza, Antoine H. F. M. Peters and Dirk Schübeler. Localized H3K36 methylation states define histone H4K16 acetylation during transcriptional elongation in *Drosophila*. *EMBO*, 2007 Dec 12; 26 (24): 4974-84.

Annette N.D. Scharf und Axel Imhof. Replikation des Chromatins-dispersiv statt semikonservativ? *BIOspektrum*, September 2007.

Notes

Notes
